

**A Renormalization Group Study
of
Supersymmetric Field Theories**

DISSERTATION

zur Erlangung des akademischen Grades
Doctor rerum naturalium (Dr. rer. nat.)

vorgelegt dem Rat der
Physikalisch-Astronomischen Fakultät
der Friedrich-Schiller-Universität Jena

von Dipl.-Phys. Marianne Heilmann
geboren am 22.01.1986 in Suhl

Gutachter:

1. Prof. Dr. Andreas Wipf, Jena
2. Dr. Frank Saueressig, Nijmegen, Niederlande
3. Prof. Dr. Hidenori Sonoda, Kobe, Japan

Tag der Disputation: 13.05.2015

Contents

1	Introduction	3
2	The Functional Renormalization Group	6
2.1	Effective Action	7
2.2	Renormalization Group Equation	9
2.3	Truncations	11
2.4	Fundamental Properties from Fixed Points	12
3	Supersymmetry	14
3.1	The Super-Poincaré Algebra	15
3.2	The Concept of Superspace	17
3.3	Spontaneous Supersymmetry Breaking	18
3.4	Aspects of Supersymmetry from the FRG	19
4	Supersymmetric Quantum Mechanics	20
4.1	Introducing the Model	21
4.2	Supersymmetric Renormalization Group Flow	24
4.2.1	Supercovariant Derivative Expansion	24
4.2.2	Choosing the Regulator Functional	25
4.2.3	Flow Equations	26
4.3	Unbroken Supersymmetric Quantum Mechanics	28
4.3.1	Effective Potential	30
4.3.2	First Excited Energy	32
4.4	Supersymmetry Breaking	34
4.4.1	Expansion Issues	34
4.4.2	Numerical Results	36
5	The Three-Dimensional $\mathcal{N} = 1$ Wess-Zumino Model	38
5.1	Introducing the Model	40
5.2	Flow Equations	41
5.3	Wilson-Fisher Fixed Point	43

5.4	Superscaling Relation	46
6	Supersymmetric $O(N)$ Theories	48
6.1	Introducing the Model	52
6.2	Supersymmetric Renormalization Group Flow	53
6.2.1	Truncation	54
6.2.2	Choosing the Regulator Functional	54
6.2.3	Flow Equations	55
6.3	Exploring the Limit of Infinitely Many Fields	57
6.3.1	RG Flow and Boundary Condition	58
6.3.2	Fixed-Point Structure	60
6.3.3	Universality	68
6.3.4	Renormalized Theory	73
6.3.5	Effective Theory	80
6.3.6	Comparison and Discussion	87
6.3.7	Spontaneous Breaking of Scale Invariance	90
6.4	Physics at Finite N - Radial Mode Fluctuations	92
6.4.1	Exact Fixed Point	92
6.4.2	Exact Critical Exponents	93
6.4.3	Global Scaling Solution	94
7	Conclusions	97
A	Technical Details for SUSY-QM	101
B	Pseudo-Spectral Methods	106
C	Technical Details for the $\mathcal{N} = 1$ Wess-Zumino Model	107
D	Technical Details for Supersymmetric $O(N)$ Theories	109

Chapter 1

Introduction

Since its development in the 1970's, the Standard Model of elementary particles describing the electromagnetic, weak, and strong nuclear interactions has been a grand achievement. The recent discovery of the Higgs boson at the Large Hadron Collider [1, 2] at a mass of 125 GeV joins a series of experimental confirmations giving further credence to the Standard Model. However, although the Standard Model has been proven very successful in explaining physics around the electroweak scale, it leaves a door ajar for certain still unexplained physical phenomena and observations. Examples thereof are [3]: *How might the gravitational force be incorporated into a unified theory? Why does the universe expand in the observed accelerated way? What is the nature of dark matter and dark energy required by cosmological observations? Why does matter predominate over antimatter? What is the origin of the hierarchy problem? Why does quantum chromodynamics not seem to break the CP-symmetry? How do the neutrino masses as predicted by neutrino oscillation experiments arise?* Due to these open issues, the Standard Model is not considered a fundamental theory valid on all scales rather than an effective theory of the electroweak and strong interactions. There are a variety of theoretical developments striving for an extension of the Standard Model as the Minimal Supersymmetric Standard Model (MSSM) [4, 5] or entirely novel theoretical concepts such as string theory [6, 7], M-theory [8, 9] and extra dimensions [10].

The most popular and promising theories beyond the Standard Model have one thing in common: *supersymmetry*. Indeed, supersymmetry represents the only non-trivial extension of space-time symmetry [11]. It implies each bosonic (fermionic) particle of the Standard Model to be associated with a similar fermionic (bosonic) one whose spin differs by one-half and is called 'superpartner'. Via extensions including supersymmetry, conceptual shortcomings of the Standard Model such as the hierarchy problem, the strong CP problem, the occurrence of dark matter and the unification of interactions at high energies may be entirely or partly solved [12–15].

If supersymmetry is unbroken in nature, it predicts mass-degenerate multiplets of bosonic and fermionic particles. This prediction could not be confirmed experimentally, meaning

supersymmetry to break spontaneously at a certain energy scale. So far the Large Hadron Collider failed to find direct evidence for supersymmetry and no signs of superpartners below 1 TeV have been found yet [16]. Nevertheless, the observed Higgs mass is consistent with the prediction of the MSSM that the lightest Higgs boson should weigh $\lesssim 130$ GeV [17]. Moreover, measurements of Higgs couplings to other particles are in accordance with the forecasts of many supersymmetric models [18]. The current scientific atmosphere about supersymmetry may be put into words best by John Ellis [19]:

“Obviously we theorists working on supersymmetry are playing for big stakes. We’re talking about dark matter, the origins of mass scales in physics, unifying the fundamental forces. You have to be realistic: if you are playing for big stakes, very possibly you’re not going to win.”

In order to get insight into supersymmetric extensions of the Standard Model it is resorted to simplified theories still exhibiting all generic properties. Famous prototypes are so-called *Wess-Zumino theories* [20] modelling the matter sector of the MSSM. Due to a lack of gauge degrees of freedom, they are of a quite simple structure.

If the description of nature is intrinsically supersymmetric, it is necessary to acquire a basic understanding of supersymmetric theories not only perturbatively but also in the non-perturbative regime. This is of particular importance as spontaneous supersymmetry breaking is believed to be a non-perturbative effect [21, 22]. In this regard, characteristics of the phase transition separating the supersymmetric from the non-supersymmetric phase are of special interest.

There exist several conceptually different approaches to strongly-coupled supersymmetric field theories. For instance, physics at criticality in higher dimensions is nicely described in the *mean field approximation* [23]. However, due to a different treatment of fermions and bosons, this scheme breaks supersymmetry [24]. *Lattice calculations* replacing space-time by a discrete lattice offer a further approach. In particular, lattice regularization combined with statistical Monte-Carlo methods have become quite successful over the last years [25–27]. Since the supersymmetry algebra inevitably involves generators of translations, a complete implementation of continuum supersymmetry on the lattice is impossible. Nevertheless, supersymmetry may be realized as an accidental symmetry of the continuum limit of the lattice-regularized theory. Generically, such a limit may be achieved by a fine-tuning of the relevant operators [28, 29]. Also, a partial restoration of supersymmetry is feasible for theories with extended supersymmetry [30]. Alternatively, a third conceptual path may be taken: the *functional renormalization group* (FRG) [31, 32]. This method takes into account quantum fluctuations in the path-integral momentum shell by momentum shell. Physics on large scales gets connected to microscopic interactions via the introduction of a scale-dependent effective average action. Its determination requires the solution of a functional differential equation as obtained by reformulating the functional integral. The

FRG has been applied to a variety of physical phenomena in the past, ranging from the QCD phase diagram [33, 34] and the Higgs sector of the Standard Model [35–37] to nuclear physics [38–40], non-equilibrium systems [41, 42] and quantum gravity [43–46]. In recent years, the fundamentals of utilizing the FRG to explore supersymmetric Wess-Zumino models in various dimensions have been elaborated [47–55]. The renormalization group equations have been formulated in a manifestly supersymmetric way, thus allowing for a sound analysis of spontaneous supersymmetry breaking. This thesis starts and follows up at this point.

The focus of the work presented here is on the application of the functional renormalization group to scalar supersymmetric field theories. It is motivated by the following questions:

Are the physical properties, especially the behaviour at criticality and in non-perturbative regimes addressed adequately via applying the FRG framework? What new non-perturbative aspects of supersymmetry may be deduced from this? Of what quality are the derived results regarding their precision, especially in comparison with other methods as e.g. variational calculations, large- N expansions and Schwinger-Dyson equations?

This work is organized as follows: chapter 2 introduces the functional renormalization group. The main aspects of supersymmetry as necessary for subsequent chapters are explained in chapter 3. The remaining chapters comprise the findings obtained by applying the FRG to different supersymmetric models. Firstly, supersymmetric quantum mechanics is explored in chapter 4. Here, it is focussed on the ground- and excited-state energies for unbroken as well as spontaneously broken supersymmetry. Subsequently, a detailed analysis of the phase structure of the three-dimensional $\mathcal{N} = 1$ Wess-Zumino theories is given in chapter 5. Finally, supersymmetric $O(N)$ models in three-dimensions are discussed in chapter 6. Here, the phase structure and interesting phenomena like spontaneous breaking of scale invariance are studied at infinite as well as finite N .

The compilation of this thesis is solely due to the author. However, a large part of the work presented here has been published in a number of articles and in collaboration with several authors. Chapter 4 and chapter 5 rely on work in collaboration with Markus Ansorg, Tobias Hellwig, Benjamin Knorr and Andreas Wipf [56]. Chapter 6 is founded on work in collaboration with Daniel F. Litim, Franziska Synatschke-Czerwonka and Andreas Wipf [57–59]. The Mathematica program used to calculate the numerically exact values of the first excited energies in chapter 4 has been provided by Georg Bergner. The C++ program implementing spectral methods for the numerical investigation of the flow equations has been developed by Benjamin Knorr and Julia Borchardt.

Chapter 2

The Functional Renormalization Group

Our nature behaves quite differently on various length or energy scales. As an example, consider the nuclear forces between protons and neutrons, mediated by pions. In a wide range of practical applications in chemistry and physics, the microscopic structure consisting of quarks and gluons turns out to be redundant knowledge. Similarly, the nuclear forces ranging up to a few fm are not of relevance on atomic scales of the order of some Å. Here, the effective description suffices. In particular, many physical properties of a theory are altered by the transition from microscopic to macroscopic scales. Examples are given by the relevant degrees of freedom, the conserved symmetries, the phase structure and the fundamental couplings. Often, the effective picture of a theory only depends on a few effective “relevant” parameters which are determined by the microscopic theory. Hence, a bridge between microscopic and macroscopic physics is built. Different microscopic theories may result in the same effective dynamics. Hence, we are in need of a tool allowing for a scale-dependent description of a certain physical setup. We are thereby specifically interested in accessing regimes, where physics is governed by non-perturbative effects and strong correlations. This is in particular interesting for supersymmetric theories, since this allows for an analysis of spontaneous supersymmetry breaking, as the latter is known to be an infrared (IR) effect [60]. In the subsequent section, a suitable tool allowing for an examination of physics on different scales, namely the functional renormalization group (FRG), is discussed.

Mathematically, the FRG represents a functional method, aimed to determine the scale-dependent modified Legendre transform of the scale-dependent generating functional $W_k[J]$ of the connected correlation functions. This modified Legendre transform is called *effective average action* $\Gamma_k[\Phi]$. Its determination requires the solution of a functional differential equation with certain initial conditions - the *flow equation*. The latter describes the evolution of Γ_k as a function of the energy scale parameter k , influenced by quantum fluctuations. Thereby, at a certain scale k , all quantum fluctuations with momenta $|p| > k$ are taken into

account. Hence, Γ_k interpolates between the microscopic action S in the ultraviolet (UV) and the full quantum effective action $\Gamma_{k \rightarrow 0} = \Gamma$ in the IR. The FRG has been applied to a variety of physical problems and theories as gauge theories [61–63], scalar field theories [31, 64, 65], supersymmetric models [47–50, 56–59], gravity [43–46], statistical physics [31, 66], nuclear physics [38–40] or non-equilibrium systems [41, 42].

In this chapter, the conventions follow [32, 67] if not stated otherwise. All formulations and considerations are worked out in Euclidean space-time. Regarding the formulations in Minkowski space-time, the reader is referred to textbooks by M.E. Peskin and D.V. Schroeder [67], J. Zinn-Justin [68] or S. Weinberg [69].

2.1 Effective Action

The effective action acts as the generating functional of correlation functions. Thus, it delivers important information about e.g. scattering processes. The correlators or n -point functions for a scalar field φ thereby emerge as the product of n field operators, located at different points in space-time, averaged over all quantum fluctuations (field configurations) and weighted with an exponential of the action $S[\varphi]$:

$$\langle \varphi(x_1) \cdots \varphi(x_n) \rangle = \mathcal{N} \int \mathcal{D}\varphi \varphi(x_1) \cdots \varphi(x_n) e^{-S[\varphi]} \quad \text{with} \quad \langle 1 \rangle = 1. \quad (2.1)$$

Here, \mathcal{N} denotes the normalization constant. Note that equivalent formulations hold for fermionic, vector and tensor fields. All n -point functions (2.1) may be generated by the regularized¹ generating functional

$$Z[J] = \int \mathcal{D}\varphi e^{-S[\varphi] + \int J\varphi} \quad (2.2)$$

via functional differentiation:

$$\langle \varphi(x_1) \cdots \varphi(x_n) \rangle = \frac{1}{Z[0]} \left(\frac{\delta^n Z[J]}{\delta J(x_1) \cdots \delta J(x_n)} \right) \Big|_{J=0}, \quad (2.3)$$

where the abbreviation $\int J\varphi = \int d^d x J(x)\varphi(x)$ has been used. The generating functional of connected correlation functions, the ‘‘Schwinger functional’’

$$W[J] = \ln Z[J] \quad (2.4)$$

emerges as the logarithm of $Z[J]$. Finally, the generating functional of all one-particle irreducible correlation functions - the *effective action* $\Gamma[\phi]$ - is introduced. It is defined as

¹We assume the existence of a proper regularized, symmetry-preserving definition of the path-integral measure, i.e. of a UV-regularized form. This may be a complicated issue in anomalous theories, where no regularization compatible with the symmetries of the theory may exist.

the Legendre transform

$$\Gamma[\phi] = \sup_J \left(\int J\phi - W[J] \right) \quad (2.5)$$

of the Schwinger functional $W[J]$, where J is transformed to ϕ . The Legendre transform of a convex function is reversible². Thus, it transforms a convex Schwinger functional to a convex effective action. The above definition states that for arbitrarily given ϕ a special $J = J_{\text{sup}} = J[\phi]$ has to be found which maximizes (2.5). Setting $J = J_{\text{sup}}$ yields

$$0 = \frac{\delta}{\delta J(x)} (J\phi - W[J]) \quad \Rightarrow \quad \phi = \frac{\delta W[J]}{\delta J} = \frac{1}{Z[J]} \frac{\delta Z[J]}{\delta J} = \langle \varphi \rangle_J. \quad (2.6)$$

Hence, the macroscopic field ϕ corresponds to the expectation value of the microscopic field φ in presence of an external source J . For a given action S , the equations of motion (EOM) may be derived by functional differentiation with respect to the fields. Likewise, the functional derivative of the effective action with respect to ϕ at J_{sup} delivers the quantum EOM

$$\frac{\delta \Gamma[\phi]}{\delta \phi} = J, \quad (2.7)$$

triggering the dynamics of the macroscopic field. The microscopic EOM may differ significantly from the effective, macroscopic EOM for ϕ . The latter takes into account all quantum fluctuations and will therefore generically include effective interactions which are not present in the microscopic dynamics.

The effective action is, in thermodynamic terms, an extensive quantity proportional to the volume of space-time. By scaling out the volume for constant macroscopic fields³, we derive at the *effective potential* [67]

$$V_{\text{eff}} = \Omega^{-1} \Gamma[\phi]. \quad (2.8)$$

For vanishing source, the EOM (2.7) simplifies to

$$\frac{\delta \Gamma[\phi]}{\delta \phi} = 0, \quad (2.9)$$

corresponding to $\partial V_{\text{eff}}/\partial \phi = 0$ in terms of the effective potential. Hence, the absolute minimum of the effective potential represents the state of lowest energy density and thus is the stable vacuum state. If V_{eff} exhibits several minima with equal energy, one minimum is chosen among these vacua and spontaneous symmetry breaking may occur.

²The Legendre transform of a non-convex function is identical to the Legendre transform of the convex hull of the function considered.

³Under certain circumstances, this state does not give the true minimum energy configuration for states with given ϕ . Here, a field theoretic analogue of the Maxwell construction for the free energy, corresponding to an interpolation between local minima, has to be applied in order to obtain a convex $V_{\text{eff}}[\phi]$.

2.2 Renormalization Group Equation

This section concretizes the ideas of the FRG presented in the introduction of this chapter. In this regard, the *flow equation* represents the vital object of interest by connecting physics on different momentum scales k .

The name *renormalization group* (RG) appeared for the first time in the 1950s [70]. It was motivated by the expectation to express fundamental physics by symmetry and group theoretic concepts rather than dynamics. The first implementation relied on K. Wilson [71–73]. He suggested the idea of performing the Euclidean path-integral momentum-shell-wise by introducing a floating IR-cutoff k . This leads to scale-dependent actions, connected via continuous RG transformations. The RG flow then describes the change of the couplings under the RG transformation [74]. A quite intuitive approach to the RG is given by Kadanoff’s idea of block spinning [75]. Physics of the Ising spin system at low momenta (large distances) is described by averaging microscopic spins over a finite region of space. Then, the system is characterized by averaged spins. Next, the system is rescaled such that when looking on the same size of the sample, a larger number of microscopic spins is considered. Graphically, Kadanoff’s idea corresponds to “zooming out” from the Ising spin system. During this procedure of block spinning, interactions of increasing range, compatible with the symmetries of the system, have been taken into account. The concept of locality is thereby a crucial ingredient of the procedure: If an interaction is non-local, no sensible averaging of quantum fluctuations over a finite region in space can be performed. Typically, the microscopic picture of usual QFTs is of local nature and non-local interactions should only emerge in the macroscopic effective limit, where all fluctuations have been integrated out.

Now, the above idea of integrating out quantum fluctuations successively is formalised. Thereby, the concept of an effective average action generalizes the block spin picture established by Kadanoff [75] to continuous space. This is realized by introducing the continuous momentum shell parameter k and deriving an equation for the interpolating action Γ_k : the *Wetterich equation* [76, 77]. To begin with, the discussion is restricted to scalar fields. A generalization to fermionic or gauge fields is straightforward and will be considered later on.

A momentum-shell-wise integration of quantum fluctuations may be implemented by defining an IR regulated, scale-dependent generating functional

$$Z_k[J] = e^{W_k[J]} = \int_{\Lambda} \mathcal{D}\varphi e^{-S[\varphi] + \int J\varphi - \Delta S_k} \quad \text{with} \quad \Delta S_k = \int_p \varphi(-p) R_k(p^2) \varphi(p) \quad (2.10)$$

as well as a scale-dependent effective average action

$$\Gamma_k[\phi] = \sup_J \left(\int J\phi - \ln Z_k[J] \right) - \Delta S_k[\phi]. \quad (2.11)$$

The latter is constructed via a modified Legendre transform, implying Γ_k not to be necessarily convex for finite $k > 0$. The regulator functional ΔS_k introduced in (2.10) is quadratic in the fields and acts as a momentum-dependent mass term. It includes the regulator function⁴ $R_k(p^2)$ satisfying certain conditions. Firstly, $R_k(p^2) > 0$ for $p^2/k^2 \rightarrow 0$ ensures IR regularization by suppressing contributions of quantum fluctuations with momenta below k^2 . Furthermore, the regulator function R_k is chosen to vanish for $k^2/p^2 \rightarrow 0$. Hence, the standard generating functional (2.2) as well as the full effective action (2.5) is recovered in the IR limit. Finally, the behaviour $R_k(p^2) \xrightarrow{k \rightarrow \infty} \infty$ ensures that the functional integral is dominated by the stationary points of the action in this limit, filtering out the bare action $\Gamma_{k \rightarrow \Lambda \rightarrow \infty} \rightarrow S + \text{const.}$.

Hence, the flowing action (2.11) defines a set of effective, k -dependent theories describing the dynamics at a momentum scale k and interpolating smoothly between the classical action S in the UV and the effective action Γ in the IR. By employing the fundamental definitions (2.10) and (2.11), the *Wetterich equation*

$$\partial_t \Gamma_k[\phi] = \frac{1}{2} \text{Tr} \left[\partial_t R_k \left(\Gamma_k^{(2)}[\phi] + R_k \right)^{-1} \right], \quad t = \ln(k/\Lambda) \quad (2.12)$$

can be derived straightforwardly [77]. The dimensionless scale-parameter t is defined as the ratio of the running scale k and the UV cutoff scale Λ . The following references offer a selection of reviews discussing the flow equation: [31, 63, 78–81].

The Wetterich equation (2.12) is a functional differential equation for the scale derivative of Γ_k . Since ΔS_k is chosen to be quadratic in the fields, the flow equation is of a one-loop structure. Nevertheless, it is an exact equation containing the fully dressed propagator in the loop. Contrary to perturbative expansions, it does not rely on the existence of a small parameter. In fact, it holds for arbitrary values of the couplings and perturbation theory can be reproduced to any order by an iterative application of (2.12), c.f. [82, 83]. Furthermore, the Wetterich equation is automatically UV as well as IR finite. The latter follows from construction whereas UV finiteness is secured by the scale derivative of the regulator function R_k in the numerator of the flow as it vanishes for momenta $p^2 \gg k^2$.

As stated above, a generalization of (2.12) to several scalar fields, fermionic fields, gauge fields or superfields is possible [47, 84–87]. Then, taking the trace not only involves an integration over Euclidean or momentum space, but also includes a summation over all internal and external indices. In supersymmetric theories considered within this thesis, the flowing action is a functional of one or several scalar superfields Φ . The flow equation then

⁴Generically, the regulator function depends on the kinetic operator of the theory. The latter may coincide with the momentum squared in simple cases. However, it could also be an appropriate covariant operator, e.g. the supercovariant derivative in Wess-Zumino models. Then, the regulator R_k is a function of the eigenvalues of the kinetic operator and \int_p a continuous or discrete sum over all the eigenvalues.

reads

$$\partial_t \Gamma_k[\Phi] = \frac{1}{2} \text{STr} \left[\partial_t R_k \left(\Gamma_k^{(2)}[\Phi] + R_k \right)^{-1} \right] \quad \text{with} \quad \left(\Gamma_k^{(2)} \right)_{ab} = \frac{\overrightarrow{\delta}}{\delta \Phi_a} \Gamma_k \frac{\overleftarrow{\delta}}{\delta \Phi_b}, \quad (2.13)$$

where a, b summarize internal and Lorentz indices as well as superspace coordinates. Besides, the integration measure is now given by the measure of the corresponding superspace involving an integration over Grassmann variables.

2.3 Truncations

The Wetterich equation represents an exact one-loop equation. It constitutes an infinite tower of coupled differential equations. To this, consider the flow of the n -point vertex, i.e. the n th functional derivative of the Wetterich equation with respect to the field. As, for instance,

$$\frac{\delta}{\delta \phi} \left(\Gamma_k^{(2)} \right)^{-1} = - \left(\Gamma_k^{(2)} \right)^{-1} \Gamma_k^{(3)} \left(\Gamma_k^{(2)} \right)^{-1}, \quad (2.14)$$

the flow of $\Gamma_k^{(n)}$ depends on $\Gamma_k^{(n+1)}$ and $\Gamma_k^{(n+2)}$. Solving this infinite number of coupled equations is not possible in general. Therefore, it is necessary to truncate Γ_k in theory space⁵, i.e. making an ansatz in which Γ_k depends on certain classes of operators. As a first example, Γ_k may be expanded in operators containing an increasing number of derivatives. This expansion scheme is intrinsically of a non-perturbative nature and thus a suitable tool for exploring non-perturbative aspects of a theory. Furthermore, a vertex expansion may be selected. This scheme is complementary to the derivative expansion in the sense that an infinite number of operators of the derivative expansion can contribute to a single operator in the vertex expansion (involving e.g. an arbitrary function of momenta). Both approaches are systematic expansions as the “truncated” effective action should converge to the true effective action by including more and more operators up to a definite order in the truncation. A systematic control of the error made by truncating the action is desirable. Unfortunately, this is a highly challenging issue. An error estimate is possible by studying the regulator dependence of Γ_k . In the IR limit $k \rightarrow 0$, the regulator dependence of an untruncated Γ_k vanishes. However, within a certain truncation there remains a residual regulator dependence in the IR, giving an estimate for the error made by the chosen truncation. Nevertheless, the real distance of $\Gamma_{k \rightarrow 0}$ from the true result may be larger than this error. Optimization techniques have been formulated for constructing an optimized regulator in order to minimize the truncation error [88]. Notice, that the necessity to truncate also bears the possibility of analysing the origin of physical effects. Thus, it may be studied which operators create certain physical phenomena such as e.g. spontaneous symmetry breaking.

⁵The theory space is spanned by all operators (as e.g. $\varphi^n, \partial_\mu \varphi \partial^\mu \varphi, \dots$) determining the effective action.

2.4 Fundamental Properties from Fixed Points

A fundamental quantum field theory (QFT) exhibits an RG trajectory extending over all scales $k \in [0, \infty)$. Indeed, this is fulfilled if the trajectory has a *fixed point* in theory space. This specific point is characterised by invariance under RG transformations, i.e. invariance under a change in scale k . A fixed-point analysis may be performed by expanding the effective average action in the infinite sum

$$\Gamma_k = \sum_i a_i(k) \mathcal{O}_i \quad (2.15)$$

of operators \mathcal{O}_i with scale-dependent coefficients $a_i(k)$. Then, the Wetterich equation describes the evolution of the running couplings, given by an infinite tower of coupled, ordinary differential equations. The rescaled flows

$$\partial_t a_i(t) = \beta_i(a_k), \quad (2.16)$$

expressed in dimensionless quantities, are called β *functions*. The latter form a vector field over theory space. Fixed points in the space of couplings then satisfy the condition

$$\beta_i(a_{k*}) = 0 \quad \forall i. \quad (2.17)$$

Infrared fixed points dominate the long-distance behaviour of correlation functions and are relevant for the understanding of continuous phase transitions and universal scaling laws [68]. Ultraviolet fixed points, in contrast, control the short-distance behaviour of quantum field theories. It is widely believed that the existence of a UV fixed point is mandatory for a definition of quantum field theory on a microscopic level, e.g. asymptotic freedom of QCD or asymptotic safety of gravity [89, 90]. In general, the fixed point structure of a given theory depends on its field content, the space-time dimensionality, the long-range or short-range nature of its interactions as well as the symmetries of the action.

The scaling solution (2.17) is called ‘‘Gaussian fixed-point’’ (GFP), if $a_{i*} = 0 \forall i$. Here, all interactions vanish and the theory is described by its kinetic terms only. A calculation of physical observables near the GFP via perturbative expansions in small couplings is possible⁶. An example of a GFP is given by Quantum Chromodynamics, where quarks and gluons interact very weakly (quark-gluon plasma) at high energies, where a trivial UV fixed point is approached. A fixed point is ‘‘non-Gaussian’’, if at least one a_{i*} is non-vanishing. Here, residual, possibly strong interactions occur at the fixed point and perturbative expansions may fail. In order to analyse the couplings in the vicinity of a fixed point, the flow is

⁶Note, that the numerical coefficients of an expansion in a small coupling may be fundamentally of a non-perturbative nature. For example, for electroweak plasmas, the rate of baryon number violation in the very early universe is known to be $\Gamma_B = Cg^{10}T^4 \ln g$ with a non-perturbative numerical coefficient C , c.f. [91].

linearised according to

$$\begin{aligned} \beta_i &= \beta_i(a_{k*}) + \left. \frac{\partial \beta_i}{\partial a_j} \right|_{a_{k*}} (a_j - a_{j*}) + \mathcal{O}((a_j - a_{j*})(a_k - a_{k*})) \\ &\stackrel{(2.17)}{=} B_i^j (a_j - a_{j*}) + \mathcal{O}(\Delta a^2) \quad \text{with} \quad B_i^j = \left. \frac{\partial \beta_i}{\partial a_j} \right|_{a_{k*}}. \end{aligned} \quad (2.18)$$

A diagonalization of the stability matrix B_i^j allows for the computation of the eigenvalues $\omega_n = -\theta_n$, labelled by the index n :

$$B_i^j V_j^n = \omega_n V_i^n = -\theta_n V_i^n. \quad (2.19)$$

Here V_i^n denotes the (right) eigenvector corresponding to the eigenvalue ω_n . The central objects of this fixed-point analysis are the negative eigenvalues, called *critical exponents* θ_n . They are universal numbers, independent of the regularization scheme chosen and parametrize the flow in the vicinity of a fixed point. Via (2.18) and (2.19), the evolution of the couplings close to a fixed point is given by

$$a_i(t) = a_{i*} + \sum_n C_n V_i^n e^{-\theta_n t}, \quad (2.20)$$

where the constants C_n are fixed by the UV initial conditions at $t = 0$. The evolution of the couplings to macroscopic scales clearly depends on the signs of the critical exponents: irrelevant eigendirections with $\theta_n < 0$ are exponentially suppressed by approaching the IR. Concerning a marginal eigendirection, characterized by $\theta_n = 0$, a linear ansatz (2.18) does not clarify the behaviour near the fixed point and higher orders $\mathcal{O}(a^2)$ have to be taken into account. If θ_n remains zero to all orders, the direction is truly marginal. Relevant eigendirections with $\theta_n > 0$ exponentially diverge away from the IR fixed-point for $k \rightarrow 0$. Thus, by ‘‘fine-tuning’’ the relevant couplings to their critical values, i.e. setting all C_n for $\theta_n > 0$ to zero, we are on the IR critical surface⁷ of the theory and the flow is driven into its fixed point by approaching the IR. This fine-tuning leads to the name ‘‘relevant’’ coupling as it represents a true parameter of the theory, whose microscopic value has to be fixed properly. In contrast, the IR values of the irrelevant couplings follow from the values of the relevant and marginal couplings. Note that (ir)relevance is a local attribute, defined with respect to a certain fixed point out of the set of all possible fixed points in coupling space. This set usually consists of several isolated⁸ fixed points. However, it may also be a continuum⁹ of fixed points or there may occur an even more exotic behaviour such as limit cycles [94–96].

⁷An IR (UV) critical surface is formed by all trajectories flowing into the IR (UV) fixed-point.

⁸Examples are quantum gravity [43, 44] or the three-dimensional Thirring model [92].

⁹Examples are the $\mathcal{N} = 1$ SUSY O(N) model in $d = 3$ for $N \rightarrow \infty$ [57] or the classical XY model in $d = 2$ [93].

Chapter 3

Supersymmetry

The concept of supersymmetry (SUSY) was introduced by Golfand and his student Likhtman [97] as well as by Volkov and Akulov [98, 99] in the early 1970s. Independently, in the context of string theory, supersymmetry was established as a symmetry of a two-dimensional world-sheet theory [100, 101].

Supersymmetry represents a proposed extension of space-time symmetry that relates two basic classes of elementary particles: bosons, having an integer-valued spin, and fermions, having a half-integer spin. Each bosonic particle is associated with a fermionic particle, called its superpartner, whose spin differs by one-half.

At first, an apparent question arises: Why is supersymmetry physically and conceptually interesting?

The group theoretician would immediately answer: Supersymmetry represents a non-trivial generalization of the Poincaré symmetry. First studies regarding an extension of the Poincaré symmetry have been made in the famous *Coleman-Mandula theorem* [102] in 1967. This “no-go-theorem” states, how the Poincaré group \mathcal{P} might be extended via other symmetry groups \mathcal{T} to a resulting Lie group \mathcal{G} , where \mathcal{G} is a connected symmetry group of the S-matrix. Posing a few physical assumptions, the theorem states that \mathcal{G} has to be locally isomorphic to the direct product $\mathcal{P} \otimes \mathcal{T}$, where \mathcal{T} is a compact Lie group with internal symmetry. In 1971, Golfand and Likhtman were the first to show that the Poincaré algebra might be non-trivially extended by the introduction of four anticommuting spinor generators in $d = 4$, later known as supercharges [97]. Four years later, Haag, Lopuszanski and Sohnius analysed all possible superalgebras, including those with an extended number of the supergenerators and central charges [11]. This extended super-Poincaré algebra forms the basis of supersymmetric field theories. Hence, the prerequisites of the Coleman-Mandula theorem were circumvented by the transition from a Lie group \mathcal{G} to more general symmetry groups.

The theoretical particle physicist would argue as follows: supersymmetry resolves the hierarchy problem of the Standard Model. The hierarchy problem is known under the

question, why the weak force is 10^{32} times stronger than gravity or equivalently, why the Higgs mass ($m_H \approx 125 \text{ GeV}$) is so much lighter than the Planck mass ($m_P \approx 1.22 \cdot 10^{19} \text{ GeV}$). Supersymmetry explains how the tiny Higgs mass could be protected from quantum corrections, since it removes the power-law divergences of the radiative corrections to the Higgs mass above the SUSY breaking scale, which becomes the new characteristic natural scale for the Higgs mass. Technically, the quantum corrections are cancelled due to the exact annihilation of bosonic and fermionic contributions. Besides, supersymmetry allows for a precise unification of the weak, electromagnetic and strong interaction at high energies.

The astrophysicist is fascinated by supersymmetry since the superpartners of the known particles are possible candidates of dark matter particles [13, 14]. The most popular class of natural dark matter candidates is generally called weakly interacting massive particles (WIMPs). Now, the lightest supersymmetric particle, i.e. the lightest of the additional hypothetical particles of a supersymmetric theory, simply has just the physical characteristics of a WIMP.

However, up to now, no superpartners have been observed yet. Hence, when going from high to low energy scales, spontaneous SUSY breaking has to occur at a certain scale. So far, the Large Hadron Collider failed to find direct evidence for supersymmetry and no meaningful signs of superpartners have been found¹. However, the total parameter space, consistent with supersymmetric extensions of the Standard Model, is extremely diverse and cannot be definitively ruled out at particle accelerators.

In the following sections, the main features of supersymmetry will be sketched without becoming too technical. The interested reader is advised to textbooks by Weinberg [103], West [104] and Kalka, Soff [105] as well as lecture notes by Wipf [106] and Bilal [107]. Note that technical and notational details of the specific models investigated in this thesis are summarized at the beginning of the respective chapters.

3.1 The Super-Poincaré Algebra

This section is devoted to the group-theoretic concepts of supersymmetry. As mentioned in the introduction of this chapter, the Poincaré group \mathcal{P} can only be extended to a Lie group \mathcal{G} in a trivial way via the direct product $\mathcal{G} = \mathcal{P} \otimes \mathcal{T}$, where \mathcal{T} denotes an internal symmetry group [102]. The only possible extended Lie algebra consists of the generators of the translations P_μ , the homogeneous Lorentz transformations $M_{\mu\nu}$ as well as the internal symmetry group I_k . Thereby, the finitely many generators I_k commute with the generators

¹For the CMSSM model, gluino and squark masses below the order of 10^3 GeV have been excluded by the ATLAS collaboration [16].

$P_\mu, M_{\mu\nu}$ and satisfy the Lie algebra

$$[P_\mu, I_k] = 0, \quad [M_{\mu\nu}, I_k] = 0, \quad [I_k, I_l] = ic_{kl}^m I_m. \quad (3.1)$$

In particular, they act on physical states via a multiplication with spin- and momentum independent Hermitian matrices. Hence, all particles of the irreducible multiplet of the internal symmetry group have equal spin and masses.

Now, how may we build a bridge to the aforementioned *super*-Poincaré algebra? This is done by the inclusion of additional fermionic generators transforming as spinors under the Lorentz group. Therefore, \mathcal{N} fermionic generator pairs Q_k^I, \bar{Q}_{Ik} with $k = 1, \dots, 2^{\lfloor \frac{d}{2} \rfloor}$, $I = 1, \dots, \mathcal{N}$ are introduced, transforming according to the $(1/2, 0)$ and $(0, 1/2)$ spinor representation of the Lorentz group, respectively. This integration of fermionic generators - also known as supercharges - corresponds to a non-trivial extension of the Poincaré algebra. It involves transformations between particles of different spin. For illustration, the super-Poincaré algebra of Minkowski space-time $\mathbb{R}^{1,3}$, containing ten bosonic generators $P_\mu, M_{\mu\nu}$ as well as four fermionic generator pairs (Majorana spinors) Q_I reads²

$$\begin{aligned} [P_\mu, Q_I] &= 0, & [M_{\mu\nu}, Q_I] &= (\Sigma_{\mu\nu})_I^J Q_J \\ \{Q_I, \bar{Q}_J\} &= 2(\gamma^\mu)_{IJ} P_\mu, & I, J &= 1, \dots, 4, \quad \mu, \nu = 0, \dots, 3. \end{aligned} \quad (3.2)$$

This super-Poincaré algebra represents a \mathbb{Z}_2 -graded rather than an ordinary Lie algebra and thus bypasses the Coleman-Mandula theorem. Grading thereby implies the vectorspace \mathfrak{g} of the algebra to be the direct sum $\mathfrak{g} = \mathfrak{g}_0 \oplus \mathfrak{g}_1$ of two vector subspaces \mathfrak{g}_0 and \mathfrak{g}_1 . The first subspace contains the ten bosonic generators $P_\mu, M_{\mu\nu}$ of the Poincaré group, whereas the second subspace is generated by the eight fermionic generators Q_I, \bar{Q}_I of the Lorentz group. The binary operation (Lie bracket) between two fermionic generators is given by the anticommutator. Contrary, two bosonic generators as well as a fermionic and a bosonic generator are linked via the commutator. Of course, this supersymmetric theory may be extended by finitely many generators of an internal symmetry group.

The super-Poincaré algebra contains the Poincaré algebra as a subalgebra and therefore any representation of the super-Poincaré algebra gives a representation of the Poincaré algebra. Hence, as each irreducible representation of the Poincaré algebra corresponds to a particle, each irreducible representation of the SUSY algebra corresponds to a superparticle. This superparticle, in turn, thus forms a collection of several ordinary particles - the *supermultiplet*.

Further basic properties of supersymmetry emerge from the above considerations. By regarding the anticommutator of the SUSY algebra (3.2), it follows that

$$\{Q_{I\alpha}, Q_{I\alpha}^\dagger\} = 2\text{Tr}(\gamma^\mu)_{II} P_\mu = 4H \quad (3.3)$$

²The matrix $\Sigma^{\mu\nu} = \frac{i}{4} [\gamma^\mu, \gamma^\nu]$ is a representation of the generators $M_{\mu\nu}$ on the four-component spinor fields.

with $\bar{Q} = Q^\dagger \gamma^0$ and the index I arbitrarily fixed. Hence, the anticommutator leads to the Hamiltonian H . Since the left hand side of (3.3) is strictly positive, the spectrum does not contain negative energy states. If $|0\rangle$ denotes the vacuum, the ground-state energy is vanishing if and only if $Q_I|0\rangle = Q_I^\dagger|0\rangle = 0$. Thus, any ground state with positive energy $E_0 > 0$ breaks supersymmetry. The translation invariance of the supercharges furthermore implies all particles within a multiplet of unbroken supersymmetry to have coinciding masses. Besides, a supermultiplet always contains an equal number of bosonic and fermionic degrees of freedom.

The fermions of the standard model are included in the so-called scalar multiplets. Their superpartners are bosons of spin zero, e.g. the selectron, smuon et cetera. Contrary, the gauge supermultiplet contains the bosons of the standard model, whose superpartners are given by spin 1/2 fermions³ - called gauginos.

The particle content regarded in this thesis is described by an $\mathcal{N} = 1$ scalar multiplet in various dimensions $d \leq 3$. It contains a real scalar field ϕ , a Majorana fermion ψ as well as a (pseudo-scalar) auxiliary field F . An action formed by the full multiplet (ϕ, ψ, F) is called *off-shell*, since its super-Poincaré algebra closes without taking into account the equations of motion. Contrary, if F has been integrated out, the action is said to be *on-shell*. Here, the SUSY algebra closes only when applying the equations of motion. Note that in both cases, the bosonic and fermionic degrees of freedom match.

3.2 The Concept of Superspace

In 1974, A. Salam and J. Strathdee introduced the concept of superspace [108]. Analogously to the manifestly Lorentz covariant formulation of relativistic theories, superspace represents a description of supersymmetric theories in a manifestly supersymmetric way. It is an extension of ordinary space-time via the inclusion of extra anticommuting coordinates - \mathcal{N} two-component Weyl spinors θ . Hence, usual d -dimensional space-time is extended by p fermionic Grassmann coordinates to $\mathbb{R}^{d|p}$ superspace. Similar to the super-Poincaré algebra, this vectorspace shows \mathbb{Z}_2 -grading since it consists of the vector subspaces \mathbb{R}^d and \mathbb{R}^p . Thus, the superspace coordinates (x, θ) form an abelian (the Lie-brackets of all elements vanish) Lie-superalgebra. Thereby, the anticommuting variables satisfy the Grassmann algebra $\{\theta^i, \theta^j\} = 0 \forall i, j$. Functions defined over the superspace are called *superfields*. They may be expanded in a finite Taylor series in the nilpotent Grassmann variables, where the corresponding coefficients form local fields over space-time and are called component fields.

An advantage of the superfield formulation is the automatic inclusion of the non-physical auxiliary fields, needed for the off-shell closure of supersymmetry⁴. In gauge theories, a

³Particles of spin 3/2 would be non-renormalizable.

⁴Unfortunately, the present knowledge of off-shell *extended* ($\mathcal{N} > 1$) supersymmetry is limited in the sense that for most theories of such a type these non-physical fields are unknown. The difficulties in finding such

further benefit is the incorporation of compensating fields, consisting entirely of gauge degrees of freedom. Such fields are used for an enlargement of the usual gauge transformations to an entire multiplet of transformations forming a representation of supersymmetry. In combination with the auxiliary fields, they allow the algebra to be field-independent. In general, superfields are highly reducible and the irreducible components may be found by imposing supersymmetric conditions on it, e.g. chirality or hermiticity conditions.

3.3 Spontaneous Supersymmetry Breaking

Generally speaking, there are two mechanisms of supersymmetry violation: explicit and spontaneous SUSY breaking.

Explicit SUSY breaking is characterized by Lagrangians containing explicit SUSY breaking terms. If such terms have positive mass dimension, they are of no relevance in the high energy limit and thus do not spoil the advantageous UV properties of supersymmetric theories. This is called soft SUSY breaking⁵ [109].

If the dynamics of the system is invariant under supersymmetry but the ground state does not respect the symmetry, *spontaneous* breaking occurs. According to the considerations of section 3.1, the ground-state energy E_0 is then lifted to positive values. In such vacua, one or several scalar fields acquire a vacuum expectation value (VEV) of the order of the SUSY breaking scale. Due to the experimental results showing no mass degeneracy in the elementary particle spectrum for energies up to 10^3 GeV, supersymmetry has to be spontaneously broken at energies below this scale. Thus, spontaneous supersymmetry breaking is an IR effect of long range fluctuations.

If a global⁶ symmetry is spontaneously broken, the Goldstone theorem predicts a massless mode, whose quantum numbers are related to the broken symmetry. Hence, spontaneous SUSY breaking is accompanied by the occurrence of a massless fermionic spin 1/2 excitation - the *goldstino* [110]. This mode mediates between the two degenerate ground states at $E_0 > 0$. For further reading on spontaneous SUSY breaking see e.g. the review and lecture notes by M. Dine and J. Mason [60], K. Intriligator and N. Seiberg [111] or Y. Shadmi and Y. Shirman [112].

auxiliary fields from superspace are due to the highly reducible character of the superfields.

⁵Soft SUSY breaking models often arise as low energy effective descriptions of theories showing spontaneous SUSY breaking.

⁶If a theory with local supersymmetry is considered, the goldstino is absorbed by the gravitino. More precisely, it gives the gravitino a mass by becoming its longitudinal component, similar to the Higgs mechanism.

3.4 Aspects of Supersymmetry from the FRG

Studying supersymmetric models within the framework of the FRG might give insight into one important issue: the *nature* of the spontaneous SUSY breaking mechanism. In globally supersymmetric theories, as examined within this thesis, supersymmetry is broken if the vacuum energy possesses any non-zero value $E_0 > 0$. The non-renormalization theorems⁷ state that, if supersymmetry is unbroken at tree level, it is unbroken to all orders of perturbation theory, since no corrections to the superpotential can be generated. However, such theorems do not hold beyond the perturbative level. So even if supersymmetry is unbroken at tree level, there might occur different sorts of quantum effects of a *non-perturbative* nature triggering SUSY breaking. This dynamical breaking mechanism, induced by non-perturbative, exponentially small corrections, has first been suggested by Witten in 1981 [21, 22]. The exponentially small corrections lead to a SUSY breaking scale m_s much smaller than the high energy scales (e.g. the Planck scale $m_P \sim 10^{19}$ GeV):

$$m_s = m_P e^{-c/g^2} \ll m_P, \quad (3.4)$$

where c is some constant and g denotes the small, dimensionless coupling constant employed in perturbative expansions. Aside, this mechanism might account for exponentially large hierarchies as e.g. $m_H/m_P \sim 10^{-17}$.

⁷For details and a derivation of the perturbative non-renormalization theorems see e.g. [103], section 27.6.

Chapter 4

Supersymmetric Quantum Mechanics

Supersymmetric quantum mechanics (SUSY-QM) has first been formulated by H. Nicolai [113] in 1976 in connection with his search for supersymmetry in non-relativistic quantum systems. In particular, Nicolai intended to extend supersymmetry to the realm of statistical physics. Later on, E. Witten [21, 22] utilized SUSY-QM in order to understand spontaneous SUSY breaking within a simple, non-relativistic setting rather than within the complex background of supersymmetric gauge theories.

In fact, SUSY-QM created new areas of research and delivered new insight into quantum mechanics itself. As an example, it allows for a much simpler solution of the hydrogen atom¹. More general, SUSY-QM provides a very generic class of solutions to so-called shape-invariant potentials, see e.g. [115]. Besides, the concept of SUSY-QM has given useful extensions to the WKB approximation [116] and has been applied to non-quantum statistical mechanics via the Fokker-Planck equation [117]. Also, in the area of mathematical physics, SUSY-QM allows for proving index theorems for physically interesting differential operators [118].

In this chapter, $\mathcal{N} = 1$ SUSY-QM as a simple $1 + 0$ -dimensional supersymmetric field theory is examined using the functional renormalization group approach. Thereby, the main object of interest are the energies of the low lying states. Since it is possible to compute the energy spectrum by diagonalizing the Hamiltonian within numerical precision, this offers the opportunity to directly test the FRG as a non-perturbative tool. These investigations should also be regarded as a completion of corresponding lattice studies, see e.g. [119–121]. As supersymmetry involves spacetime translations, a discretization of the latter goes along with a complete loss of supersymmetry². Thus, non-perturbative continuum methods preserving supersymmetry manifestly provide ideal technical requirements for investigating SUSY in the strong coupling regimes.

$\mathcal{N} = 1$ SUSY-QM has been previously studied via the FRG by A. Horikoshi et al. [122] and M. Weyrauch [123]. Both works showed, that the non-perturbative renormalization

¹Interestingly, E. Schrödinger already noticed in 1941 certain symmetry features of solutions to his equation and showed how the Hamiltonian for the hydrogen atom may be factorized [114].

²For models with extended ($\mathcal{N} > 1$) supersymmetry, a partial restoration of SUSY may be achieved.

group is capable of describing spontaneous SUSY breaking. Horikoshi et al. evaluated the ground-state energy as well as the energy gap of anharmonic oscillators by solving the Wegner-Houghton equation in the local potential approximation (LPA). They found good agreement for the energies in regions, where quantum tunnelling is of minor importance. Weyrauch employed the Wetterich as well as the Schwinger proper time renormalization group equation (PTRG) in order to study SUSY-QM. He also extended the truncation by the inclusion of a wave-function renormalization and verified a further improvement of the results in this order. However, since both works rely on SUSY-breaking regulators, a distinction between spontaneous and explicit SUSY breaking is hardly possible³.

The first studies including a supersymmetry-preserving regularization have been done by F. Synatschke-Czerwonka et al. [47]. They also included a running wave-function renormalization and found satisfactory results in the regime, where the non-convexity of the classical potential remains small. However, spontaneous SUSY breaking has not been considered there.

The subsequent considerations tackle both issues: Firstly, the Wetterich equation is elaborated in a manifestly supersymmetric formulation for all scales k including a supersymmetric regularization. Secondly, spontaneous breaking of SUSY is examined within this setting. The truncation of the exact RG equation is thereby extended to forth-order in the supercovariant derivative expansion in order to test the convergence properties of this approximation scheme. The results presented in this chapter are published in [56].

It is organized as follows: First, the model and notational conventions are described. Then, the method of truncation as well as the specific regularization are introduced. Within this setting, the flow equations are derived in next-to-next-to-leading order (NNLO) in the supercovariant derivative expansion. The effective potential and the first excited energies for unbroken SUSY are presented all the way from weak to strong couplings including the regimes where tunnelling effects become important. Lastly, spontaneous SUSY breaking is investigated in next-to-leading order (NLO) in the supercovariant derivative expansion.

4.1 Introducing the Model

The superspace formalism [108] as elucidated already in section 3.2 is employed in order to derive the flow equations for SUSY-QM. Firstly, the Euclidean superfield $\Phi(\tau, \theta, \bar{\theta})$ as a function over $\mathbb{R}^{1|2}$ superspace is defined. The finite Taylor expansion of Φ in the constant, anticommuting Grassmann variables θ and $\bar{\theta}$ reads

$$\Phi(\tau, \theta, \bar{\theta}) = \phi(\tau) + \bar{\theta}\psi(\tau) + \bar{\psi}\theta(\tau) + \bar{\theta}\theta F(\tau). \quad (4.1)$$

³In non-supersymmetric systems, the regulators of bosons and fermions do not have to be related in any way. Contrary, in SUSY systems, they are related by supersymmetry. Only then, spontaneous SUSY-breaking effects are disentangled from explicit supersymmetry breaking.

The component fields as the corresponding expansion coefficients are: the scalar field ϕ , the auxiliary field F as well as the fermionic fields ψ and $\bar{\psi}$. Thus, the two bosonic degrees of freedom comply with the two fermionic degrees. The superpotential $W(\Phi)$ represents a function of the superfield and its expansion in Grassmann variables yields

$$W(\Phi) = W(\phi) + (\bar{\theta}\psi + \bar{\psi}\theta)W'(\phi) + \bar{\theta}\theta(FW'(\phi) - W''(\phi)\bar{\psi}\psi). \quad (4.2)$$

The one-dimensional equivalent of the four-dimensional Super-Poincaré algebra contains only translations of Euclidean time. It is generated by $\mathcal{N} = 1$ pair of conserved nilpotent fermionic supercharges

$$Q = i\partial_{\bar{\theta}} + \theta\partial_{\tau} \quad \text{and} \quad \bar{Q} = i\partial_{\theta} + \bar{\theta}\partial_{\tau}. \quad (4.3)$$

They anticommute to the super-Hamiltonian H and commute with translations. Therefore, the quantum mechanical counterpart of the Super-Poincaré algebra (3.2) reads

$$\{Q, \bar{Q}\} = 2i\partial_{\tau} = 2H, \quad [H, Q] = [H, \bar{Q}] = 0. \quad (4.4)$$

Now, consider the global supersymmetry transformation

$$(\tau, \theta, \bar{\theta}) \longrightarrow (\tau', \theta', \bar{\theta}') = (\tau + \bar{\epsilon}\theta + \bar{\theta}\epsilon, \theta - i\epsilon, \bar{\theta} + i\bar{\epsilon}), \quad (4.5)$$

where $\epsilon, \bar{\epsilon}$ denote the constant, fermionic transformation parameters. This transformation is communicated to the level of the superfields via $\Phi \rightarrow \Phi + \delta_{\epsilon}\Phi$, where $\delta_{\epsilon} = \bar{\epsilon}Q - \epsilon\bar{Q}$. Consequently, the SUSY variations act on the superfield according to

$$\begin{aligned} \delta_{\epsilon}\Phi &= \delta\tau\partial_{\tau}\Phi + \delta\theta\partial_{\theta}\Phi + \delta\bar{\theta}\partial_{\bar{\theta}}\Phi \\ &= \bar{\epsilon}(i\psi + i\theta F + \theta\dot{\phi} - \bar{\theta}\theta\dot{\psi}) - (i\bar{\psi} + i\bar{\theta}F - \bar{\theta}\dot{\phi} + \bar{\theta}\theta\dot{\bar{\psi}})\epsilon. \end{aligned} \quad (4.6)$$

From (4.6), the transformation rules

$$\delta\phi = i\bar{\epsilon}\psi - i\bar{\psi}\epsilon, \quad \delta\psi = (\dot{\phi} - iF)\epsilon, \quad \delta\bar{\psi} = \bar{\epsilon}(\dot{\phi} + iF), \quad \delta F = -\bar{\epsilon}\dot{\psi} - \dot{\bar{\psi}}\epsilon \quad (4.7)$$

of the component fields are inferred. Here and in the following, a dot denotes differentiation with respect to τ . The supercovariant derivatives, required for constructing a supersymmetric action, are $D = i\partial_{\bar{\theta}} - \theta\partial_{\tau}$ and $\bar{D} = i\partial_{\theta} - \bar{\theta}\partial_{\tau}$. They obey the anticommutation relations $\{D, D\} = \{\bar{D}, \bar{D}\} = 0$, $\{D, \bar{D}\} = -2H$ and anticommute with the supercharges. Using the

above definitions allows for modelling the supersymmetric Euclidean *off-shell action*

$$\begin{aligned} S_{\text{off}}[\phi, F, \bar{\psi}, \psi] &= \int d\tau d\theta d\bar{\theta} \left[-\frac{1}{2} \Phi K \Phi + iW(\Phi) \right] \\ &= \int d\tau \left[\frac{1}{2} \dot{\phi}^2 - i\bar{\psi} \dot{\psi} + iFW'(\phi) - iW''(\phi) \bar{\psi} \psi + \frac{1}{2} F^2 \right], \end{aligned} \quad (4.8)$$

where $K = 1/2(\bar{D}D - D\bar{D})$ denotes the kinetic operator. Here, a prime means derivation with respect to the scalar field ϕ . Eliminating the auxiliary field F by its equation of motion, $F = -iW'$ yields the *on-shell action*

$$S_{\text{on}}[\phi, \psi, \bar{\psi}] = \int d\tau \left[\frac{1}{2} \dot{\phi}^2 - i\bar{\psi} \dot{\psi} + \frac{1}{2} W'^2(\phi) - iW''(\phi) \bar{\psi} \psi \right]. \quad (4.9)$$

The interactions in (4.9) are given by the bosonic “classical” potential $V(\phi) = \frac{1}{2} W'^2(\phi)$ and the Yukawa term $W'' \bar{\psi} \psi$.

As pointed out in section 3.1, the ground-state energy E_0 vanishes, if SUSY is unbroken. This, in turn, requires the supercharges Q and \bar{Q} to annihilate the vacuum. Since the ground-state energy is given by the minimum of the effective potential, a correlation of spontaneous SUSY breaking and the superpotential $W(\phi)$ is suggestive. More precisely, it can be shown that spontaneous SUSY breaking is linked to the asymptotic behaviour⁴ of the superpotential $W(\phi)$. Let us assume $W(\phi)$ to be a polynomial in the scalar field. Then, if n is even, supersymmetry will be intact on all scales. The simplest non-trivial even superpotential is given by

$$W(\phi) = e\phi + \frac{m}{2} \phi^2 + \frac{g}{3} \phi^3 + \frac{a}{4} \phi^4 \quad (4.10)$$

and will be considered in section 4.3. Note that $W(\phi)$ represents the *microscopic* initial potential of our quantum system before fluctuations are taken into account. If n is odd, the effective potential exhibits a ground state with positive energy and supersymmetry is spontaneously broken, even if we may start with a microscopic potential with vanishing ground-state energy. This applies e.g. to cubic classical superpotentials of the form

$$W(\phi) = e\phi + \frac{g}{3} \phi^3, \quad e < 0, \quad g > 0, \quad (4.11)$$

which are examined in detail in section 4.4. The energy gap between the ground-state energy E_0 and the first excited energy E_1 can be extracted either from the pole of the IR propagator at the minimum of the effective potential or from the exponential decay of the correlator.

⁴For details and derivations, see e.g. [124], section 3.3.3.

4.2 Supersymmetric Renormalization Group Flow

In order to analyse supersymmetric quantum mechanical systems, it is resorted to Wilsonian renormalization group techniques as explained in chapter 2. According to section 2.2, the effective average action Γ_k obeys the exact functional differential equation (2.13). In $\mathbb{R}^{1|2}$ superspace, this evolution equation reads

$$\partial_k \Gamma_k = \frac{1}{2} \int dz dz' \partial_k R_k(z, z') G_k(z', z), \quad G_k = (\Gamma_k^{(2)} + R_k)^{-1}, \quad (4.12)$$

where $z = (\tau, \theta, \bar{\theta})$ denote the superspace coordinates. The second functional derivative with respect to the superfield is given by

$$(\Gamma_k^{(2)})(z, z') = \frac{\overrightarrow{\delta}}{\delta\Phi(z)} \Gamma_k \frac{\overleftarrow{\delta}}{\delta\Phi(z')}. \quad (4.13)$$

Note that the supertrace in (4.12) as well as the right- and left-derivatives in (4.13) take care of the minus signs for anticommuting fields.

4.2.1 Supercovariant Derivative Expansion

According to the reasoning of section 2.3, an exact solution of (4.12) is not possible in general. Hence, a restriction of Γ_k in theory space has to be performed. Thereby, the scale dependent action is confined to a functional of certain classes of operators. Here, an expansion of Γ_k in operators with an increasing number of supercovariant derivatives D and \bar{D} is selected - an expansion scheme of intrinsically non-perturbative character.

Unfortunately, this systematic and consistent expansion scheme of Γ_k does not guarantee convergence. One goal of the present work is to demonstrate convergence of the supercovariant derivative expansion at NNLO for numerically known values of observables. Therefore, the flow equation in the off-shell formulation with a manifestly supersymmetric regulator is derived such that in each order of the supercovariant derivative expansion the flow preserves supersymmetry.

First of all, the most general ansatz for Γ_k in NNLO has to be constructed. This ansatz, including operators containing at most four supercovariant derivatives, reads

$$\Gamma_k[\Phi] = \int dz \left[i W_k(\Phi) - \frac{1}{2} Z_k(\Phi) K Z_k(\Phi) + \frac{i}{4} Y_{1,k}(\Phi) K^2 \Phi + \frac{i}{4} Y_{2,k}(\Phi) (K\Phi)^2 \right], \quad (4.14)$$

with the scale and field dependent functions $W_k, Z_k, Y_{1,k}$ and $Y_{2,k}$ and the kinetic operator K as introduced in section 4.1. In the limiting case, where $Z_k(\Phi) = \Phi$ and $Y_{2,k}(\Phi) = Y_{1,k}(\Phi) = 0$, only the superpotential is allowed to carry a scale-dependence. This is the so-called *local potential approximation* (LPA). In NLO, the restriction $Z_k(\Phi) = \Phi$ is lifted and an arbitrary

additional scale-dependent wave-function renormalization $Z_k(\Phi)$ is admitted.

By integrating out the Grassmann variables, the action (4.14) becomes a functional of the corresponding component fields. It then takes the form⁵

$$\begin{aligned} \Gamma_k[\Phi] = \int d\tau & \left[\frac{1}{2} Z'^2 \dot{\phi}^2 - i Z'^2 \bar{\psi} \dot{\psi} - \frac{i}{2} (Y'_1 + Y_2) \dot{\bar{\psi}} \dot{\psi} - i (W'' + Z' Z'' \dot{\phi} - \frac{1}{2} Y_1'' \ddot{\phi} - \frac{1}{4} Y_1''' \dot{\phi}^2) \bar{\psi} \psi \right. \\ & + \left(i W' - Z' Z'' \bar{\psi} \psi - \frac{i}{2} (Y'_1 + Y_2) \ddot{\phi} - \frac{i}{4} Y_1'' \dot{\phi}^2 + \frac{1}{2} Y_2' (\bar{\psi} \dot{\psi} - \dot{\bar{\psi}} \psi) \right) F \\ & \left. + \left(\frac{1}{2} Z'^2 - \frac{i}{4} Y_2'' \bar{\psi} \psi \right) F^2 + \frac{i}{4} Y_2' F^3 \right], \end{aligned} \quad (4.15)$$

where the terms are ordered according to increasing powers of the auxiliary field F . It should be emphasized that the supercovariant derivative expansion is not an expansion in momenta. Thus, by inspecting (4.15), it is apparent that each order of truncation contains contributions of vanishing momenta. This fact may be utilized in order to gain the flow equations for the couplings in a simple way. The truncation scheme (4.14) rather corresponds to an expansion in the auxiliary field F . Thus, the LPA includes terms up to linear powers in F . The NLO approximation contains contributions up to F squared and the NNLO truncation terms up to F cubed.

4.2.2 Choosing the Regulator Functional

The flow of Γ_k is regularized by adding a suitable regulator functional $\Delta S_k[\Phi]$ to the action, in such a way that $R_k = \Delta S_k^{(2)}$. Following [47, 48, 50], the most general off-shell supersymmetric cutoff action (quadratic in the superfields) is of the form

$$\Delta S_k = \frac{1}{2} \int dz \Phi R_k(D, \bar{D}) \Phi. \quad (4.16)$$

As D and \bar{D} satisfy the anticommutation relation $\{D, \bar{D}\} = -2i\partial_\tau$, it can be written as

$$\Delta S_k = \frac{1}{2} \int dz \Phi \left[i r_1(-\partial_\tau^2, k) - Z'^2(\bar{\Phi}) r_2(-\partial_\tau^2, k) K \right] \Phi, \quad (4.17)$$

where Z' is evaluated at the background field $\bar{\Phi} = \bar{\phi}$. Hence, R_k is given by⁶

$$R_k(q, q', \theta, \theta') = \left[i r_1(q^2, k) - Z'^2(\bar{\phi}) r_2(q^2, k) K(q, \theta) \right] \delta(q, q') \delta(\theta, \theta') \quad (4.18)$$

in momentum space. The regulator function r_1 with mass dimension one acts like an additional momentum-dependent mass and ensures a gap $\sim k$ for the IR modes. Note that this regulator function is not spectrally adjusted via an overall multiplication with the wave

⁵Here, the index k as well as the explicit dependence of the scalar functions $W_k, Z_k, Y_{1,k}$ and $Y_{2,k}$ on the scalar field ϕ have been omitted.

⁶We abbreviate $\delta(\theta, \theta') := \delta(\bar{\theta} - \bar{\theta}') \delta(\theta - \theta')$.

function renormalization as performed in [47]. Coupling the wave-function renormalization to the mass-like regulator r_1 would rather artificially slow down the flow of the higher order operators Z, Y_1, Y_2 and thus degrade the convergence of the flow. The dimensionless regulator function r_2 can be viewed as a deformation of the momentum dependence of the kinetic term. The term $q^2 r_2(q^2/k^2)$ represents the supersymmetric analogue of the corresponding regulator function $r_k(q^2/k^2)$ in scalar field theory [125]. Here, a spectral adjustment via the inclusion of the wave function renormalization $Z'(\bar{\Phi})$ is helpful in order to provide a simple form for the flow of Γ_k [88]. However, the influence of the spectral adjustment of r_2 on the flow of Γ_k should be checked carefully.

4.2.3 Flow Equations

This section explains the derivation of the flow of Γ_k . More precisely, four partial differential equations (PDE's) for the functions $W_k, Z_k, Y_{1,k}$ and $Y_{2,k}$ have to be deduced. To begin with, the second functional derivative of Γ_k as defined in (4.13) has to be determined in order to derive its flow according to (4.12). This leads to the inverse propagator⁷

$$\begin{aligned} (\Gamma_k^{(2)} + R_k)(z, z') = & \left[i(W'' + r_1) - Z''(KZ) - Z'KZ' - Z'(\bar{\Phi})^2 r_2 K + \frac{i}{4} \left\{ Y_1''(K^2 \Phi) \right. \right. \\ & \left. \left. + Y_1' K^2 + K^2 Y_1' + Y_2''(K\Phi)^2 + 2Y_2'(K\Phi)K + 2KY_2'(K\Phi) + 2KY_2 K \right\} \right] \delta(z, z'). \end{aligned} \quad (4.19)$$

Note that the scale dependent functions W, Z, Y_1, Y_2 are functions of the superfield $\Phi(z)$, whereas the scale dependent $Z'(\bar{\Phi})$ has the background field as argument. Here, a bracket implies that the kinetic operator K only acts within the bracket. If there is no bracket, then it acts on everything to its right.

As indicated in section 4.2.1, supersymmetry allows for an advantageous projection scheme. In particular, the flow of the scalar functions $W'(\phi), Z'(\phi)$ and $Y_2'(\phi)$ may be derived via a projection onto the “purely bosonic” coefficients of F, F^2 and F^3 in (4.15) for constant (i.e. momentum independent) fields. Hence, it suffices to consider time-independent component fields in (4.19) and set $\bar{\psi} = \psi = 0$ afterwards. Switching to momentum space, the inverse propagator (4.19) then takes the form

$$\begin{aligned} (\Gamma_k^{(2)} + R_k)(q, q', \theta, \theta') = & \left[\left(i(W'' + r_1) + Z'Z''F + \frac{i}{2}(Y_1' + Y_2')q^2 + \frac{i}{4}Y_2''F^2 \right) \delta(\theta, \theta') \right. \\ & + \left(iW'''F + (Z'Z''' + Z''^2)F^2 + Bq^2 + \frac{i}{4}Y_2'''F^3 + i\left(\frac{1}{2}Y_1'' + Y_2'\right)Fq^2 \right) \bar{\theta}\theta\bar{\theta}'\theta' \\ & \left. + \left(B + \frac{3}{2}iFY_2' \right) + \left(B + iFY_2' \right) q(\bar{\theta}'\theta - \bar{\theta}\theta') + \left(Z'Z''F + \frac{i}{2}Y_2''F^2 \right) (\bar{\theta}\theta + \bar{\theta}'\theta') \right] \delta(q, q'), \end{aligned} \quad (4.20)$$

⁷The functional derivative with respect to the superfields is defined such that $\int dz \frac{\delta \Phi(z)}{\delta \Phi(z')} = \int dz \delta(z, z') = 1$, where $\delta(z, z') := \delta(\tau, \tau')\delta(\theta, \theta')$.

where the background field enters via $B = Z'^2 + r_2 Z'^2(\bar{\phi})$. The Greens function in superspace, $G_k = (\Gamma_k^{(2)} + R_k)^{-1}$, is determined by

$$\int \frac{dq'}{2\pi} d\theta' d\bar{\theta}' G_k^{-1}(q, q', \theta, \theta') G_k(q', q'', \theta', \theta'') = \delta(q, q'') \delta(\theta, \theta''). \quad (4.21)$$

This implies the Greens function to be of the general form

$$G_k(q, q', \theta, \theta') = (a + b \bar{\theta}\theta + c \bar{\theta}'\theta' + d \bar{\theta}\theta' + e \bar{\theta}'\theta + f \bar{\theta}\theta\bar{\theta}'\theta') \delta(q, q'). \quad (4.22)$$

The ansatz (4.22) represents a finite expansion in the Grassmann variables. Of course, the expansion coefficients are functions of the scalars appearing in (4.20) and the momentum q . Solving equation (4.21) leads to the coefficients (a, b, c, d, e, f) , whose specific structure is given in (A.3), appendix A. Finally, the flow of Γ_k , projected onto its time-independent, bosonic part is given by

$$\begin{aligned} \partial_k \Gamma_k |_{\dot{\phi}=\dot{F}=\dot{\psi}=\dot{\bar{\psi}}=0} &= \int d\tau \left(i \partial_k W' F + \frac{1}{2} \partial_k Z'^2 F^2 + \frac{i}{4} \partial_k Y_2' F^3 \right) \\ &= \frac{1}{2} \int \frac{dq}{2\pi} \frac{dq'}{2\pi} d\theta d\bar{\theta} d\theta' d\bar{\theta}' (\partial_k R_k)(q', q, \theta', \theta) G_k(q, q', \theta, \theta') \\ &= \frac{1}{2} \int d\tau \frac{dq}{2\pi} \left[i(\partial_k r_1)(b + c + d + e) + \partial_k (r_2 Z'^2(\bar{\phi})) (f + a q^2 - e q + d q) \right]. \end{aligned} \quad (4.23)$$

By extracting the coefficients of F, F^2 and F^3 on the right hand side of (4.23), the flow equations for W', Z' and Y_2' are obtained. Their explicit form is comprised in (A.5) and (A.6) in appendix A.

However, the system of partial differential equations is not yet closed as the flow of Y_1 is missing. Since Y_1 couples solely to time-dependent terms, c.f. (4.15), a different projection scheme has to be applied here. To derive the evolution of Y_1 , the right hand side of the Wetterich equation is projected onto $\dot{F}\dot{\phi}$, delivering the flow of $Y_1'(\phi) + Y_2(\phi)$. This requires an expansion of the inverse propagator around field configurations of F and ϕ exhibiting a small momentum dependence. The calculation follows quite analogously the procedure applied in scalar $O(N)$ models [125, 126]. Again, only the bosonic part of the superfield in the inverse propagator is considered and the fermionic fields ψ and $\bar{\psi}$ are set to zero. In detail, the background field configurations

$$\begin{aligned} \phi(p) &= \phi \delta(p) + \delta\phi(p) (\delta(p - Q) + \delta(p + Q)) \quad \text{and} \\ F(p) &= F \delta(p) + \delta F(p) (\delta(p - Q) + \delta(p + Q)) \end{aligned} \quad (4.24)$$

in momentum space are chosen with small fluctuations $\delta\phi(p) \ll \phi, \delta F(p) \ll F$. Note that $\phi(p) = \phi^*(-p)$ is real and $F(p) = -F^*(-p)$ purely imaginary. An insertion of the above

configurations (4.24) into the ansatz (4.15) for Γ_k yields

$$\frac{i}{2}(Y'_1 + Y_2) = \frac{1}{\Omega} \lim_{Q^2 \rightarrow 0} \frac{\partial}{\partial Q^2} \frac{\delta^2 \Gamma_k}{\delta(\delta\phi(Q))\delta(\delta F(-Q))} \Big|_{\phi, F=\psi=\bar{\psi}=\delta F=\delta\phi=0}, \quad (4.25)$$

where Ω denotes the total volume of “space” and should be taken to infinity at the end. Thus, according to (4.25), all terms quadratic in the mixed fluctuations have to be considered by evaluating the right hand side of the Wetterich equation. The detailed calculation is presented in appendix A.

Finally, four flow equations may be simplified via the redefinitions

$$Y := Y'_2 \quad \text{and} \quad X := Y'_1 + Y_2. \quad (4.26)$$

Hence, it remains to solve for the evolution of the four scale and field dependent functions W' , Z' , X and Y . The subsequent sections of this chapter discuss and examine the solutions to the obtained flow equations for specific initial UV conditions and adequately chosen regulator functions.

4.3 Unbroken Supersymmetric Quantum Mechanics

This section comprehends the examination of quantum mechanical systems with unbroken supersymmetry. In particular, two physical quantities will be of importance here: the effective potential V_{eff} and the first excited energy state E_1 . In order to analyse those effective quantities, the PDEs for W' , Z' , Y and X as derived in the previous section have to be solved. This requires a specification of the regulator functions r_1 and r_2 in (4.18). *Supersymmetric* quantum mechanics is free from UV divergences. Ergo the IR regularization comes to the fore. It is therefore intuitive and sufficient to consider only the regulator r_1 guaranteeing a gap $\sim k$ for the IR modes by setting⁸ $r_2 = 0$. The simplest choice is given by the Callan-Symanzik regulator

$$r_1(q^2, k) = k \quad (4.27)$$

which will be selected here. By inserting (4.27) into the flow equations, the momentum integration can be performed analytically. This yields the flow

$$\partial_k W'(\phi) = \frac{Z' \mathcal{W}''^2 (X' Z' + 4X Z'') - \mathcal{W}''' Z' (3\mathcal{W}'' X + Z'^4)}{4\mathcal{W}''^2 (2\mathcal{W}'' X + Z'^4)^{3/2}}, \quad \mathcal{W}'' = W'' + k \quad (4.28)$$

of the superpotential $W'(\phi)$. The remaining flow equations are not given here explicitly as the expressions are quite long. Note that the right hand side of the flow equations depends

⁸This directly implies the flow equations to be independent of the background field as introduced in (4.17), since the latter couples only to r_2 .

on the superpotential only via W'' and W''' .

The corresponding microscopic action in the UV is given by (4.9). As this section is devoted to the analysis of unbroken SUSY-QM, the focus is laid on quartic classical superpotentials of the form (4.10). By choosing such quartic superpotentials, supersymmetry is expected to be unbroken for all scales $k \in [0, \Lambda]$. Thus, the initial conditions at the UV cutoff $k = \Lambda$ read

$$W'_\Lambda(\phi) = e + m\phi + g\phi^2 + a\phi^3, \quad Z'_\Lambda(\phi) = 1, \quad Y_\Lambda(\phi) = X_\Lambda(\phi) = 0. \quad (4.29)$$

In SUSY-QM, the fluctuations in the UV are suppressed and the flow freezes out for $k \rightarrow \Lambda \rightarrow \infty$. Hence, the initial conditions are stable for large UV-cutoffs. Indeed, plugging (4.29) into the flow equations yields

$$\partial_k W'|_\Lambda = \mathcal{O}(\Lambda^{-2}), \quad \partial_k Z'|_\Lambda = \mathcal{O}(\Lambda^{-4}), \quad \partial_k X|_\Lambda = \mathcal{O}(\Lambda^{-5}), \quad \partial_k Y|_\Lambda = \mathcal{O}(\Lambda^{-6}). \quad (4.30)$$

Note that the initial superpotential W_Λ becomes non-convex for $g^2 > 3ma$.

The set of the four coupled partial differential equations for W', Z', X, Y is solved numerically with *spectral methods* [127, 128]. More precisely, it is solved by the use of Chebyshev polynomials as basis in the domain where the flowing potential becomes flat or concave and rational Chebyshev functions in regions showing a convex potential. For the RG evolution, another Chebyshev spectralization has been applied. This procedure allows for constructing *global solutions* to the truncated flow equations with unmatched numerical accuracy. Appendix B gives further details on spectral methods.

Besides, the calculations have been cross-checked via the implicit Runge-Kutta method of `NDSolve` of *Mathematica* 9. Here, the scalar field has been limited to the region $\phi \in (-100, 100)$. Furthermore, the four functions are kept at their classical values at the boundary for all scales as the flows vanish for $|\phi| \rightarrow \infty$. Both methods deliver agreeing results for physical quantities. For example, the first excited energies coincide to three significant digits, c.f. section 4.3.2.

A solution to the flow equations for initial conditions (4.29) with $(e, m, g, a) = (1, 1, 1.8, 1)$ in the large coupling regime is illustrated in figures 4.1 and 4.2. Besides, the following deviation of the solutions at $k = 0$ from their classical values (4.29) at $k = \Lambda$ is inferred for large values of $|\phi|$:

$$W'_0 - W'_\Lambda \sim \frac{1}{2\phi}, \quad Z'_0 - Z'_\Lambda \sim \frac{1}{12\phi^4}, \quad X_0 - X_\Lambda \sim \frac{1}{18\phi^6}, \quad Y_0 - Y_\Lambda \sim -\frac{1}{9\phi^7}. \quad (4.31)$$

As expected, the higher-order operators show a faster decay for large field values, see figures 4.1 and 4.2.

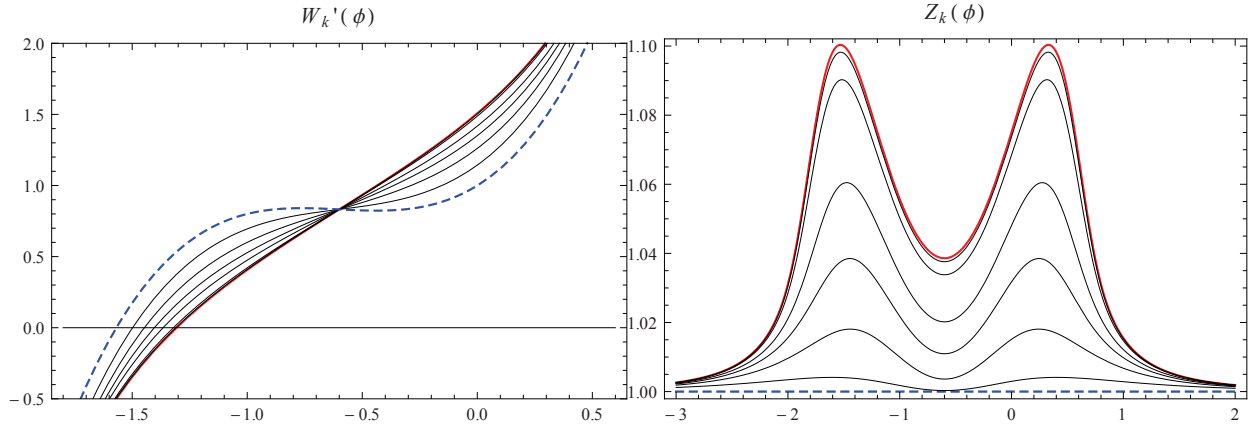


Figure 4.1: The superpotential $W'_k(\phi)$ and the wave function renormalization $Z'_k(\phi)$ for different scales k . Starting in the UV at $k = \Lambda = 10^4$ (blue, dashed line) the flow evolves to the IR at $k = 0$ (red solid line). The intermediate scales are $k = 5, 2, 1, 0.5, 0.1, 0.02$.

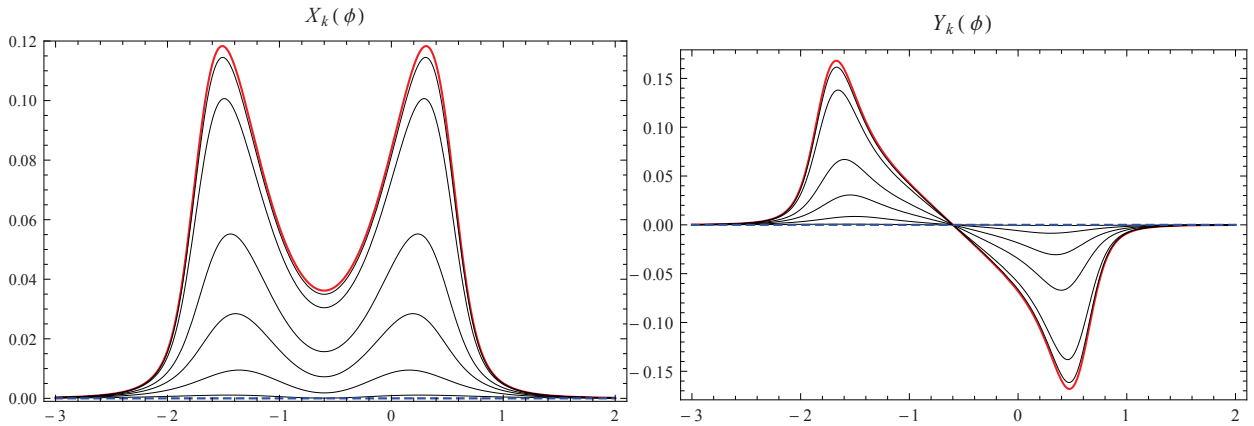


Figure 4.2: The flow of the fourth-order couplings $X_k(\phi), Y_k(\phi)$ for different scales k . Starting in the UV at $k = \Lambda = 10^4$ (blue, dashed line) the flow evolves to the IR at $k = 0$ (red solid line). The intermediate scales are $k = 5, 2, 1, 0.5, 0.1, 0.02$

4.3.1 Effective Potential

This section takes a closer look at the bosonic on-shell effective potential $V_{\text{eff}} = V_{k=0}$. As the ground-state energy E_0 is given by the minimum of V_{eff} , the effective potential delivers information about spontaneous SUSY breaking. The scale-dependent effective average potential, denoted by V_k , is computed by considering the truncated action (4.15) for vanishing fermionic fields. Next, the auxiliary field is eliminated by inserting its equation of motion

$$F = -\frac{2i}{3Y} \left(\sqrt{Z'^4 + \frac{3}{4}(4W' - 2X\ddot{\phi} - (X' - Y)\dot{\phi}^2)Y - Z'^2} \right). \quad (4.32)$$

Contrary to the NLO approximation, where $X = Y = 0$, the auxiliary field becomes dynamical in NNLO in the derivative expansion. Next, the equation of motion (4.32) is inserted into the truncated action (4.15). It suffices then to consider $\Gamma_k[\phi]$ for $\phi = \text{const.}$ in

order to extract V_k , yielding

$$V_k(\phi) = \frac{2}{27Y^2} \left(\sqrt{3W'Y + Z'^4} - Z'^2 \right) \left(6W'Y + Z'^4 - Z'^2 \sqrt{3W'Y + Z'^4} \right). \quad (4.33)$$

Let $\phi = \text{const.}$ be a solution of the effective equation $\delta\Gamma[\phi]/\delta\phi = 0$. Then, this is equivalent to $\partial V_{\text{eff}}(\phi)/\partial\phi = 0$, providing the minimum value of the effective potential.

How does the bosonic potential, floating with the energy scale k , look like? Figure 4.3

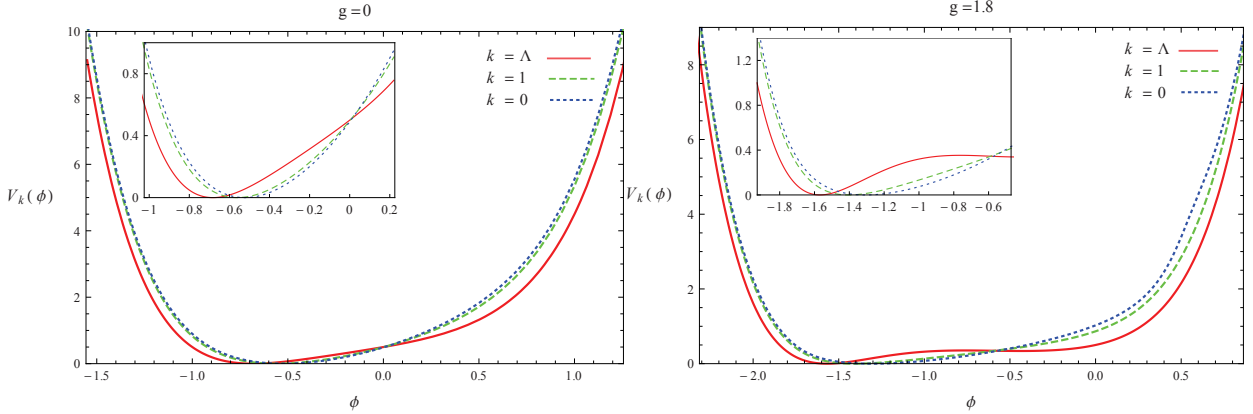


Figure 4.3: Flow of the effective average potential $V_k(\phi)$ as obtained by solving the system of PDEs numerically in NNLO in the derivative expansion with initial conditions (4.29), where $e = m = a = 1$ and $g = 0$ (left panel) and $g = 1.8$ (right panel).

gives an impression of $V_k(\phi)$, where the classical potential has been chosen to be of the form $W'_\Lambda(\phi) = 1 + \phi + g\phi^2 + \phi^3$ with $g = 0$ and $g = 1.8$. As expected, the minimum value of V_k is zero for all scales. Thus the ground-state energy vanishes and supersymmetry remains intact on all scales. Apparently, non-convexities appearing in the classical potential diminish as more and more long-range quantum fluctuations are taken into account. Hence, the running potentials in figure 4.3 approach their convex form in the IR limit. However, it should be noted that the structure of the flow equation (2.12) forces rather the superpotential than the scalar potential to become convex in the IR. Since the scalar potential is a complicated function of W', Z, Y , i.e. of the form (4.33), the flow equation does not immediately imply $V_{k \rightarrow 0}$ to be convex.

Interestingly, the scale-dependent potential V_k becomes complex for couplings $g \gtrsim 2$ and scales smaller than some $k_0 > 0$. This behaviour occurs for field values close to the local minimum of W'_Λ . Technically, it is due to the expression $\sqrt{3W'Y + Z'^4}$ appearing in (4.33) which becomes complex near the local minimum of W'_Λ for non-convex initial potentials, owing to an increasingly negative Y with decreasing scale k ; see also figure 4.2, right panel. This leads to the conclusion that the effective average potential acts like an indicator of the validity of the used approximation scheme. The running potential shows the NNLO approximation to break down at large couplings $g \gtrsim 2$ by becoming complex. Note that the poles of the propagator also deliver important information about the quality of the

approximation. This issue is discussed in the next section.

4.3.2 First Excited Energy

The energy of the first excited state E_1 can be calculated by considering the effective propagator $G_{k=0}$. Unbroken supersymmetry implies V_k to vanish at its minimum ϕ_{\min} or equivalently $W'_k(\phi_{\min}) = 0$ according to (4.33). Actually, in the strong coupling regime there exists a second solution for which $[4W'(Y + Z'^4)](\phi_{\min}) = 0$. However, we believe this solution to be non-physical as explained later on. For a constant ϕ_{\min} , the auxiliary field F in (4.32) vanishes if $W'_k(\phi_{\min}) = 0$. Thus, the excited energies E_1 are determined by considering the propagator (4.22) for constant fields ϕ and $W' = F = 0$. Integrating over the Grassmann variables then yields

$$G_k(q, q', \theta, \theta')|_{\bar{\theta}\theta\bar{\theta}'\theta'} = \frac{Z'^2 q^2}{Z'^4 q^2 + (W'' + 1/2 X q^2)^2} \delta(q - q'). \quad (4.34)$$

Now, the square of the excited-state energy E_1^2 is given by the pole of the propagator at the minimum of the effective potential:

$$\lim_{k \rightarrow 0} \left(Z'^4 q_0^2 + (W'' + \frac{1}{2} X q_0^2)^2 \right) \Big|_{\phi_{\min}} = 0 \quad \text{with} \quad q_0^2 = (iE_1)^2. \quad (4.35)$$

This equation possesses the two solutions

$$E_1^2 = \lim_{k \rightarrow 0} \frac{2}{X^2} \left(Z'^4 + XW'' \pm Z'^2 \sqrt{Z'^4 + 2XW''} \right) \Big|_{\phi_{\min}}, \quad (4.36)$$

where the solution with the negative sign is the correct one, since it reduces to the known limiting value $E_1 = |W''(\phi_{\min})|$ in LPA. The other solution with positive sign diverges in this limit.

Note that if supersymmetry is spontaneously broken, $W'_k(\phi_{\min}) \neq 0$ and the corresponding auxiliary field F does not vanish. Then, the first excited energy E_1 is extracted from the pole of the general propagator (4.22), i.e. of

$$\lim_{k \rightarrow 0} G_k(q, q', \theta, \theta')|_{\bar{\theta}\theta\bar{\theta}'\theta'} \quad (4.37)$$

at the constant minimum ϕ_{\min} of the potential, where F has to be replaced by its equation of motion (4.32).

Table 4.1 displays the energy gap $E_1(g)$ for $e = a = m = 1$ and various values of the coupling g . For comparison, the energies obtained by solving the PDEs in LPA, NLO and the exact values are listed as well. Figure 4.4 shows the first excited energy E_1 as well as the relative deviation from the exact values $e_{\text{trunc}} = (E_1 - E_1^{\text{ex}})/E_1^{\text{ex}}$ as a function of the

g	E_1^{LPA}	E_1^{NLO}	E_1^{NNLO}	E_1^{ex}
0.0	2.202	2.086	2.038	2.022
0.2	2.136	2.028	1.986	1.970
0.4	2.061	1.957	1.920	1.905
0.6	1.978	1.876	1.842	1.827
0.8	1.889	1.784	1.752	1.738
1.0	1.797	1.687	1.653	1.639
1.2	1.709	1.584	1.547	1.534
1.4	1.632	1.486	1.440	1.426
1.6	1.583	1.398	1.337	1.323
1.8	1.590	1.339	1.250	1.235
2.0	1.702	1.337	1.199	1.173
2.2	2.005	1.442	1.216	1.153
2.4	2.627	1.764	1.378	1.183
2.6	3.661	2.525	1.895	1.254
2.8	4.988	3.961	3.195	1.343

Table 4.1: Energy E_1^{NNLO} of the first excited state, calculated according to (4.36) for $r_1 = k$, $e = m = a = 1$ and various g . For comparison, also the results E_1^{LPA} obtained in LPA, E_1^{NLO} derived in NLO as well as the exact values E_1^{ex} from numerically diagonalizing the Hamiltonian are given. Here, E_1^{LPA} , E_1^{NLO} and E_1^{NNLO} were derived by solving the respective partial differential equations numerically.

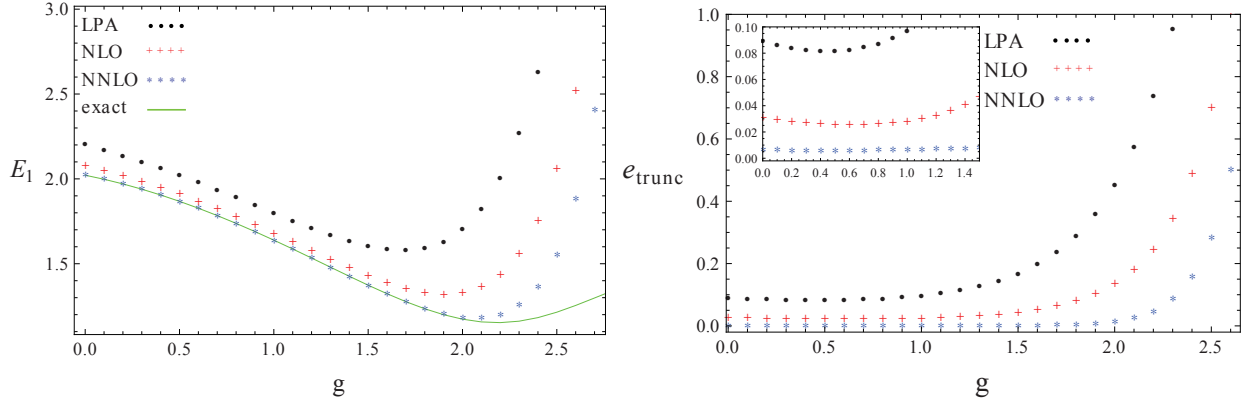


Figure 4.4: Energy gap $E_1(g)$ (left panel) and relative error e_{trunc} of the energy gap (right panel) for classical superpotentials of the form $W'_\Lambda(\phi) = 1 + \phi + g\phi^2 + \phi^3$ and various g . For convex initial potentials ($g < \sqrt{3}$), a nice convergence quantified by a relative error of 1% is achieved in NNLO. For couplings larger than $g \approx 2$, where the classical potential becomes non-convex, significant deviations from the exact results are observed.

coupling g . Obviously, an inclusion of terms of fourth-order in the supercovariant derivative expansion improves the results considerably. A relative error of less than 1% is obtained for couplings $g < \sqrt{3}$. For larger couplings $\sqrt{3} < g < 2.3$, the relative deviations from the exact results lie within a 10% error. As figure 4.4 illustrates, the error increases exponentially for couplings larger than $g \approx 2$ and the supercovariant derivative approximation breaks down. By inspecting the poles of the propagator, this breakdown is also indicated by the appearance of a further mass at $g \approx 1.7$, splitting in two masses for even larger couplings g . This is due to the formation of one (two) further minima of the effective potential, where

$4W'Y + Z'^4|_{\phi_{\min}} = 0$ holds. Here, the fourth-order correction Y is of the same magnitude as the leading and next-to-leading order terms W' and Z' indicating the invalidity of the truncation. The corresponding masses become parametrically quite large. Such large masses in the strong coupling regime are probably an artefact of the regularization and have no physical significance. Similar artefacts are encountered in $O(N)$ symmetric Wess-Zumino models [59] as discussed in section 6.3.5.

Hence, a very good convergence of the derivative expansion is observed in case of a small local barrier of the classical potential. However, as the non-convexity of V_Λ increases, tunnelling events are exponentially suppressed and are no longer captured by the derived flow equations.

4.4 Supersymmetry Breaking

As explained in section 3.3, spontaneous SUSY breaking occurs if the vacuum/ground state does not respect supersymmetry. This breaking is accompanied by the occurrence of a massless, fermionic excitation - the goldstino.

This section analyses the scale dependence of quantum mechanical systems, whose microscopic classical superpotential is of the form $W'_\Lambda(\phi) = \mathcal{O}(\phi^n)$ with highest power n even. As mentioned in section 4.1, supersymmetry then breaks spontaneously at some scale k , even if the microscopic theory is supersymmetric. Spontaneous SUSY breaking becomes an IR effect of long-range fluctuations. Hence, the FRG turns out to be a perfectly suitable method for exploring the *dynamical*, scale-dependent behaviour of SUSY-QM and most importantly, allows for studying strong-coupling effects in the non-perturbative regime triggering the symmetry breaking.

4.4.1 Expansion Issues

In order to study SUSY breaking within the FRG framework, the theory is confined to simple microscopic superpotentials of the form (4.11). Since the microscopic superpotential $W'_\Lambda(\phi) = e + g\phi^2$ represents a \mathbb{Z}_2 symmetric function, it will remain \mathbb{Z}_2 symmetric for all scales $k < \Lambda$ as the RG flow preserves this symmetry.

For unbroken supersymmetry, an expansion in the auxiliary field around $F = 0$ has been employed to derive the flow equations in terms of the scalar fields (c.f. equation (4.23)). However, this expansion point is inappropriate when supersymmetry gets spontaneously broken since the vacuum expectation value of the average field F becomes non-vanishing. For illustration, let us take a closer look at the flow equation for the superpotential in LPA, derived via an expansion around $F = 0$. Here, $W''(\phi)$ represents the ‘‘mass term’’ in the denominator of the flow. As it is now an odd function, the mass like regulator r_1 does not regulate since $\mathcal{W}''(\phi) = W''(\phi) + k$ will vanish for some value(s) of ϕ . This

means that the RG equation detects the massless fermionic excitation - the goldstino mode - associated with the spontaneous breaking of supersymmetry [120]. Hence, at the minimum of $V(\phi)$ the denominator in the flow equation simply contains the squared goldstino mass $m_G^2 = W''(0)^2 = 0$. Thus, the flow of the superpotential diverges in the IR limit at the origin. This apparently leads to infinitely large excited energies, since $E_1 = W'(0)W^{(3)}(0) > 0$ for broken supersymmetry. This divergence occurs independently of the choice of the regulator r_2 and the order of truncation⁹.

The above considerations lead to the conclusion that a Taylor expansion in powers of $F - F_0$ with non-vanishing F_0 is more adapted to systems showing spontaneous SUSY breaking. Unfortunately, the flow equations become of a much more complex form when applying this expansion scheme. Therefore, the following examinations are restricted to the NLO approximation with $W_k(\phi)$ and *field-independent* wave-function renormalization Z_k .

To begin with, an adequate expansion point F_0 has to be selected. To this, consider the equation of motion

$$F = -iW'_k(\phi)/Z'_k{}^2 \quad (4.38)$$

for the auxiliary field in NLO. From the truncated action (4.15) in NLO, the effective average potential

$$V_k(\phi) = \frac{1}{2} \left(\frac{W'_k(\phi)}{Z'_k} \right)^2 \quad (4.39)$$

emerges. Hence, SUSY is spontaneously broken, if $W'_k(\phi) > 0$ for all ϕ . If W' ceases to have a zero, (4.38) implies the auxiliary field to acquire a non-vanishing vacuum expectation value as well. An expansion of the flow of Γ_k around a non-zero auxiliary field - determined by its equation of motion - then reads

$$\begin{aligned} \partial_k \Gamma_k &= i(\partial_k W')F + \frac{1}{2}(\partial_k Z'^2)F^2 + \mathcal{O}(F^3) \\ &= \frac{W'(Z'\partial_k W' - W'\partial_k Z')}{Z'^3} + i \left(\partial_k W' - \frac{2W'\partial_k Z'}{Z'} \right) (F - F_0) \\ &\quad + Z'(\partial_k Z')(F - F_0)^2 + \dots, \end{aligned} \quad (4.40)$$

where $F_0(\phi) = -iW'(\phi)/Z'^2$. Obviously, NNLO contributions of $\mathcal{O}(F^3)$ would contribute to all orders around this new expansion point. Besides, there exists no unique projection onto the flows of W' and Z' . Different flow equations can be derived by projecting onto the constant, the linear or the quadratic term in $(F - F_0)$. Hence, the system is overdetermined. By solving all three equations using an expansion of the right hand side of the Wetterich equation, no consistent solution is found as higher derivative operators contribute to these

⁹Of course, this IR problem represents a low dimensional issue as the divergences diminish with increasing dimension d , see e.g. [48–50].

lower orders as well. To obtain a maximally self-consistent truncation it is therefore necessary to minimize these contributions. Assuming a nice convergence behaviour of the derivative expansion, it is sensible to project onto the lowest orders in $(F - F_0)$.

4.4.2 Numerical Results

In the NLO approximation with uniform wave-function renormalization, the right hand side of the RG equation (4.12) simplifies to

$$\begin{aligned} \partial_k \Gamma_k = & \frac{1}{2} \int_{-\infty}^{\infty} \frac{dq}{2\pi} \left(\partial_k (Z'^2 r_2) (\mathcal{W}''^2 - B^2 q^2) - 2(\partial_k r_1) B \mathcal{W}'' \right) \left[\frac{W' W'''}{\mathcal{N}(\mathcal{N} Z'^2 + B W' W''')} \right. \\ & \left. + \frac{i W''' Z'^4}{(\mathcal{N} Z'^2 + B W' W''')^2} (F - F_0)^1 + \frac{B (W''')^2 Z'^6}{(\mathcal{N} Z'^2 + B W' W''')^3} (F - F_0)^2 + \dots \right] \quad (4.41) \\ \text{with } \mathcal{N} = & B^2 q^2 + \mathcal{W}''^2, \quad B = Z'^2 (1 + r_2), \quad \mathcal{W}'' = W'' + r_1. \end{aligned}$$

Note that the wave-function renormalization $Z'(\bar{\phi})$ accompanying the regulator function r_2 has been identified with the field-independent Z' . To analyse the flow of the effective average potential it is proceeded in two steps. Firstly, the flow starts with the classical superpotential (4.11) at the cutoff $k = \Lambda$. Down to some scale $k_0 > 0$, W' will have a zero and SUSY remains unbroken. In this regime $k \in [k_0, \Lambda]$, the flow equations obtained by an expansion around $F = 0$ are employed. At the scale k_0 , W' ceases to have a zero and SUSY becomes spontaneously broken. Thus, physics in the regime $k \in [0, k_0)$ is described by the flow equations derived via an expansion around $F_0 \neq 0$.

Next, the regulator functions have to be specified. As explained above, r_1 does not perform as an IR regulator here and is thus set to zero. The regulator function r_2 is chosen to be of the form [50]

$$r_2(q^2, k) = \left(\frac{k^2}{q^2} - 1 \right) \theta \left(\frac{k^2}{q^2} - 1 \right). \quad (4.42)$$

The ground state energies E_0 are calculated by Taylor-expanding W' about its minimum $\phi = 0$ up to some order. The system of coupled ordinary differential equations thus obtained is solved numerically. This is a sensible approach when W' becomes flat in the IR. Due to supersymmetry, physics happens at vanishing field. This is in contrast to e.g. models exhibiting a global $O(N)$ symmetry [57, 59], where the situation is exactly opposite: in the unbroken regime, the derivative of the potential is positive, whereas in the broken phase, one has a zero.

Similar to unbroken SUSY-QM, the results for the energies are compared with the ones obtained by numerically diagonalizing the Hamiltonian of the system. Figure 4.5 displays the ground state energy E_0 and the relative error e_{trunc} in LPA and NLO as obtained via two different projection methods.

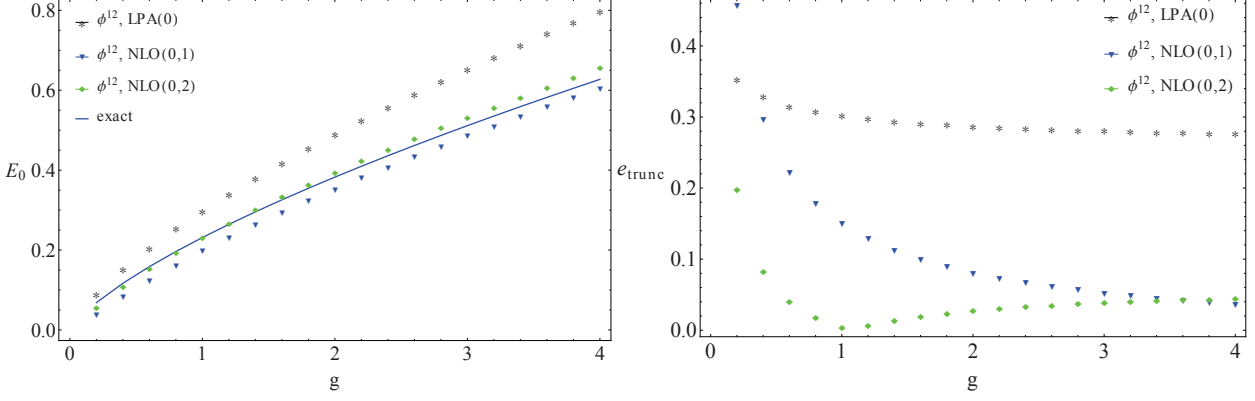


Figure 4.5: Ground-state energy E_0 (left panel) and relative error e_{trunc} of E_0 (right panel) for initial potentials of the form $W_\Lambda = -0.1\phi + \frac{g}{3}\phi^3$ as a function of the coupling g obtained via a polynomial expansion of $W'_k(\phi)$ up to ϕ^{12} . The brackets encode the projection scheme, i.e. (i, j) corresponds to a projection onto $(F - F_0)^i$ and $(F - F_0)^j$.

Apparently, the results are significantly improved by including a constant wave-function renormalization. In particular, this applies to large couplings g , where the relative error is approximately 4%. Contrary to unbroken supersymmetry, the relative error increases with decreasing g . This originates from the fact that for decreasing g the minima of the potential drift apart and tunnelling effects become more prominent, see e.g. [129].

In NLO, a $(0, 2)$ -projection shows a smaller relative error than the $(0, 1)$ -projection up to some $g_{\text{max}} \approx 3.6$, since the flow of Z' slows down when including the higher order term $(F - F_0)^2$ resulting in a higher ground-state energy $E_0 = V(0) = W'(0)/Z'^2$. However, for large $g > g_{\text{max}}$ the $(0, 1)$ -projection leads to superior results. This is due to a larger truncation error in $(F - F_0)^2$ compared to $(F - F_0)^1$ with increasing coupling g , originating from the missing higher order terms X, Y , which are of importance there.

Chapter 5

The Three-Dimensional $\mathcal{N} = 1$ Wess-Zumino Model

In 1974, a paper by J. Wess and B. Zumino was published, where they answered the question “[...] whether one can define supergauge transformations in four dimensional space-time” [20]. Indeed, they showed this to be possible and delivered some examples of representations of supergauge transformations on multiplets of fields. They also considered the scalar multiplet and the corresponding Lagrangian density

$$\mathcal{L} = -\frac{1}{2}(\partial S)^2 - \frac{1}{2}(\partial P)^2 - \frac{1}{2}\bar{\psi}\not{\partial}\psi \quad (5.1)$$

of a free massless model in $d = 4$ - the well known *Wess-Zumino model*. It contains a real scalar S , a real pseudoscalar P and a Majorana spinor ψ as field content¹. Hence, this multiplet consists of two bosonic states of spin zero and two fermionic states of spin one-half. It gained huge attention since the chiral multiplet of the Wess-Zumino model in $d = 4$ represents the simplest matter field system coupling to supergravity by making supersymmetry local [130].

This chapter explores the physics of the $\mathcal{N} = 1$ Wess-Zumino model in *three-dimensional* space-time. Its particle content is given by one scalar ϕ of spin-zero as well as one uncharged Majorana fermion ψ of spin one-half. Hence, the (on-shell) degrees of freedom halved compared to the four-dimensional counterpart. As shall be seen later, scalar as well as Yukawa-type bosonic-fermionic interactions are introduced by adding a general superpotential to the Lagrangian density.

The Wess-Zumino model is investigated via the FRG in order to explore its features beyond the realm of perturbative expansions. Hence, from a structural point of view, the technical findings, i.e. the flow equations, may be regarded as the direct generalization of

¹It should be mentioned that the same kind of SUSY algebra was formulated already by Golfand and Likhtman in 1971 [97] as well as by Volkov in 1972 [98]. However, the work by Wess and Zumino really gave the final stimulus for the exploration of supersymmetric field theories in $d = 4$.

$\mathcal{N} = 1$ SUSY-QM as discussed in the previous chapter. This theory thus serves as a second testing ground for the convergence properties of the supercovariant derivative expansion. Contrary to SUSY-QM, the model now exhibits a rich phase structure. In detail, there exists both a supersymmetric as well as a non-supersymmetric phase for certain classes of potentials. The scale-free transition between both phases is covered by a second-order phase transition described by the supersymmetric equivalent of the so-called Wilson-Fisher fixed point.

Several works have already utilized functional methods in order to gain insight into Wess-Zumino models in various dimensions. A Wilsonian effective action for the four-dimensional Wess-Zumino model has been formulated by H. Sonoda and K. Ülker in 2008 [53]. Thereby, they applied the exact renormalization group perturbatively by introducing a cutoff to the propagators. However, this procedure has been carried out not in superspace but rather in an on-shell formulation. At the same time, O. J. Rosten studied this model via a Polchinski-type RG equation in order to deduce the non-perturbative non-renormalization theorem [55]. The results presented in this chapter build on earlier studies by F. Synatschke-Czerwonka et al. [48–50]. Here, a manifestly supersymmetric functional RG flow has been constructed for the two- and three dimensional $\mathcal{N} = 1$ Wess-Zumino model. In particular, those works delivered an insight into dynamical SUSY breaking. In two dimensions [49, 50], they identified a maximally IR-attractive fixed point featuring one relevant direction and triggering SUSY breaking. Besides, they found a discrete set of scaling solutions corresponding to different UV completions, i.e. different non-perturbatively renormalized versions of the model. Similarly, Synatschke-Czerwonka et al. analysed the three-dimensional Wess-Zumino model [48]. Here, they studied the Wilson-Fisher fixed point, separating the supersymmetric (spontaneously broken \mathbb{Z}_2) from the spontaneously SUSY broken (\mathbb{Z}_2 symmetric) phase at zero and finite temperatures. Besides they showed that at non-vanishing temperature, where soft SUSY breaking occurs, global \mathbb{Z}_2 symmetry may be spontaneously broken or not, depending on the temperature.

The results stated in this chapter are published in [56]. It is composed as follows: The first section introduces the main properties of the model and the notational conventions used. Section 5.2 then comprises the derivation of the flow equations in NNLO in the supercovariant derivative expansion. It is thereby proceeded along the lines of the analysis in SUSY-QM as presented in section 4.2.3. Therefore, only the main aspects as well as differences in comparison to the quantum mechanical system are explained. Note, however that there are no Majorana fermions in three Euclidean dimensions. Thus, the RG equations are derived in $d = 3$ Minkowski space-time and are Wick-rotated afterwards². The physical findings are then presented in sections 5.3 and 5.4. Here, the fixed-point structure of the theory featuring a Wilson-Fisher fixed point is analysed. Furthermore, a superscaling equation, relating the

²For a derivation of the flow equations in Minkowski space see e.g. [48], appendix A.

leading critical exponent to the dimension of space, is derived.

5.1 Introducing the Model

This section includes the essential fundamentals of the $\mathcal{N} = 1$ Wess-Zumino model in three-dimensional Minkowski space-time. Firstly, consider the Lorentz group $SO(1, 2)$ of Lorentz transformations in $\mathbb{R}^{1,2}$. This group is formed by three generators. The corresponding Clifford algebra is given by

$$\{\gamma^\mu, \gamma^\nu\} = 2\eta^{\mu\nu} \mathbb{1}_{2 \times 2}, \quad \mu, \nu = 0, 1, 2 \quad (5.2)$$

with $\eta^{\mu\nu} = \text{diag}(1, -1, -1)$. The gamma matrices, appearing in (5.2) form an irreducible 2×2 matrix representation³ of the Clifford algebra. In the following, the representation

$$\gamma^\mu = (\sigma_2, i\sigma_3, i\sigma_1) \quad (5.3)$$

with σ_i denoting the Pauli matrices is selected. The generators $P_\mu, M_{\mu\nu}$ of $SO(1, 2)$ in $d = 3$ Minkowski space-time as well as the fermionic pair of generators Q, \bar{Q} thus satisfy the Super-Poincaré algebra

$$\begin{aligned} [P_\mu, Q] &= 0, & \{Q, \bar{Q}\} &= 2i\phi \\ [M_{10}, Q] &= \frac{i}{2}\sigma_1 Q, & [M_{20}, Q] &= -\frac{i}{2}\sigma_3 Q, & [M_{12}, Q] &= \frac{1}{2}\sigma_2 Q, & \mu &= 0, 1, 2. \end{aligned} \quad (5.4)$$

Next, the superspace formalism (c.f. section 3.2), concretized to $\mathbb{R}^{3|2}$ superspace is discussed. Here, the superspace (x, θ) is spanned by three real spacetime coordinates $x = (x^0, x^1, x^2)$ plus two Grassmann variables $\theta = (\theta^1, \theta^2)$. A superfield $\Phi(x, \theta)$ then represents a bijection from $\mathbb{R}^{3|2}$ superspace to the set of real numbers. The Taylor expansion

$$\Phi(x, \theta) = \phi(x) + \bar{\theta}\psi(x) + \frac{1}{2}\bar{\theta}\theta F(x). \quad (5.5)$$

of the real scalar superfield in the constant Grassmann variables contains the real scalar field ϕ , the real auxiliary field F and the real Majorana fermion ψ as expansion ‘‘coefficients’’. Note that the fermionic variables have been combined via $\theta = (\theta^1, \theta^2)^T$ and $\bar{\theta} = (i\theta^2, -i\theta^1)$ to constant Majorana spinors⁴. The three-dimensional counterpart of the global supersymmetry transformation (4.5) reads

$$(x^\mu, \theta) \longrightarrow (x'^\mu, \theta') = (x^\mu + i\bar{\theta}\gamma^\mu\epsilon, \theta + \epsilon), \quad (5.6)$$

³In arbitrary dimensions d , an irreducible $n \times n$ matrix representation may be constructed, where $n = 2^{\lfloor \frac{d}{2} \rfloor}$.

⁴The spinor fields, obeying the Majorana condition $\psi = \psi_C = -\sigma_2 \bar{\psi}^T$, are given by $\psi = (\chi, \bar{\eta})^T$ and $\bar{\psi} = \psi^\dagger \gamma^0 = (i\bar{\eta}, -i\chi)$ with $\chi, \bar{\eta} \in \mathbb{R}$.

where ϵ denotes the constant fermionic transformation parameter. Correspondingly, the superfields transform according to $\Phi \rightarrow \Phi + \delta_\epsilon \Phi$, where

$$\delta_\epsilon \Phi(x, \theta) = \delta x^\mu \frac{\partial \Phi}{\partial x^\mu} + \delta \theta \frac{\partial \Phi}{\partial \theta} = (\bar{\epsilon} \psi) + \bar{\theta} (F + i \not{\partial} \phi) \epsilon + \frac{i}{2} \bar{\theta} \theta (\bar{\epsilon} \not{\partial} \psi). \quad (5.7)$$

By using (5.5), the transformation behaviour of the component fields

$$\delta_\epsilon \phi = (\bar{\epsilon} \psi), \quad \delta_\epsilon \psi = (F + i \not{\partial} \phi) \epsilon \quad \text{and} \quad \delta_\epsilon F = i (\bar{\epsilon} \not{\partial} \psi) \quad (5.8)$$

automatically emerges. Via the identification $\delta_\epsilon \equiv i \bar{\epsilon} Q$, the fermionic supersymmetry generators⁵

$$Q = -i \partial_{\bar{\theta}} - \not{\partial} \theta \quad \text{and} \quad \bar{Q} = -i \partial_\theta - \bar{\theta} \not{\partial} \quad (5.9)$$

are defined. Naturally, they obey the super-Poincaré algebra (5.4). Defining a Lagrangian invariant under SUSY transformations requires the introduction of a further object commuting with the SUSY variations - the supercovariant derivatives. They are given by $D = \partial_{\bar{\theta}} + i \not{\partial} \theta$ and $\bar{D} = -\partial_\theta - i \bar{\theta} \not{\partial}$ and fulfil the anticommutation relation $\{D_k, \bar{D}_l\} = -2i \not{\partial}_{kl}$.

The above definitions allow for a construction of an off-shell supersymmetric action in $\mathbb{R}^{3|2}$ superspace:

$$S[\Phi] = \int dz \left[-\frac{1}{2} \Phi K \Phi + 2W(\Phi) \right], \quad K = \frac{1}{2} (\bar{D} D - D \bar{D}), \quad (5.10)$$

where $z = (x, \theta, \bar{\theta})$ denotes the superspace coordinates. Integrating out the constant Majorana spinors $\theta, \bar{\theta}$ and eliminating the auxiliary field F via its equation of motion $F = -W'(\phi)$ leads to the on-shell action

$$S_{on}[\phi, \psi, \bar{\psi}] = \int d^3x \left[\frac{1}{2} \partial_\mu \phi \partial^\mu \phi - \frac{i}{2} \bar{\psi} \not{\partial} \psi - \frac{1}{2} W'^2(\phi) - \frac{1}{2} W''(\phi) \bar{\psi} \psi \right]. \quad (5.11)$$

On-shell, there exists one degree of freedom in the bosonic and fermionic sector respectively. The action (5.11) describes interactions among the scalars ϕ themselves as well as between the scalars ϕ of spin zero and the uncharged fermions ψ of spin one-half. Besides, the potential self-energy $V(\phi) = W'^2(\phi)/2$ of the scalars can directly be inferred from (5.11).

5.2 Flow Equations

In the following, the flow equation

$$\partial_k \Gamma_k = \frac{i}{2} \text{STr} \left\{ \partial_k R_k \left[\Gamma_k^{(2)} + R_k \right]^{-1} \right\} \quad (5.12)$$

⁵Interestingly, the transformed superfield $\Phi' = (1 + i \bar{\epsilon} Q) \Phi = e^{i \bar{\epsilon} Q} \Phi$ may be written as an exponential map, acting on the original superfield. This illustrates the generation of *finite* SUSY transformations.

in three-dimensional Minkowski space-time is employed [48]. Once the flow equations are derived, a Wick rotation of the zeroth momentum component is performed to obtain the corresponding flows in Euclidean space.

Analogously to eq. (4.14), the general ansatz for the scale-dependent effective average action in NNLO in the supercovariant derivative expansion reads

$$\Gamma_k[\Phi] = \int dz \left[2W_k(\Phi) - \frac{1}{2}Z_k(\Phi)KZ_k(\Phi) - \frac{1}{8}Y_{1,k}(\Phi)K^2\Phi - \frac{1}{8}Y_{2,k}(\Phi)(K\Phi)^2 \right]. \quad (5.13)$$

Here, the scale- and field-dependent functions $W_k, Z_k, Y_{1,k}, Y_{2,k}$ have been introduced. The prefactors of each term have been chosen such that the resulting flow equations in $d = 3$ Euclidean space exactly match the corresponding flow equations derived in supersymmetric quantum mechanics with $\int \frac{dq}{2\pi} \rightarrow \int \frac{d^3q}{(2\pi)^3}$ (c.f. (??), appendix A). Integrating out the Grassmann variables in (5.13) yields

$$\begin{aligned} \Gamma_k[\Phi] = & \int d^3x \left[\frac{1}{2}(\partial_\mu Z)(\partial^\mu Z) - \frac{i}{2}(Z'\bar{\psi})\not{\partial}(Z'\psi) - \frac{1}{4}Y_1'\bar{\psi}\partial^2\psi - \left(\frac{1}{2}W'' + \frac{1}{8}Y_1''(\partial^2\phi)\right)\bar{\psi}\psi \right. \\ & + \frac{1}{4}Y_2(\partial^\mu\bar{\psi})(\partial_\mu\psi) + \left(W' - \frac{1}{2}Z'Z''\bar{\psi}\psi + \frac{1}{2}(Y_1' + Y_2)(\partial^2\phi) + \frac{1}{4}Y_1''(\partial_\mu\phi)(\partial^\mu\phi) + \frac{i}{2}Y_2'\bar{\psi}\not{\partial}\psi\right)F \\ & \left. + \left(\frac{1}{2}Z'^2 + \frac{1}{8}Y_2''\bar{\psi}\psi\right)F^2 - \frac{1}{4}Y_2'F^3 \right], \end{aligned} \quad (5.14)$$

where again all terms have been ordered in powers of the auxiliary field F . In analogy to (4.17), the supersymmetric cutoff action is assumed to be of the form

$$\Delta S_k[\Phi] = \frac{1}{2} \int dz \Phi \left[2r_1(-\partial^2, k) - Z_k'^2(\bar{\Phi})r_2(-\partial^2, k)K \right] \Phi, \quad (5.15)$$

with Z_k' evaluated at the background field $\bar{\Phi} = \bar{\phi}$. As in quantum mechanics, the scale dependence of W', Z' and Y_2' is extracted by projecting the right hand side of (5.12) onto F, F^2 and F^3 for constant component fields and a vanishing Majorana spinors. For details, it is referred to appendix C. Finally, the evolution equations in Euclidean space with metric $-\delta_{\mu\nu}$ follow via a Wick rotation of the zeroth momentum component, i.e. $q^0 \rightarrow iq^0$. As mentioned above, these equations are by construction identically to (??) as derived in $\mathcal{N} = 1$ supersymmetric quantum mechanics up to an integration over a three-dimensional momentum space.

The missing flow of $Y_1' + Y_2$ is derived in an exactly similar manner to $d = 1$ as explained in section 4.2.3. Here, momentum-dependent fields ϕ and F have to be considered and the final flow is deduced by projecting onto all contributions of the order $Q^2\delta\phi(Q)\delta F(-Q)$. Contrary to SUSY-QM, an additional Wick rotation of q^0 is applied afterwards. Finally, the definitions (4.26) are imposed in order to simplify the obtained flow equations.

5.3 Wilson-Fisher Fixed Point

Before going into a detailed analysis of the phase structure of the three-dimensional Wess-Zumino model, the earlier findings of Synatschke-Czerwonka et al. [48] are shortly recapitulated. This study employed the supercovariant derivative expansion in NLO with uniform (field-independent) wave-function renormalization. The corresponding flow equations have been solved by applying a polynomial approximation of the superpotential. A maximally IR stable supersymmetric analogon of the Wilson-Fisher fixed point with one IR-relevant direction has been identified. Thereby, the relevant direction is triggered by the minimum of the superpotential $W'(\phi)$. Depending on the choice of this parameter, macroscopic physics may show spontaneous SUSY breaking or not. If the microscopic potential furthermore respects the internal \mathbb{Z}_2 symmetry, the breaking of this symmetry is directly linked to SUSY breaking. Thus spontaneous SUSY breaking implies the ground state to be lifted above zero and therefore guarantees \mathbb{Z}_2 symmetry. Contrary, a supersymmetric ground state with $W'(\phi)$ even goes along with a non-vanishing VEV for the scalar field and hence spontaneous \mathbb{Z}_2 breaking. In addition, a *superscaling relation* of the form

$$\theta_0 = \frac{3 - \eta}{2} \quad (5.16)$$

has been deduced, where θ_0 denotes the critical exponent of the relevant direction and η the anomalous dimension. It also has been shown that in the phase featuring spontaneous SUSY breaking, the RG flow drives the theory into a massless limit.

This section contains a discussion of the fixed-point structure in NNLO in the supercovariant derivative expansion. Similar to the study of the quantum mechanical equivalent in sections 4.3 and 4.4, it is focused on the convergence properties of this truncation scheme. Besides, it is aimed at *globally* solving the fixed-point equations via spectral methods rather than employing polynomial approximations of a finite radius of convergence. This approach ensures the numerical validity of the obtained results which are naturally free from boundary effects usually present when applying a domain truncation.

To begin with, suitable regulator functions have to be chosen. In the following, the possible microscopic superpotentials W'_Λ are restricted to even polynomials of the field. Then, its leading power remains even during the flow allowing for dynamical SUSY breaking to occur by approaching the IR. Besides, the flow equations automatically force $W'(\phi)$ to remain even for all scales $k < \Lambda$. Furthermore, the equations also imply $Z'(\phi)$ and $Y(\phi)$ to be even and $X(\phi)$ to be an odd function.

What implications can be inferred from the global behaviour of $W'(\phi)$ regarding the choice of regulators? If $W'(\phi)$ tends asymptotically to an even power, $W''(\phi)$ always shows a node. The mass-term W'' however appears in the propagator and is IR regulated by r_1 as introduced in (5.15). Apparently, the node of $W''(\phi)$ is merely shifted but not screened

by a mass-like regulator like r_1 . This is exactly analogous to the situation in $d = 1$ with spontaneous SUSY breaking as discussed section 4.4. Thus, r_1 is set to zero whereas r_2 is selected to be of the form⁶ (4.42). Besides, the value of the background field appearing in the cutoff action (5.15) is identified with the minimum of the potential, i.e. $\bar{\phi} = \phi_0$. It should be emphasized that the background field $\bar{\phi}$ is not identified with the fluctuation field ϕ - an approximation well known in the context of background field flows [47, 131, 132]. It will be commented on this issue later on in this section.

The Wilson-Fisher fixed-point characterizes a second-order phase transition or equivalently a scale-free theory. Here, the correlation length diverges, indicating fluctuations on all scales to be important for the dynamics of the effective theory. Thus, the flow equations have to be formulated in terms of dimensionless quantities. By using dimensionless couplings, the true scale-independence of the effective average action at a fixed point is ensured. The canonical dimensions of the field and the couplings are given by

$$[\phi] = 1/2, \quad [W] = 2, \quad [Z'] = 0, \quad [X] = -1, \quad [Y] = -3/2. \quad (5.17)$$

Hence, dimensionless quantities are defined via

$$\begin{aligned} \chi &= Z'(\phi_0)k^{-1/2}\phi, & w(\chi) &= W(\phi)k^{-2}, & z'(\chi) &= Z'(\phi)/Z'(\phi_0), \\ x(\chi) &= X(\phi)k/Z'^2(\phi_0), & y(\chi) &= Y(\phi)k^{3/2}/Z'^3(\phi_0) \end{aligned} \quad (5.18)$$

with ϕ_0 denoting the minimum of the potential. Employing the definition of the anomalous dimension

$$\eta(k) = -\frac{d}{dt} \ln \left(Z'^2(\phi_0) \right), \quad t = \ln(k/\Lambda) \quad (5.19)$$

as well as the dimensionless momentum variable $u = q^2/k^2$, the flow of the dimensionless superpotential reads

$$\begin{aligned} \partial_t w' + \frac{1}{2}(3 - \eta)w' - \frac{1}{2}(\eta + 1)\chi w'' = \\ \frac{1}{2\pi^2} \int_0^1 du \frac{\sqrt{u}(\eta(u - 1) + 2) (\alpha'(u\alpha^2 - 4\beta^2) + 16\alpha u z' z'' \beta)}{2(u\alpha^2 + 4\beta^2)^2}. \end{aligned} \quad (5.20)$$

Above, the abbreviations $\alpha := ux + 2w''$ and $\beta := 1 + u(z'^2 - 1)$ have been used. The left hand side of (5.20) includes the dimensional and anomalous scaling. In contrast, the right hand side encodes the interactions amongst the operators according to the ansatz of Γ_k . Note that of the fourth-order contributions only x and not y directly couples to the flow of the superpotential. The expressions of the remaining flows are rather long and therefore not written down explicitly.

⁶The choice $r_2(q^2, k) = \left(\frac{k}{|q|} - 1 \right) \Theta \left(\frac{k^2}{q^2} - 1 \right)$ as utilized in [48] would lead to IR divergent flows of the fourth-order operators X and Y .

In section 2.4, the fixed-point condition (2.17) has been introduced. Therefore, the Wilson-Fisher fixed point satisfies

$$\partial_t \mathcal{C}_* = 0, \quad \text{with} \quad \mathcal{C} = (w', z', x, y). \quad (5.21)$$

For large fields $|\chi| \gg 1$, the right hand side of (5.20), i.e. the non-trivial flow, vanishes as $|w_*''|$ is generally expected to be large for a \mathbb{Z}_2 -symmetric system. This holds for the remaining flows as well. Thus, the fixed-point solution for large χ is fixed by the anomalous and canonical scaling, leading to the asymptotic behaviour

$$w'_*(\chi) \sim \chi^{\left(\frac{3-\eta}{\eta+1}\right)}, \quad z'_*(\chi) \sim \chi^{-\left(\frac{\eta}{\eta+1}\right)}, \quad x_*(\chi) \sim \chi^{-2}, \quad y_*(\chi) \sim \chi^{-3}. \quad (5.22)$$

Consequently, the higher order functions vanish for large fields if η is assumed to be positive.

Next, the numerical results to the fixed-point equations are presented. The scaling equations are solved globally via a combination of Chebyshev and rational Chebyshev polynomials (see appendix B). Figure 5.1 illustrates the scaling solutions of the four operators considered. The IR relevant coupling $w'_*(0)$, the location χ_0 of the minimum of the potential as well as the anomalous dimension η and leading critical exponents for different truncations are displayed in table 5.1. A nice convergence behaviour with increasing order in the derivative expansion is observed. Hence, the quantitative relevance of the operators in Γ_k seems to correlate with their scaling dimension (canonical plus anomalous scaling) D with $D_{w'} > D_{z'} > D_x > D_y$. They are determined in terms of η as follows:

$$D_{w'} = \frac{1}{2}(3 - \eta), \quad D_{z'} = -\frac{\eta}{2}, \quad D_x = -(1 + \eta), \quad D_y = -\frac{3}{2}(1 + \eta). \quad (5.23)$$

approximation	$w'_*(0)$	χ_0	η	θ_0	θ_1	θ_2	θ_3
LPA	-0.0420	0.147		3/2	-0.702	-3.800	-7.747
NLO	-0.0292	0.150	0.186	1.407	-0.771	-1.642	-3.268
NNLO	-0.0294	0.149	0.180	1.410	-0.715	-1.490	-2.423

Table 5.1: Value of the superpotential $w'_*(\chi = 0)$ at the origin, location of minimum χ_0 of the fixed-point potential, anomalous dimension and subleading critical exponents of the Wilson-Fisher fixed point for different orders in the supercovariant derivative expansion.

Finally, it is commented on not applying the background field approximation (BFA) $\phi = \bar{\phi}$ for the spectrally adjusted regulator $Z_k'^2(\bar{\phi})r_2$. According to (5.22), the fixed-point solution z'_* vanishes for large fields $|\chi| \rightarrow \infty$. Implementing the BFA goes along with the replacement $z'(\chi_0) = 1 \rightarrow z'(\chi)$ in the dimensionless regulator. Thus, the regulator is suppressed artificially for large fields. This in turn can lead to instabilities. Indeed, during the numerical investigation of the fixed-point equations, no global solution in NNLO could be found when employing the background field approximation, even though a solution via

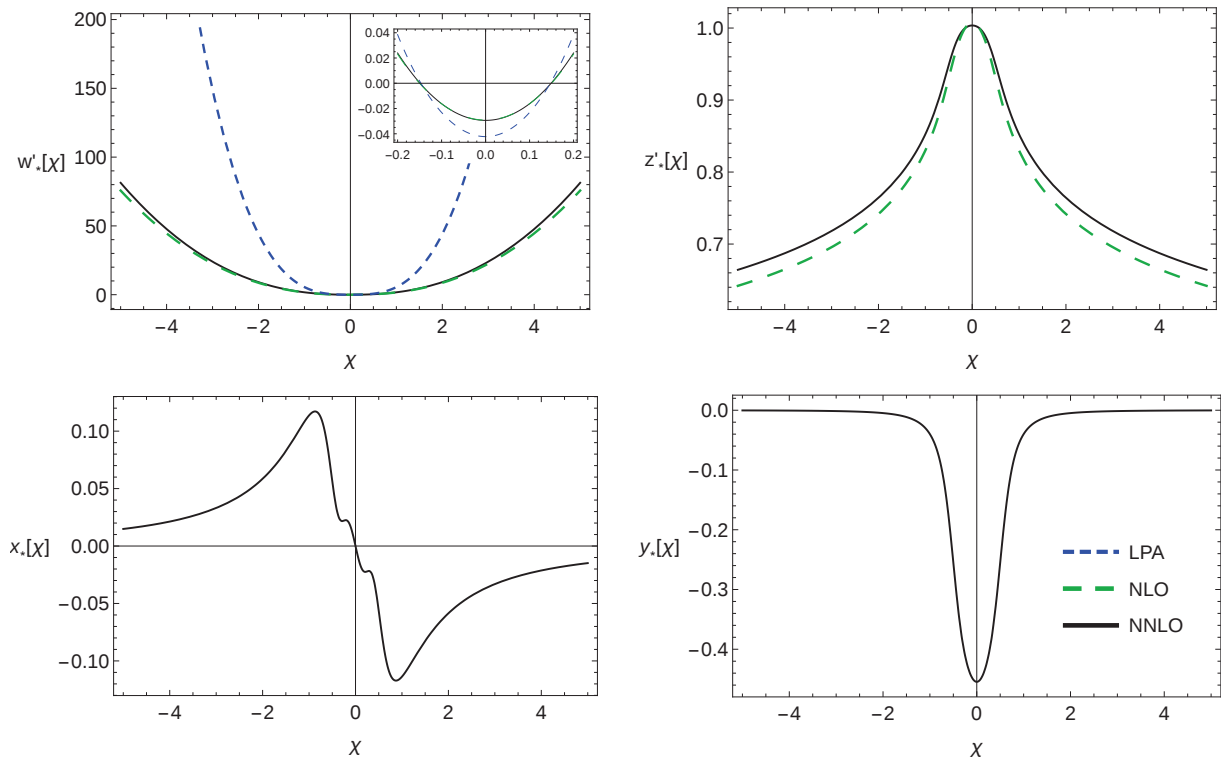


Figure 5.1: Fixed-point solution of the three-dimensional Wess-Zumino model in LPA, NLO and NNLO. The change in asymptotics when going from LPA to NLO induced by the anomalous dimension is clearly visible. Also, the potential as well as the wave function renormalization change only mildly when going from NLO to NNLO, indicating once more a good convergence of the derivative expansion.

a Taylor expansion seems to exist. The difference between the physical quantities (critical exponents etc.) obtained by a Taylor expansion with BFA and the spectral method without BFA are almost identical. Thus one might argue that the error made in this approximation is irrelevant. However, one should bear in mind that a fixed-point potential better be globally defined, and that there might be systems that are unstable against such types of approximations. Note also that when integrating the dimensional flow equations, the difference should be even smaller as $Z'(\phi)$ does not fall off asymptotically.

5.4 Superscaling Relation

As mentioned in the previous section, the superscaling relation (5.16) has been derived in [48]. It relates the critical exponent $\theta_0 = 1/\nu_w$ of the IR unstable direction $w'_*(0)$ to the anomalous dimension η . This is especially interesting as such a relation is unknown in standard spin systems. In Ising-like systems, the thermodynamic main exponents as e.g. $\alpha, \beta, \gamma, \delta$ are related among each other by scaling relations. Besides, they may be deduced from the correlation exponents ν and η by so-called hyperscaling relations involving the dimension of space d . However, there exists no general relation between ν and η . The superscaling relation (5.16) thus represents a special feature of the Wess-Zumino model. Below, this superscaling

relation will be shown to hold true to all orders in the supercovariant derivative expansion of Γ_k . In particular, the superscaling relation is derived for arbitrary dimension $d \geq 2$.

To begin with, note that the only flow equation depending explicitly on w' is the one for w' itself. In the subsequent derivation, η is assumed to be a free parameter, see e.g. [48, 133]. Next, consider small fluctuations around the fixed-point solution in w' -direction,

$$w'(t, \chi) = w'_*(\chi) + \delta w'(t, \chi), \quad (5.24)$$

and possible higher order operators evaluated at the fixed point. Now, the flow (5.20) - generalized to d dimensions⁷ - is linearized in $\delta w'$. This yields the fluctuation equation

$$\partial_t \delta w' = \left(\frac{\eta - d}{2} + \mathcal{F}(\chi) \partial_\chi + \mathcal{G}(\chi) \partial_\chi^2 \right) \delta w'. \quad (5.25)$$

Here, \mathcal{F} and \mathcal{G} are functionals obtained from the linearization. The critical exponents then correspond to the negative eigenvalues of the operator on the right hand side of (5.25). Apparently, a constant variation represents an eigenfunction to this operator with eigenvalue $(\eta - d)/2$. Since the flow equations of all higher operators of Γ_k remain independent of w' , this is true to all orders. Hence, the superscaling relation

$$\theta_0 = 1/\nu_w = \frac{1}{2}(d - \eta), \quad d \geq 2 \quad (5.26)$$

has been verified.

⁷The right hand side of (5.20) holds for arbitrary d up to a different dimensional prefactor of $1/(2^{d-1}\pi^{d/2}\Gamma(d/2))$.

Chapter 6

Supersymmetric $O(N)$ Theories

This chapter is devoted to the exploration of scalar models featuring two global, continuous¹ symmetries: Supersymmetry and $O(N)$ symmetry. The first implies invariance under global external transformations involving space and time, whereas the latter means invariance of the action under internal orthogonal transformations, keeping the scalar product of N superfields unaffected. The following sections thereby focus on the supersymmetric $O(N)$ model in three dimensions.

Purely scalar $O(N)$ theories lacking SUSY have been extensively studied in the past with perturbative methods as well as non-perturbative approaches. Due to the striking resemblance in many characteristics to the supersymmetric $O(N)$ models, some features of the purely scalar $O(N)$ theories are summarized before it is passed on to supersymmetric $O(N)$ theories.

In general, scalar $O(N)$ models represent the prototype for investigating the phenomenon of symmetry restoration at high temperatures. Especially, the scalar $(\phi^2)_{d=3}^2$ theory has gained much attention the past. Often, the limit of infinitely many fields $N \rightarrow \infty$ has been considered, since this solvable spherical model gives a qualitatively accurate picture of the phase structure. The $(\phi^2)_{d=3}^2$ theory exhibits an IR attractive Wilson-Fisher fixed point corresponding to a second order phase transition between the $O(N)$ symmetric and the spontaneously broken phase [65]. Many different physical systems can be described by the scalar $(\phi^2)_{d=3}^2$ model. Some applications are e.g. the description of statistical properties of long polymer chains ($N = 0$), the liquid-vapour transition ($N = 1$) or the Helium superfluid transition ($N = 2$). The $O(3)$ model is of relevance in condensed matter physics, where it pictures the ferromagnetic phase transition. The $O(4)$ model is of physical importance as well, since it corresponds to the scalar sector of the electroweak standard model in the limit of vanishing gauge and Yukawa couplings. It is also used for modelling the chiral phase transition in QCD in the limit of two quark flavours [134–137].

In contrast to the $O(N)$ model with a microscopic ϕ^4 potential, the scalar $(\phi^2)_{d=3}^3$

¹Note that for $N = 1$ scalar field, the symmetry becomes discrete.

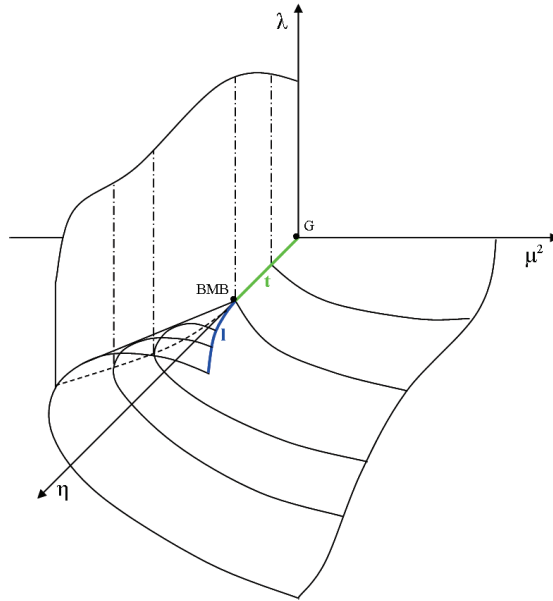


Figure 6.1: Phase structure of the scalar $O(N)$ model at infinite N including the BMB fixed point, according to [139] (see text).

model shows a more complex phase structure [65, 138–140]. Depending on the renormalized couplings μ^2, λ and η of the operators ϕ^2, ϕ^4 and ϕ^6 , one observes a first-order phase transition at strong coupling without universal behaviour or a second-order phase transition with universal behaviour. Both regimes are separated by a tricritical line t , characterized by vanishing couplings μ^2 and λ as depicted in figure 6.1. A surface of first-order transitions continues into the $O(N)$ symmetric phase for couplings with $\eta > \eta_c$ and ends at a gas-liquid transition line l . Scale invariance is an exact symmetry of the tricritical theory, but at the endpoint $(0, 0, \eta_c)$, scale invariance is spontaneously broken. The free coupling η is dimensionally transmuted to an undetermined mass scale m and a massless Goldstone-boson (dilaton) shows up. In the large- N limit, this non-trivial and UV-stable *Bardeen-Moshe-Bander* (BMB) fixed point marks the point where the tricritical line t and the gas-liquid line l meet. Hence, the tricritical line connects the Gaussian fixed point and the BMB fixed point. One expects that at finite N the tricritical line extends all the way to infinite η and the BMB point disappears [141]. Note that the BMB fixed point is also of interest as a fundamental UV fixed point, allowing for a non-Gaussian continuum limit for the $(\phi^2)_{d=3}^3$ theory with non-classical scaling.

Unfortunately, the spontaneous breakdown of the $O(N)$ symmetry goes along with the appearance of $N - 1$ massless Goldstone bosons. Fluctuations of the latter generate IR power singularities. This, in turn has a great impact on perturbative calculations as the presence of such divergences destroys the convergence of the perturbative series. Ergo, the order and details of the phase transition are not resolvable in any finite order in perturbation theory, see e.g. [142–145]. Fortunately, such divergence issues appearing on macroscopic scales become manageable via the non-perturbative RG approach utilized in this thesis.

Since the early nineties, there have been elaborated plenty of works applying the renormalization group idea to scalar $O(N)$ models. The subsequent review of publications has to be regarded only as a small selection out of those works. The scalar ϕ^4 theory in $d = 2, 3, 4$ has been examined at infinite as well as finite N by Wetterich et al. in [31, 125, 126]. Here, a derivative expansion of Γ_k has been applied up to NLO with uniform wave function renormalization, leading to satisfying values for critical exponents and a description of the phase structure. References [146, 147] considered the four-dimensional $O(N)$ model. W.A. Bardeen and M. Moshe [146] thereby examined the large- N limit of the model to become a free field theory. In contrast, M. Reuter et al. [147] focused on the model at finite temperatures featuring a high-temperature phase transition of second order. The bosonic $O(N)$ model with classical ϕ^6 potential has been investigated by N. Tetradis and D. Litim [65], W.A. Bardeen et al. [140] and F. David et al. [138] in the large- N limit. They have identified the complex phase structure described above showing first- as well as second-order phase transitions, both regimes separated by a tricritical line t . The works [138, 140] thereby focused on the BMB phenomenon and showed it to be of an intrinsically non-perturbative nature. David et al. suggested the BMB phenomenon not to survive at finite N , which they fortified in [139]. This conjecture has been supported by F. Karsch et al. [141], who numerically studied the BMB fixed point at finite N by considering the limit of an infinitely large ϕ^6 coupling. More recently, the scalar $O(N)$ model in *fractional* dimensions has been analysed by Codello et al. [148, 149]. Here, the critical exponents for various N in fractional dimensions ranging from two to four have been computed in LPA, including the scaling exponents for the bicritical Wilson-Fisher and the tricritical phase transition for general d and N . Besides, the model in $4 < d < 5$ has been looked at in [150] by R. Percacci and G.P. Vacca. They negated the speculation that a non-trivial UV fixed point - implying an asymptotically safe theory - might exist in $d = 5$. More precisely, they showed the scaling solutions to be either unbounded from below or singular and not globally defined in LPA at infinite N . Rather methodical studies regarding the convergence behaviour of the derivative expansion and aiming at a high-precision determination of critical exponents have been performed by B. Delamotte et al. [64, 151]. They restricted to the Ising model in $d = 3$ up to fourth order in the derivative expansion, leading to very accurate critical exponents. Another expansion scheme has been developed by Blaizot et al. [152–154] allowing for the computation of the full momentum dependence of correlation functions.

Now, the question arises, how the phase structure and physical quantities of the $O(N)$ model change, when supersymmetry is introduced. Then, additional fermionic degrees of freedom are present and their fluctuations modify the quantum effective theory. First of all, the $O(N)$ symmetric Wess-Zumino model with a microscopic $(\Phi^2)_{d=3}^2$ superpotential is determined by only *two* renormalized parameters. Hence, critical and tricritical theories are identical. Note that a superpotential quartic in the superfields implies the bosonic potential

to be of order ϕ^6 . Thus, the supersymmetric $(\Phi^2)_{d=3}^2$ model is expected to be quite similar to the scalar $(\phi^2)_{d=3}^3$ theory with constraint, i.e. linked couplings.

Since the mid-eighties, its phase structure has attracted ongoing attention [155–162]. Most works thereby utilized the large- N expansion as a non-perturbative approach. In 1985, W.A. Bardeen et al. [155] tried to understand the mechanism of spontaneous breaking of scale invariance. Thus they hoped to get insight into the origin of the very different orders of magnitude of mass scales appearing in particle physics. Similar to the observations in scalar $(\phi^2)_{d=3}^3$ models, they indeed found a supersymmetric version of the BMB fixed point at a critical coupling. Here, the bosons and fermions become massive while a Goldstone boson (dilaton) and a Goldstone fermion (dilatino) are dynamically generated. Besides, the authors identified four different phases, including peculiar degenerate $O(N)$ symmetric phases with several mass scales. In the same year, a further study of the $1/N$ expansion was realized by R. Gudmundsdottir and G. Rydell [160], where the authors found a non-trivial UV fixed-point and a stable dilaton phase. At next-to-leading order, the dilaton acquires a mass of order $1/N$ showing that a phase with spontaneously broken scale invariance only exists in the limit of infinitely many superfields, similar to the observations in scalar $(\phi^2)_{d=3}^3$ theories. These findings were confirmed two years later by Y. Matsubara et al. [162]. Later on, J.F. Dawson et al. [157] analysed the phase structure of the supersymmetric $(\Phi^2)_{d=3}^2$ model at zero and finite temperature by applying several non-perturbative methods. By performing the $1/N$ expansion, the Hartree approximation and Schwinger-Dyson equations, they observed a rich degenerate ground-state structure. Further studies regarding the softly SUSY broken phase at finite temperature with similar findings to [157] have been developed by M. Moshe et al. [161, 163].

Finally, the following question arises: what new features and interesting physics of supersymmetric $O(N)$ models does the FRG approach deliver? The advantages are threefold. Firstly, it allows for investigating the renormalized theory, where the UV scale Λ is removed. The obtained phase structure thus can be directly compared with earlier results based on gap equations and Schwinger-Dyson equations [155–157]. Beyond this limit, however, one can take the effective field theory perspective as well. Here, the UV cutoff Λ remains a finite parameter. The boundary condition at $k = \Lambda$ then has been achieved by integrating out all fluctuations with momenta larger than Λ . Via this procedure, an analysis of the physical origin of the complex phase structure exhibiting several masses is made possible. Besides, the effects of changes in the boundary conditions and higher order couplings on the phase diagram become transparent. Most importantly, the flow equations comprise physics on all scales $k < \Lambda$. Thus, a discussion of a *scale-dependent* phase diagram is feasible. This is quite of importance for supersymmetric $O(N)$ models as such an analysis shows the latter to be plagued by Landau poles and multivalued effective average potentials; c.f. sections 6.3.4 and 6.3.5. Besides, the origin of e.g. phases with two or even more $O(N)$ symmetric ground

states becomes illustrative due to the characteristics of the scale-dependent bosonic potential. Especially those physical observations are not directly visible from the IR limit only.

The results reported in this chapter are published in [57], [59] and [58]. It is organized as follows: The main features of supersymmetric $O(N)$ models are explained in section 6.1. The second section is devoted to the derivation of a supersymmetric RG flow equation in leading order in the derivative expansion. The large- N limit offers an exact analytical solution of the derived flow equations which is discussed in section 6.3. Here, a detailed account of the fixed-point solutions (section 6.3.2) and related universal quantities (section 6.3.3) is given, including the critical exponents of a Wilson-Fisher type fixed-point. Then, the renormalized ($\Lambda \rightarrow \infty$) as well as the effective (Λ finite) field theories are examined in sections 6.3.4 and 6.3.5 respectively. Subsequently, section 6.3.7 illustrates the supersymmetric BMB phenomenon in the large- N limit. Finally, at finite N , an exact fixed point to leading order in a gradient expansion is derived (section 6.4). Moreover, its impact on the phase transition is evaluated and the fate of the BMB mechanism revealed.

6.1 Introducing the Model

In this section, the relevant features of the three-dimensional $\mathcal{N} = 1$ supersymmetric $O(N)$ models are sketched. This picture will be painted quite quickly, since the theory corresponds formally to the N -fold copy of the $\mathcal{N} = 1$ Wess-Zumino model. Thus, the conventions utilized in section 5.1 regarding the representation of the gamma matrices, Majorana spinors, supercharges and supercovariant derivatives are adopted. Similarly, the supersymmetry transformations are given by (5.6) and the super-Poincaré algebra (5.4) holds.

Contrary to the $\mathcal{N} = 1$ Wess-Zumino model, the real superfield now represents a map $\Phi : \mathbb{R}^{3|2} \rightarrow \mathbb{R}^N$ from $\mathbb{R}^{3|2}$ superspace onto the flat \mathbb{R}^N . The chosen N coordinates $\{\Phi^i\}$, $i = 1, \dots, N$ on \mathbb{R}^N can be summarized to a N -component vector superfield $\vec{\Phi}$. A single component of this real vector superfield reads

$$\Phi^i(x, \theta) = \phi^i(x) + \bar{\theta}\psi^i(x) + \frac{1}{2}\bar{\theta}\theta F^i(x), \quad i = 1, \dots, N \quad (6.1)$$

in accordance with (5.5). The supersymmetric action, built up from (6.1) then describes the interactions of N uncharged Majorana fermions ψ^i of spin one-half with N pseudoscalar particles F^i and N scalars ϕ^i of spin zero. Supersymmetry guarantees all particles to be of the same mass. Besides it implies the bosonic and the fermionic sector to have $2N$ degrees of freedom each (off-shell). Similar to the Wess-Zumino model, the scalars interact among each other as well as with the fermions. Since the action should respect $O(N)$ symmetry, the superpotential only depends on the invariant composite superfield $R = 1/2\bar{\Phi}^i\Phi_i$. In

components, it reads

$$R = \frac{1}{2}\Phi^2 = \bar{\rho} + (\bar{\theta}\psi)\phi + \frac{1}{2}\bar{\theta}\theta \left(\phi F - \frac{1}{2}\bar{\psi}\psi \right), \quad (6.2)$$

wherein the composite scalar field $\bar{\rho} \equiv \phi^2/2$ has been introduced. Note that here and in the following, the internal summation index is suppressed. The starting point for further investigations will be the manifestly supersymmetric action

$$S = \int d^3x \left(-\frac{1}{2}\Phi K \Phi + 2W(R) \right) \Big|_{\bar{\theta}\theta} \quad \text{with} \quad K = \frac{1}{2}(\bar{\mathcal{D}}\mathcal{D} - \mathcal{D}\bar{\mathcal{D}}). \quad (6.3)$$

Inserting the Taylor expansions of the superfields and integrating out the Grassmann spinors then yields the off-shell action

$$S_{off}[\phi^i, \psi^i, F^i] = \int d^3x \frac{1}{2} \left[-\phi\partial^2\phi - i\bar{\psi}\not{\partial}\psi + F^2 + 2W'(\bar{\rho})(\phi F) - W'(\bar{\rho})(\bar{\psi}\psi) - W''(\bar{\rho})(\bar{\psi}\phi)(\psi\phi) \right]. \quad (6.4)$$

Here, a prime denotes a derivative with respect to $\bar{\rho}$. By eliminating the auxiliary fields F^i through their algebraic equation of motion, $F^i = -W'(\bar{\rho})\phi^i$, the on-shell action

$$S_{on}[\phi^i, \psi^i] = \int d^3x \frac{1}{2} \left[-\phi\partial^2\phi - i\bar{\psi}\not{\partial}\psi - 2\bar{\rho}(W'(\bar{\rho}))^2 - W'(\bar{\rho})(\bar{\psi}\psi) - W''(\bar{\rho})(\bar{\psi}\phi)(\psi\phi) \right] \quad (6.5)$$

is obtained. The field-dependent fermion mass m_ψ , the bosonic potential V , and the field-dependent Yukawa-type coupling λ_Y all follow from the superpotential W as

$$\begin{aligned} m_\psi &= W'(\bar{\rho}) \\ V &= \bar{\rho} [W'(\bar{\rho})]^2 \\ \lambda_Y &= \frac{1}{2}W''(\bar{\rho}). \end{aligned} \quad (6.6)$$

All salient features of the classical theory are encoded in the functions (6.6). For a polynomial superpotential, the scalar field potential always has a minimum at $V(0) = 0$ implying that global supersymmetry is unbroken by construction.

6.2 Supersymmetric Renormalization Group Flow

The derivation of the flow equations in superspace form the content of this section. There are many formal similarities to the $\mathcal{N} = 1$ Wess-Zumino model and the respective considerations as given in section 5.2. Hence, only the relevant steps and formulas are sketched below.

Firstly, the truncation scheme is introduced, followed by a discussion of the cutoff functional. Finally, the derivation of the flow equation for the superpotential in LPA is explained.

6.2.1 Truncation

Analogously to the Wess-Zumino theories (c.f. chapter 5), the Wetterich equation (5.12) in three-dimensional Minkowski space-time is employed. Therein, the second functional derivative with respect to the superfields is defined as

$$\left(\Gamma_k^{(2)}\right)_{mn}(z, z') = \frac{\overrightarrow{\delta}}{\delta\Phi_m^*(z)} \Gamma_k \frac{\overleftarrow{\delta}}{\delta\Phi_n(z')}, \quad (6.7)$$

where m, n denote the internal superfield indices and $z = (q, \theta)$ the superspace coordinates². Here and in the following, it is switched to momentum space. Note that the superfields are real and hence $\Phi_m(-q, \theta) = \Phi_m^*(q, \theta)$. In order to solve (5.12), an efficient truncation scheme has to be developed. Again, an expansion in increasing powers of the supercovariant derivatives D and \bar{D} is selected. Keeping in mind the fact that Γ_k should respect $O(N)$ symmetry, the general ansatz in NLO in the supercovariant derivative expansion is given by

$$\Gamma_k = \int dz \left(2W_k(R) + \frac{1}{2}Z_k(R)\bar{D}\Phi^i D\Phi_i + \frac{1}{4}Y_k(R)\bar{D}R DR \right). \quad (6.8)$$

The scale dependence is encoded in the field-dependent superpotential $W_k(R)$ and wave-function renormalizations $Z_k(R)$ and $Y_k(R)$ respectively. The derivation of the evolution equations for the wave function renormalizations would require an expansion around a momentum-dependent background. The latter equations then lead to the determination of the anomalous dimensions η and $\tilde{\eta}$ of the radial mode as well as the $N - 1$ Goldstone modes. Here, it will be limited to the leading order in the super-derivative expansion, i.e. the LPA. It amounts to setting the wave function renormalization $Z_k = 1$ throughout as well as $Y_k = 0$. This is expected to be a satisfactory approximation for large N , where RG corrections to the wave-function renormalization Z_k of the relevant degrees of freedom, the Goldstone modes, are suppressed as $1/N$. In scalar $O(N)$ theories, the LPA delivers already very good results for the scaling of the Wilson-Fisher fixed point [31, 125, 126, 164]. Here, the LPA does retain the full field- and scale-dependence of the superpotential W_k .

6.2.2 Choosing the Regulator Functional

The flow equation 5.12 contains a suitable momentum cutoff R_k , ensuring UV and IR regularization and thus guarantees a finite flow of Γ_k . In this section, it will be proceeded

²The functional derivative with respect to the superfields is defined such that $\int dz \frac{\delta\Phi_i(z)}{\delta\Phi_j(z')} = \int dz \delta(z - z')\delta_{ij} = \delta_{ij}$, where $\delta(z - z') := \delta(q - q')\delta(\bar{\theta} - \bar{\theta}')\delta(\theta - \theta')$.

analogously to the construction of the cutoff functional in supersymmetric quantum mechanics as presented in section 4.2.2 and [47, 48, 50–52]. Additionally to the requirements stated in section 4.2.2, the regulator functional now preserves *both* supersymmetry and $O(N)$ symmetry for all scales. Being quadratic in the fields, it should be of the form

$$\Delta S_k[\Phi^i] = -\frac{1}{2} \int \frac{d^3q}{(2\pi)^3} d\theta d\bar{\theta} \Phi^i R_k(\bar{D}D) \delta_{ij} \Phi^j. \quad (6.9)$$

Utilizing the anticommutator $\{D_k, \bar{D}_l\} = -2q_\mu (\gamma^\mu)_{kl}$ yields

$$\left(\frac{1}{2}\bar{D}D\right)^{2n} = q^{2n} \quad (6.10)$$

in momentum space, such that a supersymmetric and $O(N)$ -invariant regulator term is the superspace integral of

$$\frac{1}{2}\Phi_i R_k(\bar{D}D)\Phi^i = \frac{1}{2}\Phi_i \left(2r_1(q^2) - r_2(q^2) K\right) \Phi^i. \quad (6.11)$$

Expressed in component fields, the cutoff function may be written as

$$\Delta S_k = \frac{1}{2} \int (\phi, F) R_k^B \begin{pmatrix} \phi \\ F \end{pmatrix} + \frac{1}{2} \int \bar{\psi} R_k^F \psi, \quad (6.12)$$

where the bosonic and fermionic momentum cutoffs R_k^B and R_k^F are of the form

$$R_k^B = \begin{pmatrix} q^2 r_2 & r_1 \\ r_1 & r_2 \end{pmatrix} \otimes \mathbb{1}_N \quad \text{and} \quad R_k^F = -\left(r_1 + r_2 \not{q}\right) \otimes \mathbb{1}_N. \quad (6.13)$$

Apparently, the two free regulator functions $r_1 \equiv r_1(q^2/k^2)$ and $r_2 \equiv r_2(q^2/k^2)$ are left at our disposal. Hence, choosing an appropriate regulator seems to lighten. Nevertheless, there are additional restrictions as supersymmetry relates the regulators of bosonic and fermionic fields. This puts further constraints on the admitted cutoff functions r_1 and r_2 in a supersymmetric theory.

6.2.3 Flow Equations

Next, it is turned to the supersymmetric RG flow in the local potential approximation, i.e. Γ_k is given by (6.8) with $Z_k(R)$ and $Y_k(R)$ set to zero. The flow of the renormalized superpotential $W_k(\bar{\rho})$ in Euclidean space is obtained by considering the spatially constant field configuration

$$\Phi_i(q, \theta) = \phi \delta_{i1} \delta(q), \quad (6.14)$$

corresponding to setting the fermions and the auxiliary fields to zero and projecting onto one of the N components of the scalars. After the evolution equation has been derived in Minkowski space-time, a Wick-rotation of the zeroth momentum is performed. Appendix D presents an elaborate derivation of the flow of $W_k(\bar{\rho})$.

The regulator function r_1 acts as a mass-like IR regulator rather than as UV-regulator. In contrast, r_2 serves both as IR and UV regulator. Thus, r_1 is neglected and r_2 used in what follows. Then, the scale-dependence of the superpotential is determined by

$$\partial_t W_k = -\frac{1}{2} \int \frac{d^3 q}{(2\pi)^3} \partial_t r_2 \left(\frac{(N-1)W'_k}{(1+r_2)^2 q^2 + W_k'^2} + \frac{W'_k + 2W_k'' \bar{\rho}}{(1+r_2)^2 q^2 + (W'_k + 2W_k'' \bar{\rho})^2} \right). \quad (6.15)$$

Similar to the bosonic $O(N)$ model, the flow receives contributions from the $N-1$ Goldstone modes (the first term) and from the radial mode (second term). Following [48, 88, 165, 166], the regulator r_2 is chosen to be of the form

$$r_2(q^2) = \left(\frac{k}{|q|} - 1 \right) \theta \left(\frac{k^2}{q^2} - 1 \right). \quad (6.16)$$

This choice implies $\partial_t r_2$ to vanish identically for $q^2 > k^2$, and the inverse propagators

$$(1+r_2)^2 q^2 + X = \begin{cases} q^2 + X & \text{for } q^2 > k^2 \\ k^2 + X & \text{for } q^2 < k^2 \end{cases}$$

become flat (momentum independent) in the regime where the right hand side of (6.15) is non-vanishing. In the LPA, this is a solution to the general optimization condition for scalar $O(N)$ theories [88, 165, 166] and is therefore expected to lead to an improved convergence and stability of the RG flow. In order to achieve a relatively simple form of the flow, the rescaling

$$\bar{\rho} \rightarrow \frac{N}{8\pi^2} \bar{\rho}, \quad W \rightarrow \frac{N}{8\pi^2} W \quad (6.17)$$

of the fields and the superpotential is employed. Note that W' is invariant under the rescaling which absorbs the redundant overall factor $1/(8\pi^2)$, originating from the momentum integration, into the field and the superpotential. The additional rescaling with N also removes the leading N -dependence from the RG equation. In these conventions, and with given initial condition $W_{k=\Lambda}(\bar{\rho})$, the RG flow determines the superpotential in the infrared limit $k \rightarrow 0$. Considering the above rescaling and inserting the regulator function (6.16) then yields the flow

$$\frac{N}{k^2} \partial_t W = -(N-1) I \left(\frac{W'}{k} \right) - I \left(\frac{W' + 2\bar{\rho} W''}{k} \right) \quad (6.18)$$

of the superpotential, where $I(x) = x/(1+x^2)$. It is understood that W and its derivatives

are functions of the RG scale k and the fields and the index k will be omitted in the following. The first term on the right hand side of (6.18) describes the contribution of the $N - 1$ Goldstone modes and the last term is the contribution of the single radial mode. Note that the right hand side of the flow vanishes for $W' \equiv 0$, and for $1/|W'| \rightarrow 0$, corresponding to the classical limit where the couplings and the potential (6.6) are independent of the RG scale.

To study the critical behavior of the theory, the flow is rewritten in dimensionless quantities. In particular, it is switched to a dimensionless field variable ρ , a dimensionless superpotential w and a dimensionless scalar potential v according to

$$\rho = \frac{\bar{\rho}}{k}, \quad w(\rho) = \frac{W(\bar{\rho})}{k^2}, \quad v(\rho) = \frac{\bar{\rho}}{k} \left(\frac{W'(\bar{\rho})}{k} \right)^2. \quad (6.19)$$

In terms of (6.19) the flow equation (6.18) then reads

$$\partial_t w + 2w - \rho w' = -\left(1 - \frac{1}{N}\right)I(w') - \frac{1}{N}I(w' + 2\rho w''). \quad (6.20)$$

The evolution of the scalar potential $v(\rho)$ is determined by the scale-dependence of $w'(\rho)$. Therefore, the flow equation for $w' \equiv u$,

$$\partial_t u + u - \rho u' = -\left(1 - \frac{1}{N}\right)u' I'(u) - \frac{1}{N}(3u' + 2\rho u'') I'(u + 2\rho u') \quad (6.21)$$

is quoted for completeness.

6.3 Exploring the Limit of Infinitely Many Fields

In the previous section, the PDE (6.18) characterizing the scale-dependence of the superpotential $W_k(\phi)$ has been derived. Unfortunately, this second-order PDE is of a highly non-linear nature. Due to those properties, an analytical handling of the full equation is hardly possible. There are several ways of tackling this issue. Firstly, a numerical access would be feasible. Secondly, approximations of the full equation could be considered and possibly solved. Within this chapter, the second line is taken. In particular, the *large- N limit* with $N \rightarrow \infty$ will be explored. This approximation offers an exact analytical treatment of the PDE via the “method of characteristics”, since its order decreases by one in this limit. Moreover, it has been shown to allow for “[...] *a very detailed quantitative description for the “transition to complexity”.*”³ As this citation regarding the large- N limit of the scalar $O(N)$ model in $d = 3$ indicates, the limit of infinitely many fields is expected to describe the phase structure of the supersymmetric analogue in a quite satisfactory way. Besides,

³See [31], section 3.3, page 40.

the next-to-leading order in the supercovariant derivative expansion contains the anomalous dimension $\eta \sim 1/N$ which does not contribute in this limit.

The large- N limit has been successfully applied to various theories featuring an internal symmetry group as e.g. $SU(N)$ and $SO(N)$. For example, $SU(N)$ Yang-Mills theory can be simplified considerably in the limit where the number of colours N becomes large as proposed firstly by t'Hooft [167]. Moreover, in mean field theory it serves for modelling free particles in a constant external field as well as phase transitions [168]. A further interesting application are matrix models of $2d$ gravity. Here, space-discretized gravity is reformulated in terms of matrix integrals. The continuum is then recovered by the limit where the matrix size N tends to infinity; see [68], appendix A22.

6.3.1 RG Flow and Boundary Condition

In the large- N limit, the Goldstone modes fully dominate the dynamics and the contribution of the radial mode becomes a sub-leading effect. Besides, the anomalous dimension of the Goldstone modes vanish, as no momentum-dependent two-point function exists that contributes to the running of the kinetic term of these modes to leading order in N . This is a particular feature of the bosonic $O(N)$ models [68] and their supersymmetric extensions⁴. Consequently, the LPA approximation becomes *exact* for $N \rightarrow \infty$.

Due to the rescaling (6.17) of the fields and the superpotential respectively, the limit of infinitely many fields $N \rightarrow \infty$ is taken easily in the RG flow (6.21). The evolution equation for the first derivative of the superpotential $u \equiv w'$ then simplifies to

$$\partial_t u + u - \rho u' = -\frac{1 - u^2}{(1 + u^2)^2} u'. \quad (6.22)$$

The second-order PDE (6.21) has thus turned into the first-order PDE above which can be solved analytically via the method of characteristics. The first characteristic reads $ue^t = \text{const.}$ and the second one is

$$\frac{\rho - 1}{u} - F(u) = \text{const.} \quad \text{with} \quad F(u) = \frac{u}{1 + u^2} + 2 \arctan u. \quad (6.23)$$

Altogether, this yields

$$\frac{\rho - 1}{u} - F(u) = G(ue^t) \quad (6.24)$$

for all $\rho \geq 0$, where the function $G(ue^t)$ is determined by the boundary condition for $u(\rho)$, imposed at the initial UV scale $k = \Lambda$. The validity of the solution (6.24) is confirmed by direct insertion into (6.22). For completeness, the RG equation for the bosonic potential is

⁴A counterexample is given by Yukawa-type systems which may have large anomalous dimensions in the large- N limit [169].

given. Using (6.19) and (6.23), its evolution is determined by

$$\partial_t v + 3v - \rho v' = (v - \rho v') \frac{\rho - v}{(\rho + v)^2}. \quad (6.25)$$

Note that up to minor modifications, equation (6.22) holds for general space-time dimensions away from $d = 3$. The canonical mass dimension of u is one for all dimensions and the dependence on space-time dimensionality, therefore, only enters via the field variable leading to the replacement of $(-\rho)$ by $(2 - d)\rho$ in (6.22). This modifies the second characteristic equation, whose solution is expressed in terms of the hypergeometric function for arbitrary dimension $d \neq 1$. The analysis below restricts to the case $d = 3$.

Next, the boundary condition at the UV reference scale $k = \Lambda$ is specified according to

$$k = \Lambda : \quad \begin{cases} u(\rho) & = \tau (\rho - \kappa) \\ W'(\bar{\rho}) & = \tau (\bar{\rho} - \kappa \Lambda), \end{cases} \quad (6.26)$$

where τ denotes the dimensionless quartic superfield coupling at the cutoff. If the UV parameter κ is positive, $\kappa \Lambda$ is interpreted as VEV for the scalar field at $k = \Lambda$. Notice that according to (6.26), the classical superpotential $W_\Lambda(\Phi)$ is assumed to be quartic in the superfields. This implies the microscopic scalar potential $V_\Lambda(\bar{\rho}) = \bar{\rho} W'_\Lambda{}^2(\bar{\rho})$ to be of sixth order in the scalar fields ϕ_i . As already stressed in the introduction of this chapter, a relevant difference to the scalar $(\phi^2)_{d=3}^3$ model emerges out of this fact: the supersymmetric $O(N)$ model considered is characterized by only two renormalized parameters, contrary to the scalar counterpart (see e.g. figure 6.1) which is determined by three classical couplings. Since the bosonic potential is proportional to the superpotential squared, supersymmetry links the couplings, resulting in reduced degrees of freedom.

Taking into account the boundary condition (6.26), the function $G(x)$ adopts the form

$$G(x) = \frac{1}{\tau} - F(x) + \frac{\kappa - 1}{x} \quad (6.27)$$

in terms of the initial parameters. For initial conditions different from (6.26) the function is modified accordingly. Thus, the general implicit solution of (6.22), satisfying the boundary condition (6.26), reads

$$\frac{\rho - 1}{u} - F(u) = \frac{1}{\tau} - F(ue^t) + \frac{\kappa - 1}{ue^t}. \quad (6.28)$$

The above solution may be rewritten in order to obtain the suitable structure

$$\begin{aligned} \rho - \rho_0(t) &= c u + H(u) - H(ue^t) e^{-t} \\ \rho_0(t) &= 1 + \delta \kappa e^{-t}, \quad c = 1/\tau, \end{aligned} \quad (6.29)$$

where the non-negative function

$$H(u) \equiv u F(u) = \frac{u^2}{1+u^2} + 2u \arctan u \quad (6.30)$$

encodes the RG modifications due to fluctuations. The parameter $\delta\kappa = \kappa - 1$ measures the deviation of the VEV at the initial scale $\rho_0(t=0) = \kappa$ from its critical value $\kappa_{\text{cr}} = 1$. For any positive deviation, $\rho_0(t) \rightarrow \infty$ in the infrared limit corresponding to a finite dimensionful VEV of the scalar field. The bosonic potential V shows a second minimum at $\bar{\rho} = 0$ due to its definition (6.6). Hence, global $O(N)$ symmetry is (not) spontaneously broken if the finite (vanishing) VEV is taken. Conversely, for a negative $\delta\kappa$ we have $\rho_0(t) < 0$ in the IR limit such that the global minimum of the effective potential is achieved for vanishing $\bar{\rho}$. This leaves the global $O(N)$ symmetry intact. The case $\delta\kappa = 0$ then corresponds to the phase transition between the $O(N)$ symmetric and spontaneously $O(N)$ broken phase.

Thus, it is concluded from (6.29) that an IR repulsive mode is associated with $\rho_0(t)$, solely controlled by the initial VEV. This has been observed previously in purely scalar theories in the large- N limit [65]. All the remaining couplings included in the potential are either exactly marginal or IR attractive. Their flow is encoded in the term $H(ue^t)e^{-t}$ in the first equation of (6.29). This *factorization* of the solution is a consequence of the large- N limit and allows for a straightforward analysis of the entire phase structure of the model. The global form of solutions $u(\rho, t)$ is mainly determined by the coupling $\tau = 1/c$ and the function H , with ρ_0 only entering through a shift of the ρ -axis.

The non-negative function H appearing in the implicit solution (6.29) will be of importance below. Expanding H in powers of $1/u$ leads to

$$H = \pi |u| - 1 - \frac{1}{3u^2} + \mathcal{O}\left(\frac{1}{u^4}\right). \quad (6.31)$$

Conversely, an expansion for small u gives

$$H = 3u^2 - \frac{5}{3}u^4 + \frac{7}{5}u^6 + \mathcal{O}(u^8). \quad (6.32)$$

Since $H(u)$ is an even function, the solution (6.29) is invariant under $(c, u) \leftrightarrow (-c, -u)$. Furthermore, the scalar field potential only depends on u^2 . Thus, the following discussion is restricted to $c \geq 0$.

6.3.2 Fixed-Point Structure

Supersymmetric Fixed Points

Fixed points are scale-independent solutions of (6.22), i. e. solutions u_* satisfying $\partial_t u_*(\rho) = 0$. Besides the Gaussian fixed-point solution $u_* \equiv 0$, non-trivial fixed points follow from (6.24)

in the limit where $G(ue^t)$ becomes a t -independent constant. Hence, fixed-points of the supersymmetric $O(N)$ model obey

$$\rho = 1 + H(u_*) + cu_*, \quad (6.33)$$

where the constant c is related to the marginal quartic superfield coupling τ as $c = 1/\tau$. Apparently, a classification of possible fixed-point solutions then solely depends on the real parameter c . With $|u_*| \in [0, \infty)$ and for a fixed c , equation (6.33) identifies the range of achievable field values. Candidates for physical fixed points $u_*(\rho)$ are those solutions which extend over all fields $\rho \in [0, \infty)$. Figure 6.2 displays the entire set of solutions $\rho(u_*)$ to (6.33) for all c . Any solution $u_*(\rho)$ with parameter c is equivalent to the reflected solution $-u_*(\rho)$ with parameter $-c$, leading to physically equivalent, identical scalar potentials v_* .

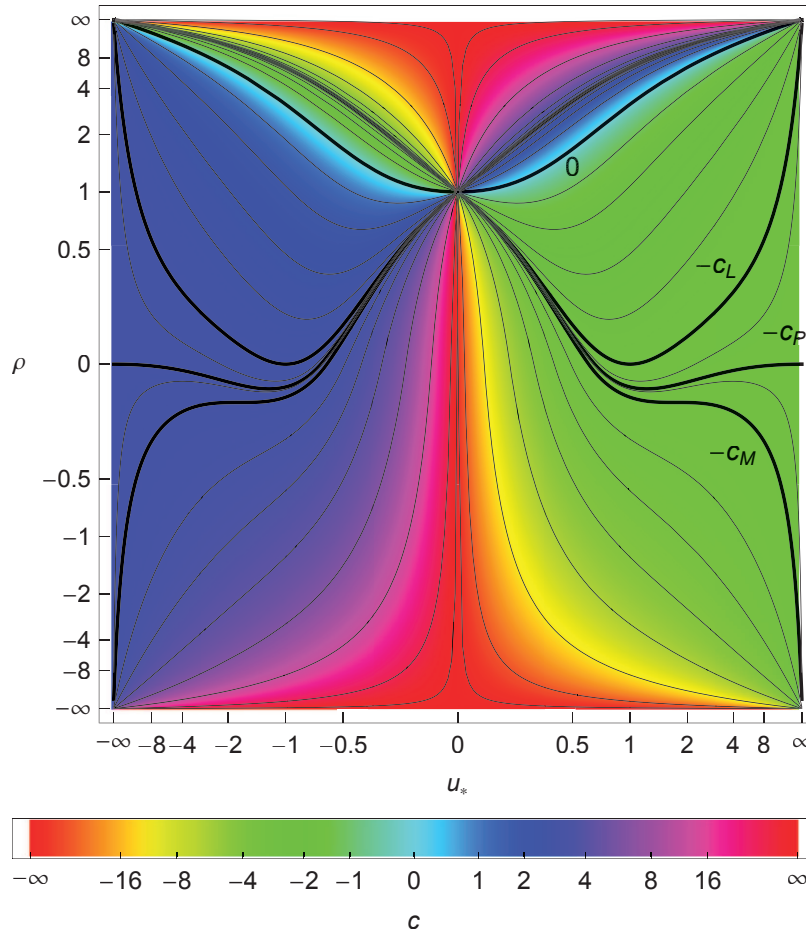


Figure 6.2: Supersymmetric fixed point solutions $\rho(u_*)$ for all fields ρ and all superfield potentials u_* , color-coded by the free parameter c . Both axes are rescaled as $x \rightarrow \frac{x}{1+|x|}$ for display purposes. Thin lines are included to guide the eye, thick lines correspond to distinguished values for c (c_I, c_L, c_P, c_M) as defined in (6.37).

Now, the fixed-point solution (6.33) is discussed in more detail. All curves pass through $(\rho, u_*) = (1, 0)$ which follows immediately from (6.33) due to $H(0) = 0$. As figure 6.3

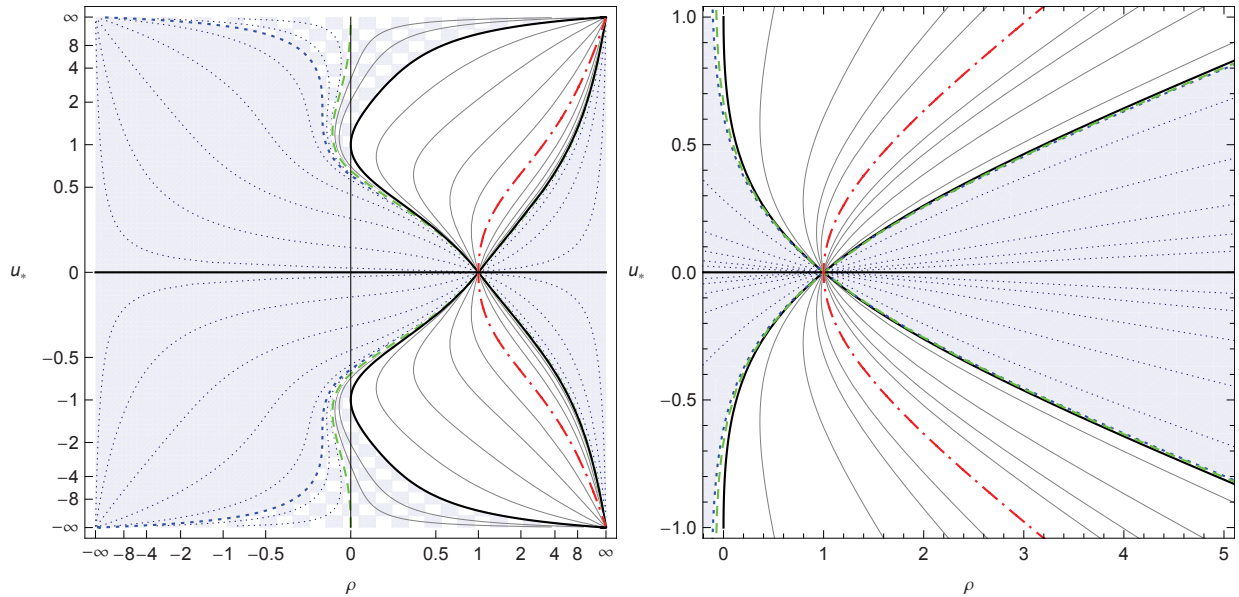


Figure 6.3: Supersymmetric fixed point solutions $u_*(\rho)$ according to (6.33), covering the entire parameter range for c . With decreasing c , fixed point curves rotate counter-clockwise around $(\rho, u_*) = (1, 0)$ starting with $c = \infty$ where $u_* = 0$ (horizontal line), passing through $c = 0$ (red, dashed-dotted line), completing a rotation of 180° at $c = -\infty$ (horizontal line). Further special lines refer to $|c| = c_M$ (blue dashed), $|c| = c_P$ (green, long dashed), $|c| = c_L$ (black, full lines), see main text. *Left panel:* fixed point solutions for all fields (both axes are rescaled as $x \rightarrow \frac{x}{1+|x|}$ for display purposes). *Right panel:* fixed point solutions for physical fields in the vicinity of $\rho = 1$.

illustrates, the fixed point solutions fall into two distinct classes, and solutions in the same class show the same global behaviour. Depending on the value of c , the solution u_* is either defined for all real ρ or it has a turning point at $|\rho_s| < \infty$ and is only defined for $\rho \in [\rho_s, \infty)$. In the latter case the solution has two branches bifurcating at $\rho = \rho_s$. This issue of the appearance of *non-unique* fixed-point solutions $u_*(\rho)$ is analysed in more detail in the subsequent section.

Next, some limiting cases of interest are considered in more detail. For small u_* , (6.33) and (6.32) lead to

$$\rho - 1 = c u_* + 3 u_*^2 + \mathcal{O}(u_*^4). \quad (6.34)$$

Hence, the potential is analytical in $\rho - 1$ in the vicinity of $\rho = 1$ for all c , except for $c = 0$ where it becomes non-analytical with $u_* \propto \sqrt{\rho - 1}$. Equation (6.34) implies all fixed-point solutions to have one simple zero at $\rho = 1$ with finite $u'_*(1)$ except for $c = 0$, where $u'_*(1)$ diverges. Consequently, the scalar fixed-point potentials $v_* = \rho u_*^2$ possess two minima at $\rho = 0$ and $\rho = 1$, the first one being a simple zero. The second minimum is a double zero for $c \neq 0$ and a simple zero for $c = 0$. Furthermore, the large- u_* limit of (6.33) is regarded, where $H(u)$ is expanded according to (6.31). The scaling solution then behaves as

$$\rho = \pi |u_*| + c u_* + \mathcal{O}(1/u_*^2). \quad (6.35)$$

Thus the asymptotic behavior of u_* is given by

$$\begin{aligned} u_* &= \frac{\rho}{c + \pi} + \text{subleading} \quad (u_* > 0), \\ u_* &= \frac{\rho}{c - \pi} + \text{subleading} \quad (u_* < 0). \end{aligned} \quad (6.36)$$

If $|c| > c_P \equiv \pi$, the expansions extend towards $\rho \rightarrow \pm\infty$ and $u_*(\rho)$ is defined for all real ρ (for illustration see figure 6.3). At $|c| = c_P$, the leading term in (6.35) vanishes and, depending on the sign of c , one of the asymptotic solutions is replaced by $u_* \sim \rho^{-1/2}$ thus corresponding to a small field regime $\rho \ll 1$. For even stronger couplings $|c| < c_P$, both expansions extend towards $\rho \rightarrow +\infty$. Hence, in this sector u_* shows two asymptotic expansions for large positive ρ .

Above, the distinguished value $c = c_P = \pi$ has already been mentioned. However, a full characterization of all fixed-point solutions according to their global behaviour requires the introduction of five specific values

$$\begin{aligned} c_I &= 0 \\ c_L &= \frac{1}{2}(\pi + 3) \\ c_P &= \pi \\ c_M &= \frac{2}{3}\pi + \frac{5}{8}\sqrt{3} \\ c_G &= \infty \end{aligned} \quad (6.37)$$

of the inverse quartic superfield coupling $1/\tau = c$. Subsequently, the different classes of scaling solutions ranging from the weakly to the strongly coupled regime are characterized. Firstly, the Gaussian fixed-point solution $u_*(\rho) = 0$ is described by a vanishing ϕ^6 coupling corresponding to $c_G = \infty$. In the

$$\text{weak coupling regime:} \quad c_P < |c| < c_G, \quad (6.38)$$

the scaling solutions extend in compliance with (6.36) over the entire real axis including the physical field space $\rho \geq 0$. For $|c| \geq c_M$, the fixed-point solutions are monotonous functions $u_*(\rho)$. In contrast, for $c_P < |c| < c_M$, a turning point $\rho_s < 0$ appears, where the field-dependent dimensionless mass term $u'_*(\rho)$ diverges. Those fixed-point solutions are single-valued in the physical regime $\rho \geq 0$ but multi-valued in the non-physical regime $\rho < 0$. In the

$$\text{intermediate coupling regime:} \quad c_L < |c| < c_P, \quad (6.39)$$

the global behaviour of the scaling solutions drastically changes. As shown above, u_* then has, simultaneously, two asymptotic expansions for large positive ρ . This implies that v_*

displays a loop consisting of two branches $v_<$ and $v_>$ which coincide at $\rho = 0$, $\rho = \infty$ and some $\rho_s < 0$, where u_* has infinite slope. This behaviour is illustrated in figure 6.4, left panel. The

$$\text{strong coupling regime:} \quad c_I < |c| \leq c_L \quad (6.40)$$

is characterized by solutions not extending over all physical fields $\rho \geq 0$, i.e. the turning point of ρ_s moves into the physical regime. Finally, the extreme value $c_I = 0$ corresponding to an infinitely large ϕ^6 coupling τ reflects the ‘would-be’ Wilson-Fisher fixed-point solution and will be discussed in more detail in section 6.3.3. Note that numerically, the ranges

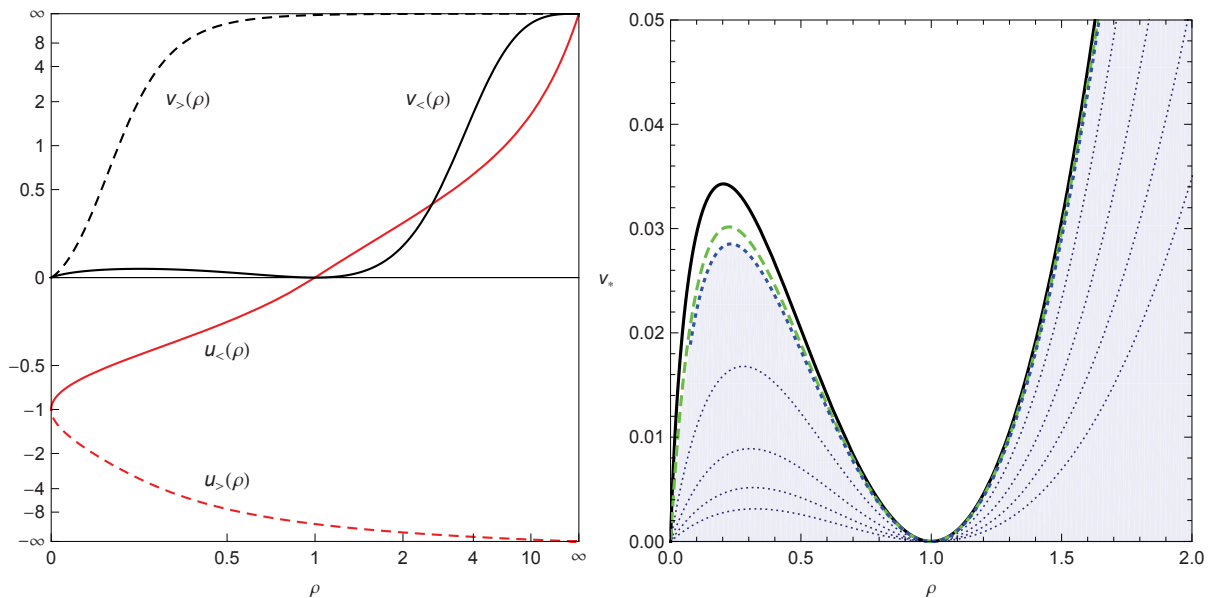


Figure 6.4: *Left panel:* Scaling solution u_* and fixed-point potentials $v_* = \rho u_*^2$ at $|c| = c_L$ showing the two branches $v_<, u_<$ (full lines) and $v_>, u_>$ (dashed lines). *Right panel:* The scalar fixed-point potential $v_*(\rho)$ for different c : c_L (black line), c_P (green, long dashed), c_M (blue, short dashed) and $c = a^n c_L$, $a = 2^{1/4}$ with $n = 1.0, 2.3, 3.6, 4.9$ (blue, dotted). For c_L and c_P just one branch is plotted.

$$\frac{c_M - c_P}{c_P} \simeq 0.011, \quad \frac{c_P - c_L}{c_P} \simeq 0.023 \quad (6.41)$$

are very small. The scalar fixed point potential v_* is displayed in figure 6.4 (right panel) for various values of c .

Non-analyticities

In the previous section, several classes of fixed-point solutions, distinguished by varying microscopic parameters c , have been presented briefly. This section explains the appearance of the non-analytic behaviour in the integrated flows at intermediate and strong couplings in more detail. This discussion completes the general description of scaling solutions above and will be of help to understand the RG flows away from critical points in section 6.3.4.

By construction, the Wetterich equation is well-defined. Furthermore, the right hand

side of the supersymmetric flow (6.22) is bounded, provided that the superpotential remains real. Incidentally, this is in contrast to the standard purely bosonic flows, which potentially may grow large in a phase with spontaneous symmetry breaking. Despite their boundedness, the supersymmetric fixed point solutions display *Landau-type poles* at strong coupling due to non-analyticities, such as cusps, of the integrated RG flow. This can be appreciated as follows: consider the field-dependent dimensionless mass term $u'(\rho)$. The fixed-point solution (6.33) implies $u'(\rho)$ to diverge, provided that

$$\left. \frac{d\rho}{du} \right|_{u_s} = c + H'(u_s) = 0. \quad (6.42)$$

This condition determines the singular value u_s and from (6.33), the value

$$\rho_s = \frac{1 - u_s^2}{(1 + u_s^2)^2} \quad (6.43)$$

of the singular field is obtained. The function $H'(u)$ is odd and bounded by $H'(u_c) = \pm c_M$. Asymptotically, it approaches $|H'(u \rightarrow \pm\infty)| = c_P < c_M$ as shown in figure 6.5. Hence, with

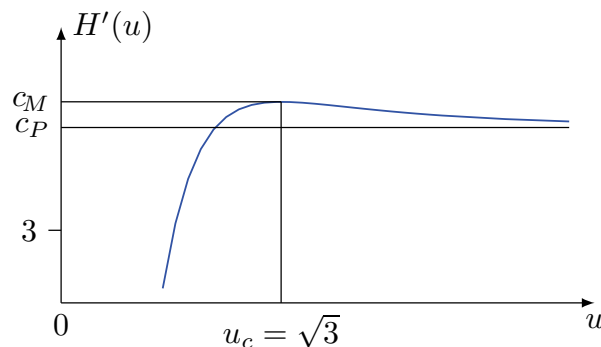


Figure 6.5: The non-monotonic odd function $H'(u)$.

decreasing $|c|$ (increasing coupling strength τ), a divergence for u' is first encountered for $|c| = c_M$. Performing an expansion of (6.33) up to the first non-trivial order yields

$$\rho - \rho_c = \frac{1}{6} H'''(u_c) (u_* - u_c)^3. \quad (6.44)$$

Note that (6.44) is continuous across $(u_*, \rho) = (u_c, \rho_c)$. Therefore, the non-analyticity in the solution can be written as

$$u_* - u_s = \pm \operatorname{sgn}(\rho - \rho_c) \left| \frac{\rho - \rho_c}{\frac{1}{6} H'''(u_c)} \right|^{1/3}, \quad (6.45)$$

where the signs refer to $c = \pm c_M$. This directly leads to the non-perturbative Landau pole

$$\frac{1}{u'_*} = \pm \frac{9}{2} |H'''(u_c)|^{1/3} |\rho - \rho_c|^{2/3} \quad (6.46)$$

in u'_* . The determined Landau pole remains invisible, because it is achieved at the negative fields $\rho_c = -1/8$. However, increasing the coupling by lowering $|c|$ below c_M , the expansion in the vicinity of $d\rho/du = 0$ becomes

$$\rho - \rho_s = \frac{1}{2} H''(u_s) (u_* - u_s)^2 \quad (6.47)$$

up to sub-leading terms, where u_s is determined through (6.42). In this regime, $H''(u_s)$ is non-zero throughout. Within the weakly coupled regime $c_P \leq |c| < c_M$, two solutions for u_s with $|u_{s1}| < |u_c| < |u_{s2}|$ and $H''(u_{s1}) < 0 < H''(u_{s2})$ can be identified. Effectively, the solution for the superpotential becomes multi-valued in a limited region of field space. For stronger couplings $|c| < c_P$, only one solution for u_s with $H''(u_s) > 0$ is left. In contrast to (6.46), the non-analyticity has turned into a square root,

$$\frac{1}{u'_*} = \pm 2 |H''(u_s)|^{1/2} (\rho - \rho_s)^{1/2} . \quad (6.48)$$

The non-analyticity (6.48) is stronger than (6.46) and the solution (6.47) cannot be continued continuously beyond the point $(u_*, \rho) = (u_s, \rho_s)$. In the strong coupling regime $|c| < c_L$ the singular field value $\rho_s(c) > 0$, i.e. the pole, moves into the physical field space.

It is interesting to note that non-analyticities, such as cusps, have been detected previously in the context of the random field Ising model, where disorder is technically introduced with the help of Parisi-Sourlas supersymmetry. Using functional renormalization, it has been argued that a cusp behaviour at finite ‘‘Larkin scales’’ $k = k_L > 0$ is at the origin for the spontaneous breaking of Parisi-Sourlas supersymmetry [170–172].

At this point it should be mentioned that the superpotential W' shows another non-analytic behaviour: It is not differentiable at its node $\bar{\rho}_0$ in the exact IR limit for arbitrary couplings $c > 0$. This issue is discussed in detail in section 6.3.5 below.

Exactly Marginal Coupling & Line of Fixed Points

This section clarifies the physical meaning of the parameter c . To this end, a polynomial expansion of the RG-time dependent superpotential $u(t, \rho)$ satisfying the flow equation (6.22) is employed. For the initial condition (6.26), there always exists a node $\rho_0(t)$ around which a Taylor expansion

$$u(t, \rho) = \sum_{i=1}^n a_i(t) (\rho - \rho_0(t))^i \quad (6.49)$$

with $\tau = a_1(0)$ and $\kappa = \rho_0(0)$ can be performed. By inserting this ansatz into the flow equation (6.22), the evolution equations

$$\partial_t \rho_0 = 1 - \rho_0 \quad (6.50)$$

$$\partial_t a_1 \equiv 0 \quad (6.51)$$

$$\partial_t a_2 = 3a_1^3 + a_2 \quad (6.52)$$

for the lowest scale-dependent couplings are derived. Several comments are in order at this point. Firstly, the running of the VEV $\rho_0(t)$ is independent of all the other local couplings. This property is typical for a supersymmetric flow and has previously been observed in the context of two- and three-dimensional $\mathcal{N} = 1$ Wess-Zumino models [48, 50, 56]. The fixed point is obtained for $\rho_0 = 1$. Secondly, the system of algebraic equations describing the t -independent fixed-point couplings can be solved recursively. This leads to fixed-point couplings $a_{i*}(a_1)$ for all $i \geq 2$. Inserting (6.49) into the expansion of the scalar field potential $v = \rho u^2 = \sum_{i=2} \lambda_i (\rho - \rho_0)^i$ and evaluating it on the fixed point leads to the fixed-point values

$$\lambda_{2*} = a_1^2 \quad (6.53)$$

$$\lambda_{3*} = a_1^2 (1 - 6a_1^2) \quad (6.54)$$

$$\lambda_{4*} = -a_1^4 (6 - 45a_1^2) \quad (6.55)$$

and similarly to higher order. Clearly, the weak (strong) coupling regimes correspond to small (large) λ_2 and hence small (large) a_1 respectively. Also, on the level of the scalar field potential the critical behaviour is independent of the sign of a_1 . Finally, and most importantly, the coupling a_1 remains un-renormalized under the supersymmetric RG flow (6.51). Therefore $a_1 = \tau$ corresponds to an *exactly marginal coupling*, and fixed points can be classified according to the value of the quartic (dimensionless) superfield interaction τ which relates to the free parameter c in the analytical solution (6.33) as

$$c = \frac{1}{\tau}. \quad (6.56)$$

Hence, the presence of the exactly marginal coupling a_1 explains the existence of a *line of fixed points* in the space of couplings. Similar findings for scalar $O(N)$ models in $d = 3$ have been nicely presented in [173] by J. Comellas and A. Travesset. The authors explored the large- N limit by using the Wegner-Houghton equation in LPA. For $N \rightarrow \infty$, they made the following observations⁵:

“[...] *the marginal operator becomes completely marginal and a line of inequivalent FP appears, though they have the critical exponents of the GFP. This might be a general feature of this*

⁵FP= fixed point, GFP= Gaussian fixed point

limit.”

Similar to the findings above, they showed the line of fixed points to be margined by the Gaussian fixed point for $c = \infty$ on the one hand and the Heisenberg fixed point for $c = 0$ on the other hand. Also, they discovered Gaussian scaling similar to the scaling behaviour of the supersymmetric counterpart analysed here (see section 6.3.3).

This section is closed by a summary of the picture that has emerged by analysing all possible scaling solutions of the SUSY $O(N)$ model. An analytical form (6.33) of the scaling equation has been derived, showing that it displays a line of non-trivial fixed points solely parametrized by the exactly marginal quartic superfield coupling $\tau = 1/c$. The line is bordered on the one side by the Gaussian fixed point $\tau = 1/c = 0$ for vanishing coupling. In the *weakly coupled regime* (6.38), a unique fixed point solution exists covering the whole physical domain $\rho \geq 0$. In the *intermediate coupling regime* (6.39) two separate fixed point solutions $u_<$ and $u_>$ exist. The former solution has a node at $\rho_0 = 1$ whereas the other solution has no node, see figure 6.4, left panel. Therefore, the corresponding scalar field potentials $v_<$ ($v_>$) have two (one) minima at $\rho = 0$ and $\rho = 1$. Both are analytical functions of ρ in the vicinity of their global minima. In the *strong coupling regime* (6.40), the theory becomes so strongly coupled that $du/d\rho|_{\rho_s}$ diverges in the physical field space. Thus, no fixed-point solution exists which extends over all fields here. Therefore, the supersymmetric $O(N)$ model displays a line of fixed points which bifurcates at $|c| = c_P$ into two fixed points, and then terminates at $|c| = c_L$. Finally the solution with $c = 0$ is closely linked to the Wilson-Fisher fixed point in the purely bosonic model [65, 164, 174], see section 6.3.3.

6.3.3 Universality

This section describes the universal behaviour of the IR fixed points marking the second-order phase transition in the large- N limit. Important universal quantities within this context are the critical exponents associated with the physics in the vicinity of the phase transition. In the beginning, the critical exponents are derived in two different ways. Firstly, a polynomial approximation of the superpotential is employed. Subsequently, the critical exponents are calculated analytically by considering small fluctuations around the scaling solution⁶. Finally, the connection between the fixed-points of the supersymmetric $O(N)$ theories and those of the scalar theory in $d = 3$ is clarified.

Critical Exponents

Fixed-point solutions are characterized by universal critical scaling exponents. The exponents can be deduced from the RG equations in several ways. For a start, it is turned towards the polynomial approximation (6.49) of the superpotential $u(t, \rho)$ of order n in terms of $n + 1$

⁶Note that the thermodynamic critical exponents are discussed later on in section 6.3.5 as well.

couplings. From their beta-functions (2.16), the universal exponents follow as the negative of the eigenvalues θ_n of their stability matrix B_i^j according to (2.18) and (2.19). By using the flow equation (6.22), the exponents

$$\theta_n = 1 - n, \quad n \in \mathbb{N}_0 \quad (6.57)$$

are derived both numerically and analytically. Hence, the fixed-point solutions found are non-Gaussian (except for $c = c_G$), yet they display Gaussian exponents. This behaviour is strikingly similar to the line of fixed points featuring Gaussian scaling in the scalar $(\phi^2)_{d=3}^3$ theory [173].

Note however, that the above analysis relies on local information of the RG flow in the vicinity of $u = 0$, showing that the scaling (6.57) is achieved mathematically for all $0 < |c| < \infty$. Physically, however, the analysis is not sensitive to the global behaviour of the solution, and consequently cannot detect that $|c| = c_L$ denotes a physical endpoint. Besides, the BMB phenomenon associated with $|c| = c_P$ requires an additional treatment. As will be shown in section 6.3.7, the scaling exponents become double-valued here due to a dissimilar scaling behaviour of different mass scales close to the fixed point. Also, the case $c = c_I$ needs special care as an analytical expansion about $u = 0$ is no longer applicable⁷.

Eigenperturbations

Interestingly, the critical exponents may also be calculated analytically without resorting to a polynomial expansion. To that end, consider small fluctuations δu about the fixed-point superpotential such that

$$u(t, \rho) = u_*(\rho) + \delta u(t, \rho). \quad (6.58)$$

Linearizing the flow equation (6.22) in δu leads to the fluctuation equation

$$\partial_t \delta u = \frac{u_*}{u_*'} \left(\partial_\rho - \frac{(u_* u_*')'}{u_* u_*'} \right) \delta u, \quad (6.59)$$

where primes denote a derivative with respect to the function's argument. Since the right hand side is independent of t , the differential equation (6.59) can be factorized via separation of variables, i.e. $\delta u(t, \rho) = f(t)g(\rho)$ with

$$\begin{aligned} (\ln f)' &= \lambda \\ (\ln g)' &= \lambda (\ln u_*)' + (\ln u_* u_*')', \end{aligned} \quad (6.60)$$

⁷At $c = c_I = 0$, the potential becomes non-analytical in the vicinity of $\rho = 1$ with $u_* \propto \sqrt{\rho - 1}$; see (6.34).

where λ denotes the eigenvalue. Integration leads to the exact solution

$$\delta u = C e^{\lambda t} u_*^{\lambda+1} u_*' \quad (6.61)$$

for the linear perturbation of the fixed-point superpotential. The allowed range of values for the eigenvalues λ is determined using regularity conditions for the eigenperturbations. As shown in (6.35), the fixed point potential u_* grows linearly with the field for large ρ and hence $\delta u \propto e^{\lambda t} \rho^{\lambda+1}$ for $\rho \gg 1$. Furthermore, for small u_* , i.e. in the vicinity of the node, the solution becomes (6.34). This leads to a finite u_*' (meaning $0 < u_*' < \infty$) for all $c \neq 0$. In summary, this yields

$$\delta u \propto e^{\lambda t} (\rho - 1)^{\lambda+1}. \quad (6.62)$$

Regularity of the perturbations requires non-negative integer values for the exponent $\lambda + 1$. Since the critical exponents are defined as the negative eigenvalues, we thus obtain (6.57).

Note that this line of reasoning assumes analyticity of the perturbation at the node which holds for all $c \neq 0$. For $c = 0$, u_* is non-analytical at $\rho = 1$ but u_*^2 instead is analytical and has a simple zero with finite $(u_*^2)'|_{u_*=0}$. Therefore, equation (6.61) may be used to relate the (regular) fluctuations of u^2 to u_*^2 , leading to

$$\delta u^2 = C e^{\lambda t} (u_*^2)^{\frac{1}{2}(\lambda+1)} (u_*^2)'. \quad (6.63)$$

Again, analyticity implies that the exponent $(\lambda + 1)/2$ is a non-negative integer and hence

$$\theta = 1 - 2n, \quad n \in \mathbb{N}_0. \quad (6.64)$$

Apparently, the above values are identical to the universal critical exponents of the 3d spherical model [173, 175]. It should be stressed, however, that this solution is not a proper scaling solution due to its limitation to field values $\rho \geq 1$.

Finally, the analysis of linear perturbations is extended to those of the function u^2 and the scalar potential $v = \rho u^2$. Starting with $u^2 = u_*^2 + \delta u^2$, an analytical solution is found by using the identity $\delta u^2 = 2u_* \delta u$ together with (6.61). The linear perturbations thus behave as

$$\delta u^2 = 2C e^{\lambda t} u_*^{\lambda+2} u_*'. \quad (6.65)$$

Note that the degree in u_* has increased by one unit. Employing the same reasoning as above for $c \neq 0$, the set of available negative eigenvalues is given by

$$\theta = 2 - n, \quad n \in \mathbb{N}_0. \quad (6.66)$$

Physically, the appearance of the eigenmode with eigenvalue -2 is due to the mass term squared, a term which on dimensional grounds is available in u^2 but not in u .

Finally, using (6.22), (6.25) and (6.65), the linear eigenperturbations about the scalar potential $v(t, \rho) = v_* + \delta v(t, \rho)$ are found as

$$\delta v = 2C e^{\lambda t} u_*^{\lambda+2} \left[u_* + u'_* \left(1 - u_*^2 F'(u_*) \right) \right]. \quad (6.67)$$

Close to $u_* = 0$, the term in round brackets reduces to one, and the square bracket becomes u'_* which is finite at $u_* = 0$. Therefore, regularity of eigenperturbations again implies (6.66). However, a non-supersymmetric scalar theory does not restrict the potential to be of the product form (6.19). Consequently, an additional eigenvalue of -3 , related to redundant shifts of the potential, becomes available.

We conclude that supersymmetry is responsible for the absence of the redundant eigenvalue -3 in the scalar potential, and for relating its two relevant eigendirections with eigenvalues -1 and -2 with the sole relevant eigendirection with eigenvalue -1 of the derivative of the superpotential.

Wilson-Fisher Fixed Point

It is interesting to understand how the supersymmetric model and its fixed points fall back onto those of the $3d$ non-supersymmetric scalar theory within the same approximation [65, 164, 174]. To that end, consider the $4d$ supersymmetric $O(N)$ model at finite temperatures T . The temperature is implemented using the imaginary time formalism. On the level of the flow equation, it amounts to the replacements [31, 88, 176]

$$\int_{-\infty}^{\infty} \frac{dq_0}{2\pi} f(q_0) \rightarrow T \sum_{n=-\infty}^{\infty} f(q_0 = 2\pi c_n T). \quad (6.68)$$

Here $2\pi c_n T$ denotes the n th Matsubara frequency with $c_n = n$ for bosons and $c_n = n + \frac{1}{2}$ for fermions. The temperature imposes periodic (anti-periodic) boundary conditions for bosons (fermions) and, consequently, softly breaks global supersymmetry. Within a derivative expansion, the relevant momentum integrals are performed analytically by using the four-dimensional version of (6.15), together with (6.68) and the momentum cutoff (6.16).

Now, what happens in the IR, where $k/T \rightarrow 0$? Due to (6.68), all fermions and bosons with non-vanishing Matsubara mass will decouple from the system, except for the bosonic zero mode. In this limit, the $4d$ supersymmetric model undergoes a dimensional reduction to a $3d$ non-supersymmetric theory, where all fermions have decoupled. In the large- N limit, the RG flow for the potential of the remaining bosonic zero mode in LPA is determined by

$$\partial_t z = -2z + \rho z' - \frac{1-z}{(1+z)^2} z', \quad (6.69)$$

where z is related to the scalar field potential via $v(\rho) = \rho z(\rho)$. The key difference to the

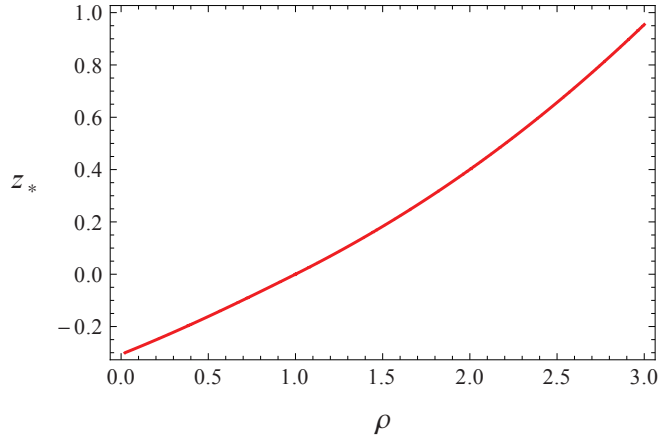


Figure 6.6: The Wilson-Fisher fixed point solution $z_*(\rho)$ of (6.69).

supersymmetric system studied previously is that the function z is no longer constrained to be the square of a superpotential derivative w' . Relaxing this constraint allows for an additional scaling solution, which follows from integrating (6.69) analytically. The general solution reads

$$\frac{\rho - 1}{\sqrt{z}} - \frac{\sqrt{z}}{1 + z} - 2 \arctan \sqrt{z} = B(z e^{2t}) \quad (6.70)$$

with $B(z e^{2t})$ fixed through initial UV conditions. For negative z , the solution is found by analytical continuation. In particular, (6.69) has a Wilson-Fisher fixed-point solution $z_* \neq 0$ with $z(\rho = 1) = 0$ corresponding to (6.70) with $B = 0$. The solution extends over all ρ with one unstable direction as pictured in figure 6.6. The eigenperturbations $z = z_* + \delta z$ are found analytically leading to (6.63) with the replacements $\delta u \rightarrow \delta z$ and $u_*^2 \rightarrow z_*$. Hence, the universal critical exponents are identical and given by (6.64).

The similarities and differences between the Wilson-Fisher fixed-point of the scalar model and the $c = c_I$ ‘would-be’ Wilson-Fisher fixed point of the supersymmetric theory can also be appreciated from the behaviour at small and large fields. In fact, for $\rho \geq 1$, $z_*(\rho)$ is positive and related to the real superpotential by $z_*(\rho) = w'_*(\rho)^2$. In turn, $z_*(\rho)$ is negative for all $\rho < 1$. Interestingly, this solution is still visible in the supersymmetric theory, where it corresponds to a purely imaginary “superpotential” $w'_*(\rho) = \pm i \sqrt{-z_*(\rho)}$. Hence, provided an imaginary superpotential is meaningful, the $c = c_I$ solution can be extended to a valid supersymmetric Wilson-Fisher fixed point for all ρ . However, the structure of the Lagrangian imposed by SUSY implies the field-dependent fermion mass term $\sim w'_*$ and the Yukawa-type fermion-boson interaction $\sim w''_*$ to become purely imaginary. Most importantly, a purely imaginary w'_* implicates the scalar potential to obey $v_*(\rho) = \rho w_*'^2 < 0$ for all fields within $0 < \rho < 1$. Unbroken SUSY requires the dimensional $V_k(\bar{\varrho})$ to remain positive for all fields and scales. In the IR limit, the dimensional potential approaches $V(\bar{\varrho}) = 64\pi^2 \bar{\varrho}^3 / N^2 \geq 0$. Hence, our results state that this potential can be approached arbitrarily close from within a phase with $O(N)$ symmetry and global supersymmetry.

6.3.4 Renormalized Theory

This section is devoted to a detailed discussion of the phase structure of the model and its spontaneous $O(N)$ symmetry breaking in the limit, where the UV scale Λ is removed.

Renormalization

Since the solution (6.29) is valid for all k and Λ , the ‘continuum limit’ $1/\Lambda \rightarrow 0$ may be taken. The explicitly t -dependent term in (6.29) thereby drops out in consequence of the limit $k/\Lambda \rightarrow 0$ for fixed and finite k and (6.32). The remaining scale-dependence solely reduces to the implicit scale-dependence of $\rho_0(k)$:

$$\rho - \rho_0(k) = c u + H(u) \quad \text{with} \quad \rho_0(k) = 1 + \bar{\rho}_0/k. \quad (6.71)$$

The dimensional parameter $\bar{\rho}_0$ has taken over the role of $\delta\kappa\Lambda$ in (6.29). Above, the VEV is the only quantity which is non-trivially renormalized in the continuum limit by requiring

$$\bar{\rho}_0 \equiv \lim_{\Lambda \rightarrow \infty} (\delta\kappa(\Lambda)\Lambda) < \infty. \quad (6.72)$$

Consequently, the canonical dimension of fields remains unchanged (no anomalous dimension). The continuum limit maps the original set of free parameters (τ, κ, Λ) to the parameters $(\tau, \bar{\rho}_0)$. All couplings of the superfield derivative – the marginal coupling c and the IR attractive higher-order couplings $u^{(n)}(\rho_0)$ – have settled on their fixed point values. The only ‘coupling’ not settled on a fixed point is the UV attractive dimensionless VEV ρ_0 . Thus, $\bar{\rho}_0$ and the non-renormalized parameter c are the free parameters of the theory, fixed by the microscopic parameters τ and κ . In terms of the dimensional quantities $\bar{\rho}$ and $W'(\bar{\rho})$, the integrated RG flow becomes

$$\bar{\rho} - \bar{\rho}_0(k) = c W' + k H(W'/k) \quad \text{with} \quad \bar{\rho}_0(k) = k + \bar{\rho}_0. \quad (6.73)$$

Note that $\bar{\rho}_0$ also has the interpretation of the physical VEV in the IR limit, provided it is positive. In the following sections, it will be advantageous to switch between the two representations (6.71) and (6.73).

Characteristic Energy

The RG flow (6.71), (6.73) carries a characteristic energy scale

$$E = |\bar{\rho}_0|, \quad (6.74)$$

meaning that the theory changes its qualitative behaviour depending on whether fluctuations have an energy larger or smaller than E . The scale is set by the UV renormalization

(6.72) of the model. For $k \gg E$, the dimensional VEV scales proportional to k . Ergo, the dimensionless parameter ρ_0 becomes a constant corresponding to a fixed point. All other dimensionless couplings equally have stopped to evolve with k and thus the entire solution approaches a high-energy (UV) fixed point. This fixed point would persist for all k provided that $E = 0$. Then, it represents an IR fixed point as well. This regime is most conveniently described using (6.71). For $E > 0$, and with decreasing k , deviations from the fixed point become visible once k reaches E . Here, the VEV displays a cross-over from linear scaling $\bar{\rho}(k) \propto k$ for $k \gg E$ to the constant value $\bar{\rho}_0$ for $k \ll E$. In full analogy, the dimensionless VEV displays a cross-over from a constant value to scaling inversely proportional to the RG scale. In addition, the running of all dimensional couplings in the potential is switched on once $k \approx E$ and below. This regime is conveniently described using (6.73) which governs the remaining RG running through its right hand side.

Gap Equations

At first, the phase structure is analysed in the IR limit $k = 0$. This allows for a direct comparison with earlier results based on gap equations and Schwinger-Dyson equations [155, 156]. Figure 6.7 displays the schematic phase diagram explained below. In the IR limit, (6.73) simplifies with (6.31) and (6.37) to

$$\bar{\rho} - \bar{\rho}_0 = c W' + c_P |W'| . \quad (6.75)$$

Since the potential shows a local minimum at vanishing field, the squared particle masses are given by

$$\bar{\mu}^2 = V''(\phi)|_{\phi=0} = W'^2(\bar{\rho})|_{\bar{\rho}=0} . \quad (6.76)$$

Thus, (6.75) becomes a gap equation for the mass parameter $\bar{\mu} \equiv W'(\bar{\rho} = 0)$,

$$\bar{\rho}_0 = -c \bar{\mu} - c_P |\bar{\mu}| . \quad (6.77)$$

The significance of (6.77) is as follows. For fixed $\bar{\rho}_0$ and c , it yields the possible IR solutions for the masses at vanishing field. Without loss of generality, the discussion is restricted to $c \geq 0$. For non-vanishing $\bar{\rho}_0$, there are two solutions

$$\begin{aligned} m = \bar{\mu} &= -\frac{\bar{\rho}_0}{c_P + c} \geq 0 & \text{and} \\ M = -\bar{\mu} &= -\frac{\bar{\rho}_0}{c_P - c} \geq 0. \end{aligned} \quad (6.78)$$

In the symmetric (SYM) regime ($\bar{\rho}_0 < 0$), the mass m is always present whereas the second mass M is available as long as $c < c_P$. Contrary, the regime allowing for spontaneous

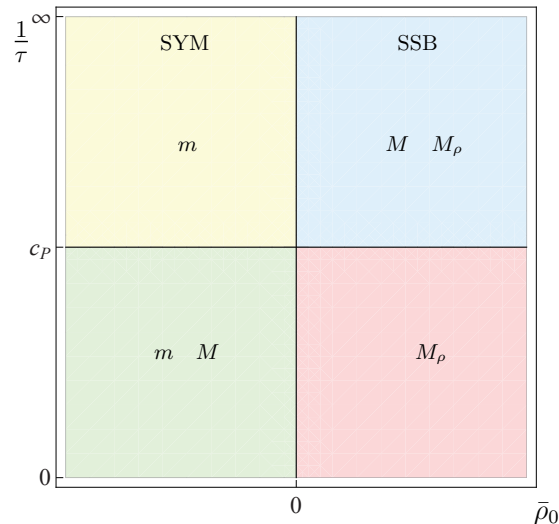


Figure 6.7: Schematic phase diagram of the supersymmetric model based on the gap equation (6.77) in the infinite cutoff limit. The results agree with earlier findings [155, 156].

$O(N)$ symmetry breaking (SSB) ($\bar{\rho}_0 > 0$) features two degenerate ground states: As expected, a non-symmetric ground state with a radial mass M_ρ is found, see section 6.3.5. However, for $c > c_P$, the gap equations show an additional symmetric ground state, characterized by the mass M . Note that changing the sign of c leads to equivalent results under the replacements

$$(c, m, M, M_\rho) \leftrightarrow (-c, M, m, -M_\rho). \quad (6.79)$$

At the phase transition ($\bar{\rho}_0 = 0$), (6.78) states that either $c = c_P$ with $M > 0$ undetermined, or $c = -c_P$ and m undetermined. Hence, at this point the gap equations reflect the phenomenon of spontaneously broken scale invariance which will be discussed in detail in section 6.3.7. These findings agree with previously obtained results [155, 156]. The sole difference is that the value for the critical coupling c_P depends on the regularization. The precise link to the conventions used in [155, 156] is given in table 6.1.

Heilmann et al. [59]	$\bar{\rho}_0$	$\tau = 1/c$
Bardeen et al. [155]	$-4\pi^2\mu\lambda^{-1}$	$(4\pi^2)^{-1}\lambda$
Moshe and Zinn-Justin [156]	$-4\pi^2(\mu - \mu_c)u^{-1}$	$(4\pi^2)^{-1}u$

Table 6.1: “Translation guide” between the conventions used in [155], [156] and our findings [59].

RG Phase Diagram

Above, the integrated evolution equation at $k = 0$ has been considered, leading to a gap equation (6.77) for the $O(N)$ bosonic and fermionic quanta. Now, the phase diagram implied by the flow equations for arbitrary k is considered and compared to the phase diagram obtained at $k = 0$. To begin with, a useful *graphical representation* of the renormalized

RG trajectories (6.71) is introduced. For vanishing $\bar{\rho}_0$, the trajectories (6.71) reduce to the scaling solutions $u_*(\rho)$ analysed in 6.3.2. The only difference is a shift of the argument, i.e.

$$u(\rho) = u_*(X), \quad \text{with} \quad X \equiv \rho + 1 - \rho_0(k) = \rho - \frac{\bar{\rho}_0}{k}. \quad (6.80)$$

The solutions and their dependence on the constant c is shown in figure 6.8.

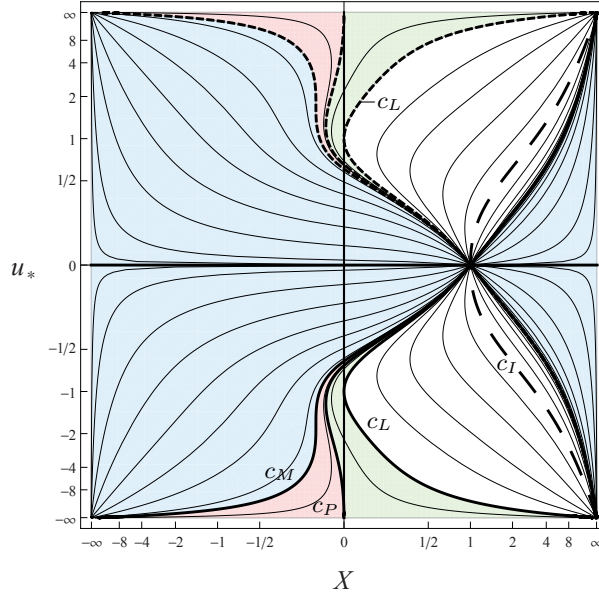


Figure 6.8: Graphical representation of the solutions $u_*(X)$ of (6.71), where $X = \rho - \bar{\rho}_0/k$. The shaded areas are separated by thick lines at $|c| = c_I, c_L, c_P, c_M$ and c_G , c.f. (6.37).

Once the free parameters are fixed, the RG evolution of a particular solution stays on a curve with constant c . By rotating counter-clockwise around $(X, u_*) = (1, 0)$ from the horizontal c_G -line to the c_I -curve (from the c_I -curve to the c_G -line), all curves with positive (negative) c are covered. Equations (6.80) and (6.71) imply

$$X \in [-\bar{\rho}_0/k, \infty) \quad (6.81)$$

for $u(\rho)$ to cover all physical fields $\rho \in [0, \infty)$. The curves $u_*(X)$ in figure 6.8 define monotonous invertible functions, provided that $X > 1$. A unique classification of curves is then achieved by choosing a value for u_* on a line of constant $X > 1$, together with fixing $\bar{\rho}_0$. Note that two different values for u_* may correspond to a single parameter c .

Firstly, it is focused on the *symmetric regime*. It is characterized by $\bar{\rho}_0 < 0$ implying X to reduce to ρ for large scales. A restriction on the coupling parameter c is imposed if the solution u is required to exist for all ρ . In the weakly coupled regime (6.38), all u_* are single-valued for non-negative arguments such that $u_*(X)$ stays well-defined for all scales, see figure 6.9 (left panel). For intermediate couplings (6.39), the theory admits two distinct effective potentials and therefore two scalar mass parameters. They are related to trajectories which either run through a node or not, depending on whether $u(0)$ is larger or smaller than

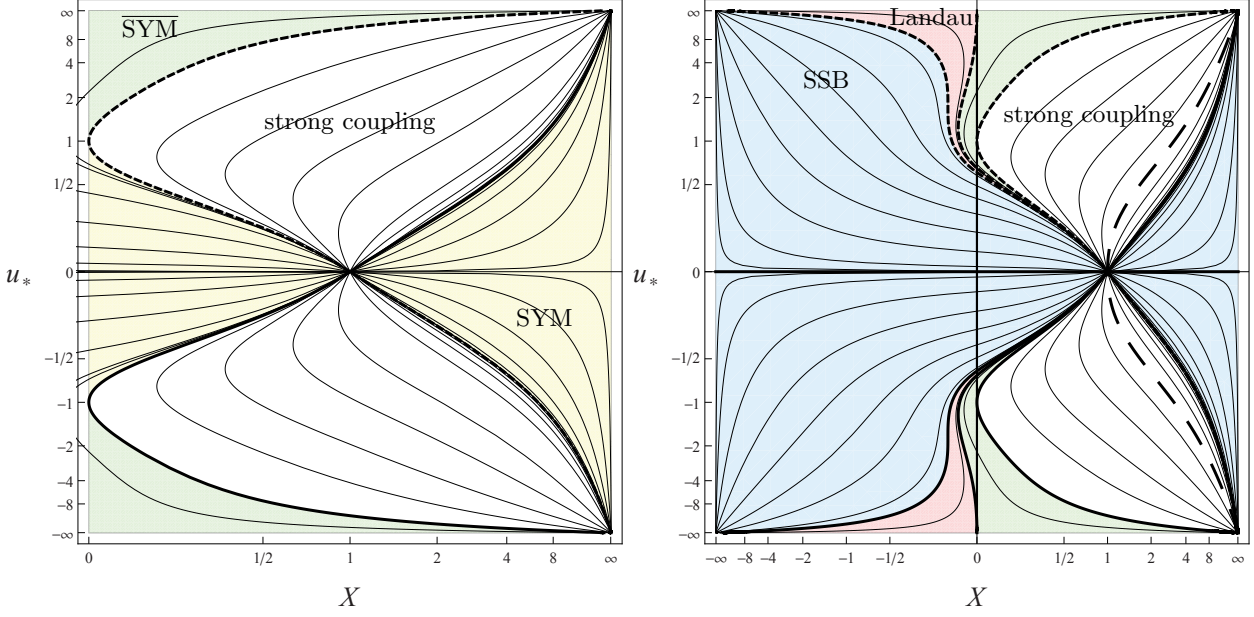


Figure 6.9: *Left figure:* RG trajectories $u_*(X)$ in the $O(N)$ symmetric phase: at weak coupling, trajectories either show a non-vanishing VEV for large scales (SYM, yellow shading), or a vanishing VEV for all scales (SYM, green shading). At strong coupling, trajectories terminate at Landau poles (white area). *Right figure:* RG trajectories $u_*(X)$ in the regions with spontaneous breaking of the $O(N)$ symmetry. Couplings are either finite for all k (SSB, blue shading), or run into a singularity (Landau, red shading). Some trajectories cannot be continued beyond the Landau pole (magenta shading). The SSB phase cannot be defined for strong coupling (white area).

one for $k \gg E$. The theory is then characterized by the coupling and the scalar mass at vanishing field. This peculiar structure has been found previously [155, 156] and will be explained below in more detail.

Next, the phase with *spontaneously broken* $O(N)$ symmetry exhibiting a positive physical VEV $\bar{\rho}_0 > 0$ is considered. This requires $u_*(X)$ to be well-defined for all real X . In view of the analytical solution illustrated in figure 6.8, this limits the achievable couplings to the weak coupling sector (6.38). Actually, for couplings $|c| \geq c_M$ within the weakly coupled domain, the function u_* is one-to-one and the theory described by $u(\rho)$ in (6.71) remains well-defined even in the IR limit. The theory is then characterized by two mass scales. The first one is given by the scalar mass at vanishing field corresponding to an $O(N)$ symmetric phase, whereas the second mass scale is given by the radial mass at $\bar{\rho} = \bar{\rho}_0$ allowing for SSB. However, if the quartic superfield coupling τ is increased or equivalently $|c|$ decreased further, the theory is not well-defined in the IR limit. Figure 6.9 (right panel) illustrates the different coupling regimes characterizing the SSB phase.

It remains to discuss the *strong-coupling* and *Landau regimes* already visualised in figure 6.9 more extensively. Firstly, take a ‘bottom-up’ view according to which the couplings evolve from the IR towards higher scales, parametrizing the effective potential in terms of local couplings in an expansion about vanishing field. Now, consider trajectories located in the strong coupling sector (6.40) within the symmetric regime ($\bar{\rho}_0 < 0$). Those trajectories

emanate from the upper/lower-right corner in figure 6.9 (left panel) for $k \approx 0$. Increasing k , consequently, corresponds to decreasing X and the running mass term and the fermion-boson coupling at vanishing field $u'(\rho = 0) \equiv u'_*(-\bar{\rho}_0/k)$ diverge at $k = k_L$. Hence, the renormalized RG flow comes to a halt: the solutions (6.71) cannot be continued beyond these points, because X cannot decrease any further along the integral curve $u_*(X)$. The potential becomes double-valued for $k < k_L$ with two different trajectories terminating at the same Landau pole. Using (6.47) together with (6.80), the non-analyticity in u reads

$$\rho - \rho_s(k) = \frac{1}{2}H''(u_s)(u(\rho) - u_s)^2 \quad \text{with} \quad \rho_s(k) = \rho_s + \bar{\rho}_0/k. \quad (6.82)$$

From the fixed point solution we know that $\rho_s \leq 1$ and therefore $\rho_s(k) \leq \rho_0(k)$ for all scales. In the IR limit, this implies that $\bar{\rho}_s(k) \rightarrow \bar{\rho}_0(k)$ from below. Here, the values for ρ_s are fixed by the coupling strength c via (6.43), where $\rho_s \geq 0$ in the strongly coupled symmetric regime with $c \leq c_L$. From (6.82) it follows that $k_L = -\bar{\rho}_0/\rho_s$ is positive, see figure 6.10. In summary, parameters c within the strong coupling region (6.40) allow for a supersymmetric model with linearly realized $O(N)$ symmetry up to scales $k = k_L$.

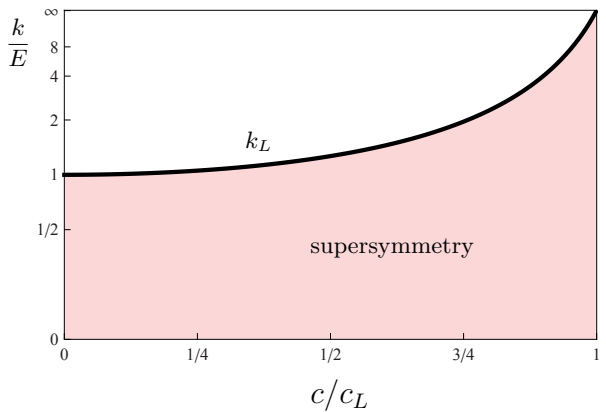


Figure 6.10: Location of the UV Landau pole for trajectories in the symmetric phase at strong couplings (6.40) (see text).

Next, trajectories of the SSB phase ($\bar{\rho}_0 > 0$) within the Landau/strong-coupling regimes are discussed. Within the weakly coupled sector (6.38), i.e. for $c_P < |c| \leq c_M$, all curves of constant c contain two Landau points with $|u_{s1}| < |u_c| < |u_{s2}|$ and $H''(u_{s1}) < 0 < H''(u_{s2})$ (see section 6.3.2). Each of them is described by (6.82) and parameters $0 > \rho_{s2}(c) > \rho_{s1}(c)$. The singularity at (ρ_{s1}, u_{s1}) corresponds to an IR Landau pole ('top-down'), whereas the one at (ρ_{s2}, u_{s2}) corresponds to a UV Landau pole ('bottom-up'). In the IR limit, the domain where u is multi-valued, collapses to a point with $\Delta\bar{\rho} = k(\rho_{s1} - \rho_{s2}) \rightarrow 0$. The location of both discontinuities approaches the VEV $\bar{\rho}_s(k) \rightarrow \bar{\rho}_0$ from below, and the discontinuity in the superpotential derivative

$$\Delta W' \equiv W'(\bar{\rho}_{s1}) - W'(\bar{\rho}_{s2}) = k(u_{s1} - u_{s2}) \quad (6.83)$$

becomes arbitrarily small. Interestingly, the UV and IR Landau poles become degenerate on

the integral curve for $|c| = c_M$ where $\rho_{s1} = \rho_{s2} = -1/8$. The non-analyticity evolves with

$$u(\rho) - u_s = \mp \operatorname{sgn}(\rho - \rho_s(k)) \left| \frac{\rho - \rho_s(k)}{\frac{1}{6}H'''(u_s)} \right|^{1/3}. \quad (6.84)$$

Here, the quartic scalar self-coupling $u'(\rho = 0)$ still diverges at the Landau pole, but the renormalized RG flow continues non-perturbatively rendering $u'(0)$ again finite. The non-analyticity (6.84) first appears for vanishing field at the scale $k_L = -\bar{\rho}_0/\rho_s$ and evolves up to the VEV $\bar{\rho}_0$ in the IR limit. At intermediate couplings (6.39), a different picture emerges. The solutions (6.80) cover all positive values for X , even for large k (see (6.81)). In a ‘top-down’ perspective, those trajectories emanate at $X \approx 0$ and continue towards decreasing X . Again, all trajectories reach the Landau pole (6.82) for the quartic superfield coupling at vanishing field with $\rho_s(c)$ taking negative values. The Landau scale reads $k_L = -\bar{\rho}_0/\rho_s > 0$, and the effective potential does not exist for fields below $\bar{\rho}_s(k) \leq \bar{\rho}_0(k)$. However, the theory still admits a radial scalar mass, set by the VEV and the quartic coupling. This is due to the existence of the one-sided derivative $\frac{dW'}{d\bar{\rho}}|_{\bar{\rho}_0}$ for fields $\bar{\rho} \geq \bar{\rho}_0$ larger than the VEV. Unfortunately, a scalar mass at vanishing field cannot be defined. Therefore it is concluded that the renormalized RG flow cannot be continued towards the IR for scales below the Landau scale $k < k_L$ for parameters c within the intermediate coupling regime. At very high couplings (6.40), a Landau pole with (6.82) and $\rho_s > 0$ occurs. Contrary to the intermediate coupling sector, the pole is located within the physical regime for all k . The integral curves have no continuation beyond this pole. In particular, the effective potential is not defined for the entire inner part $\bar{\rho} < \bar{\rho}_0$ in the IR limit and a scalar mass $W'(0)$ cannot be defined either. As in the intermediately coupled case, a radial mass proportional to the VEV still exists.

The schematic phase diagram shown in figure 6.11 summarizes the previously explained behaviour of the RG flow at various k . It is given in dependence on the coupling parameter c and the scale parameter $\bar{\rho}_0$ and should be compared to the phase structure 6.7 obtained by considering the RG equations at $k = 0$.

In the symmetric regime, the theory has a weakly coupled phase (6.38) with a scalar mass m where both the $O(N)$ symmetry and supersymmetry are preserved. At intermediate couplings (6.39), the theory admits two $O(N)$ symmetric phases featuring two mass scales m and M . This domain has a very narrow width in parameter space, see (6.41), which is sensitive to the underlying regularization. For strong couplings (6.40), the theory displays two mass scales m and M . However, it is also plagued by Landau-type singularities admitting no solution for the superpotential at scales above the Landau scale k_L . This is not visible from an evaluation of the IR gap equations alone.

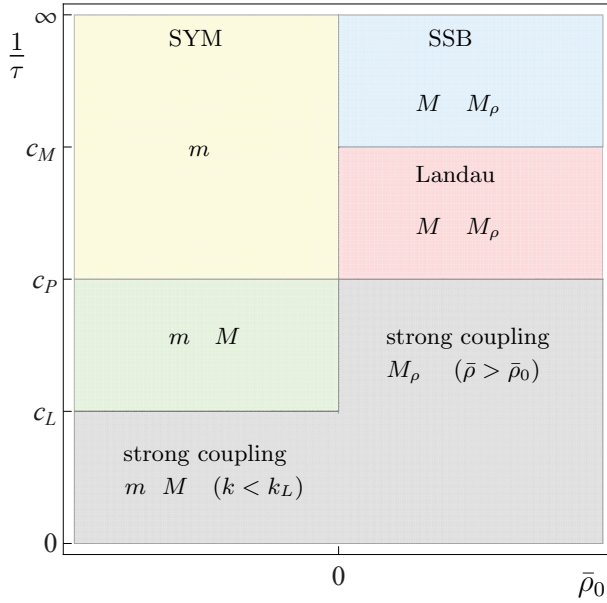


Figure 6.11: Schematic phase diagram based on the RG in the infinite cutoff limit. The scale k_L is given in figure 6.10.

In the SSB regime, the theory has a weakly coupled phase $c \geq c_M$, where the effective potential for the scalar has two degenerate minima corresponding to the mass scales M and M_ρ . With increasing coupling τ , the theory enters a narrow parameter range $c_P < |c| < c_M$, where RG trajectories run through a series of Landau poles at intermediate energies. Here, the discontinuity in field space and in the superpotential derivative shrinks to zero in the IR limit, the details of which are sensitive to the underlying regularization. For even larger couplings $|c| \leq c_P$, the theory is so strongly coupled that RG trajectories terminate at Landau poles within the physical regime.

The effective potential does not exist for fields below the non-trivial VEV $\bar{\rho} < \bar{\rho}_0$ in the IR limit. Nevertheless the potential does admit a radial mass M_ρ .

Unbroken global SUSY requires a ground state with vanishing energy and an otherwise positive dimensional effective potential for all fields and scales. Strictly speaking, the non-existence of an effective potential for small fields means that, based on the potential alone, no statement on SUSY breaking at strong couplings could be made. In fact, the results suggest that a description of the ground state in terms of constant fields may no longer be adequate at strong couplings. The occurrence of a Landau scale k_L makes it conceivable that SUSY is spontaneously broken in the strongly coupled regime, signalled by a divergence in the Ward identity. This interpretation would be consistent with the picture for the spontaneous breaking of Parisi-Sourlas supersymmetry in disordered Ising models [170], which is triggered by cusp-like non-analyticities of the RG flow at a finite ‘‘Larkin scale’’ k_L . At strong couplings, these limitations of the full effective potential and the occurrence of Landau poles are not directly visible from the IR limit only, see figures 6.7 and 6.11. Only by virtue of the fully integrated RG flow for all scales k , the structure of the effective potential at strong couplings becomes transparent.

6.3.5 Effective Theory

Within this section, the integrated RG flow is viewed from an effective theory perspective. Hence, the UV scale Λ is assumed to be finite. The boundary condition at $k = \Lambda$ has been achieved by integrating-out all fluctuations with momenta above Λ . The RG equations then detail the remaining low-energy flow of couplings for all scales $k < \Lambda$. In terms of

dimensional quantities, the solution (6.29) reads

$$\begin{aligned}\bar{\rho} - \bar{\rho}_0(k) &= cW' + H\left(\frac{W'}{k}\right)k - H\left(\frac{W'}{\Lambda}\right)\Lambda \\ \bar{\rho}_0(k) &= k + \bar{\rho}_0.\end{aligned}\tag{6.85}$$

The parameter $\bar{\rho}_0$ is given by $\bar{\rho}_0 = \Lambda(\kappa - 1)$ in terms of the microscopic parameters. Via examining (6.85), the origin of the ‘‘peculiar’’ phases discussed in the previous section is clarified. Besides, the effective theory perspective allows for assessing the effects of changes in the boundary condition on the phase structure of the theory.

Gap Equations

Similarly to the subsequent section, the flow equation (6.85) is analysed in the IR limit $k = 0$ first. The corresponding gap equation for the scalar masses $W'(0) \equiv \mu\Lambda$ at vanishing field is given in terms of the dimensionless parameter μ by

$$-\frac{\bar{\rho}_0}{\Lambda} = c\mu + c_P|\mu| - H(\mu),\tag{6.86}$$

where the expansion (6.31) has been utilized. If $\bar{\rho}_0 \neq 0$, the two possible branches

$$\begin{aligned}H(\mu) &= (c + c_P)\mu + \frac{\bar{\rho}_0}{\Lambda}, \quad (\mu > 0) \quad \text{and} \\ H(\mu) &= (c - c_P)\mu + \frac{\bar{\rho}_0}{\Lambda}, \quad (\mu < 0)\end{aligned}\tag{6.87}$$

of solutions are found⁸. The main difference to (6.77) in the infinite cutoff limit manifests in the appearance of the additional term $H(\mu)$. Figure 6.12, left panel, displays the phases of the supersymmetric $O(N)$ model based on the above gap equations at finite Λ .

In the *symmetric regime* ($\bar{\rho}_0 < 0$) there exist one, two, or three solutions to (6.87) with $m = \Lambda\mu > 0$ as well as none, one or two solutions $M = -\Lambda\mu > 0$. Thereby, three solutions for m can only exist in the very strong coupling domain with $0 < c < c_M - c_P$, cf. figure 6.5. For the dominant part of the parameter space $(1/\tau, \bar{\rho}_0/\Lambda)$, only a single scalar mass m exists. These findings are quite similar to the weak coupling phase of the renormalized theory, c.f. figure 6.7. For small $\bar{\rho}_0/\Lambda$ and strong couplings τ , a ‘‘triangle’’ opens up allowing for two additional mass scales of the type M . The borderline $c(\bar{\rho}_0/\Lambda)$ emerges analytically, starting at the point $(c, \bar{\rho}_0/\Lambda) = (c_P, 0)$ and ending at $(c, \bar{\rho}_0/\Lambda) \approx (0, -1.077)$. At very strong couplings, two further masses of type m show up in a tiny ‘‘spike’’-like region, bordered by the curves connecting $(c, \bar{\rho}_0/\Lambda) = (c_M - c_P, -9/8) \approx (0.035, -1.125)$ with $(c, \bar{\rho}_0/\Lambda) = (0, -1.077)$ and $(0, -1)$ as indicated in figure 6.12 (left panel). In summary, either a single mass m , or

⁸Again, only positive parameters $c \geq 0$ are considered as changing the sign of c amounts to interchanging $\mu \leftrightarrow -\mu$ in (6.87).

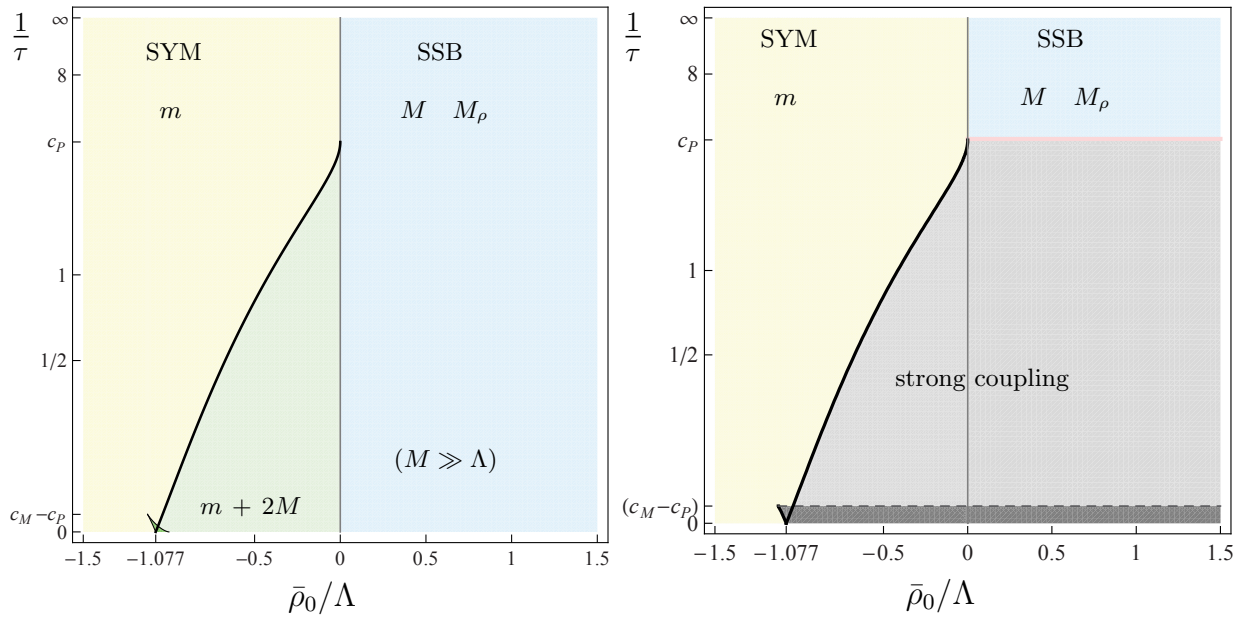


Figure 6.12: *Left panel:* Phases of the supersymmetric $O(N)$ model according to the gap equation (6.86) at finite UV scale Λ . The SYM phase displays either a single mass scale m or several ones. The SSB regime displays two scalar mass scales M and M_ρ for all couplings. The phase transition between the symmetric phase and the SSB phase is continuous with Gaussian exponents. *Right panel:* Phases according to the RG equations at finite UV scale. The SSB regime is quite similar to the result at $1/\Lambda = 0$, see Fig 6.11. The SYM phase, however, is substantially larger. The phase transition between both phases is continuous with Gaussian exponents. Note that there exists a very tiny Landau phase for couplings $c_P < |c| < c_M$ in the SSB regime (red line).

three masses $m + 2M$ or $3m$, or five different mass scales $3m + 2M$ (in the region where the triangle and the spike overlap) are identified. However, the masses appearing in the strong-coupling domain are parametrically large. Thus, these masses may be solely an artefact of the regularization and should not be trusted.

Within the regime $\bar{\rho}_0 > 0$ allowing for *spontaneous $O(N)$ symmetry breaking*, a unique scalar mass solution M to (6.87) is achieved from the branch with negative μ for all couplings c . This mass scale represents an $O(N)$ symmetric state within the phase where normally only SSB would be expected to occur. For strong couplings, its value becomes parametrically very large, i.e. of the order of the cutoff, similar to some mass solutions found in the symmetric regime. In addition, the theory shows a radial mass M_ρ .

RG Phase Diagram

Next, the phase diagram deduced from (6.85) at finite Λ for arbitrary scales k is analysed. It is graphed in figure 6.12, right panel.

Firstly, it is focused on the *symmetric domain*, meaning $\bar{\rho}_0 < 0$. If the coupling τ is small enough, the theory exhibits a single scalar mass only. Within the strongly coupled regime, the RG flow develops a Landau pole and the effective potential becomes multi-valued in the physical regime $\bar{\rho} > 0$. The boundary between the two regimes is marked by a curve

$c_{\text{cr}}(\bar{\rho}_0/\Lambda)$. The latter is determined as follows: In the IR limit, (6.85) together with the Landau-pole condition $d\bar{\rho}/dW' = 0$ evaluated at vanishing field yields

$$\frac{\bar{\rho}_0}{\Lambda} = H\left(\frac{W'_L}{\Lambda}\right) - \frac{W'_L}{\Lambda} H'\left(\frac{W'_L}{\Lambda}\right), \quad (6.88)$$

where W'_L is equal to $W'(0)$ when the Landau pole enters the physical region at $\bar{\rho} = 0$. The real roots of this polynomial equation are

$$\frac{W'_L}{\Lambda} = \pm \left(\frac{\sqrt{9 + 8\bar{\rho}_0/\Lambda} - (3 + 2\bar{\rho}_0/\Lambda)}{2(1 + \bar{\rho}_0/\Lambda)} \right)^{1/2}. \quad (6.89)$$

Here, the plus (minus) sign belongs to a Landau pole at $\bar{\rho} = 0$ in the positive (negative) half-plane of W' . Inserting (6.89) into the IR limit of (6.85) at $\bar{\rho} = 0$ yields the critical coupling

$$c_{\text{cr}} = \frac{1}{W'} \left(-\frac{\bar{\rho}_0}{\Lambda} + H\left(\frac{W'}{\Lambda}\right) \Lambda - c_P \frac{|W'|}{\Lambda} \right) \Big|_{W'_L}. \quad (6.90)$$

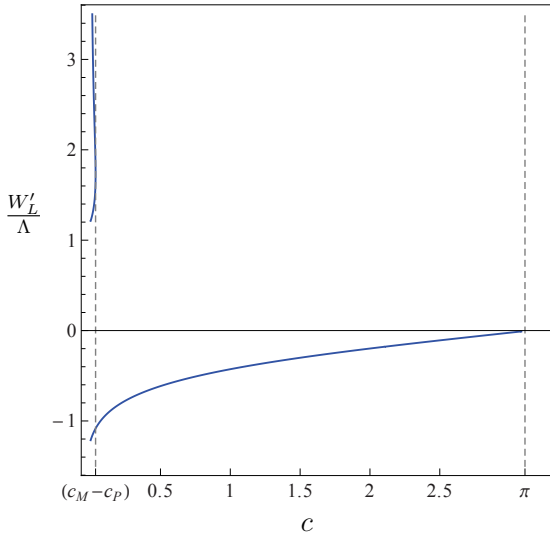


Figure 6.13: Possible values W'_L/Λ as a function of the inverse superfield coupling $c = 1/\tau$ associated with a Landau pole in the IR limit.

In general, Landau poles only occur in the parameter range $\bar{\rho}_0/\Lambda \in (-1.125, 0)$ and $c \in (0, c_P)$, i.e. the strong coupling regime. Besides ambiguities with $W'_L < 0$ for couplings $c < c_P$, Landau poles with $W'_L > 0$ occur in the very narrow strong coupling regime with $c < (c_M - c_P) \approx 0.035$. This is illustrated in figure 6.13. Hence, the different regimes of the symmetric phase as shown in figure 6.12 (right panel) are interpreted as follows: Landau poles in the physical regime with $W'_L < 0$ are observed for strong superfield couplings $c < c_{\text{cr}-}$, where the latter denotes the critical coupling (6.90), evaluated at $W'_L < 0$.

The corresponding borderline starts at $(c, \bar{\rho}_0/\Lambda) = (c_P, 0)$ and ends at $(0, -1.077)$, similar to borderline resulting from the gap equation. For very strong couplings $c < c_M - c_P \ll 1$, ambiguities with $W'_L > 0$ in the physical regime (dark shaded area in figure 6.12, right panel) are detected. However, this area is bounded by $c_{\text{cr}+}$ from below, where $c_{\text{cr}+}$ starts at $(c_M - c_P, -1.125)$ and ends at $(0, -1.077)$.

Interestingly, the available domain of couplings is substantially larger than the corresponding parameter space deduced from the RG flow in the infinite cutoff limit, c.f. figure

6.11. In addition, the equations do not admit a second mass M as for $\Lambda \rightarrow \infty$. It should be emphasized that the RG study of the phase diagram also allows for a simple descriptive explanation of the various masses emerging from the gap equation analysis as shown in figure 6.12, left panel. The two additional masses M , observed in the strong coupling domain (big triangle) result from an ambiguity of the solution W' in the negative half-plane. The borderline connecting $(c_P, 0)$ and $(0, -1.077)$ represents the special solution with $c = c_{cr-}$ showing a Landau pole in the IR exactly at vanishing field. This corresponds to an additional infinitely large mass M . Similarly, the two additional masses of type m in the spike-like strong coupling region result from ambiguities of the solution for positive W' .

Next, it is focussed on the *SSB phase*, i.e. $\bar{\rho}_0 > 0$. For weak couplings $|c| \geq c_M$, the theory displays a well-defined low-energy regime with two mass scales M and M_ρ , in line with the gap equation analysis. In the very narrow coupling regime $c_P < |c| < c_M$, IR Landau poles at $\rho_s(k)$ appear within the physical regime for scales $k < k_L$. However, similar to the renormalized theory, the poles approach the VEV $\lim_{k \rightarrow 0} \bar{\rho}_s(k) \rightarrow \bar{\rho}_0$ in the IR limit from below and the domain featuring a multi-valued W' collapses to a point. Hence, the effective Potential is well defined and unique. For stronger couplings $c < c_P$, the effective potential is plagued by Landau poles and becomes multi-valued even in the IR limit. This becomes apparent by considering the second derivative W'' of the superpotential. The latter shows a non-analyticity at $\bar{\rho}_0$ exactly in the IR limit with

$$\lim_{\bar{\rho} \rightarrow \bar{\rho}_{0\pm}} W''(\bar{\rho}) = \frac{1}{c \pm \pi}, \quad (6.91)$$

where $W'(\bar{\rho}_{0\pm}) \rightarrow \pm 0$. Apparently, the solution W' then shows a cusp with positive W'' for $W' \rightarrow +0$ and negative W'' for $W' \rightarrow -0$ in the vicinity of the node. Since there exists at most one Landau pole with $W'_L < 0$ in the IR limit (figure 6.13) and since $W'(\bar{\rho} \rightarrow -\infty) = -\infty$, it becomes apparent that there has to be a Landau pole located in the physical regime for $k \rightarrow 0$ if and only if $|c| < c_P$.

Effective Potential

As already mentioned in section 6.3.2, the relevant microscopic coupling $\kappa = \kappa_{cr} + \bar{\rho}_0/\Lambda$ determines the macroscopic physics of the model: if $\kappa < \kappa_{cr}$ ($\bar{\rho}_0 < 0$), the effective potential preserves global $O(N)$ symmetry. Contrary, if $\kappa > \kappa_{cr}$ ($\bar{\rho}_0 > 0$), the symmetry may be spontaneously broken, if the VEV $\bar{\rho}_0 > 0$ is taken. The specific UV coupling $\kappa_{cr} = 1$ marks the phase transition between the two regimes. Figure 6.14 illustrates the flow of the effective average potential $V_k(\bar{\rho})$ for different values of κ . Starting in the UV at $k = \Lambda$ with

$$V_\Lambda = \bar{\rho} (W'_\Lambda)^2 = \tau^2 \bar{\rho} (\bar{\rho} - \kappa \Lambda)^2 \quad (6.92)$$

according to (6.26), the potential evolves up to the IR limit $k \rightarrow 0$.

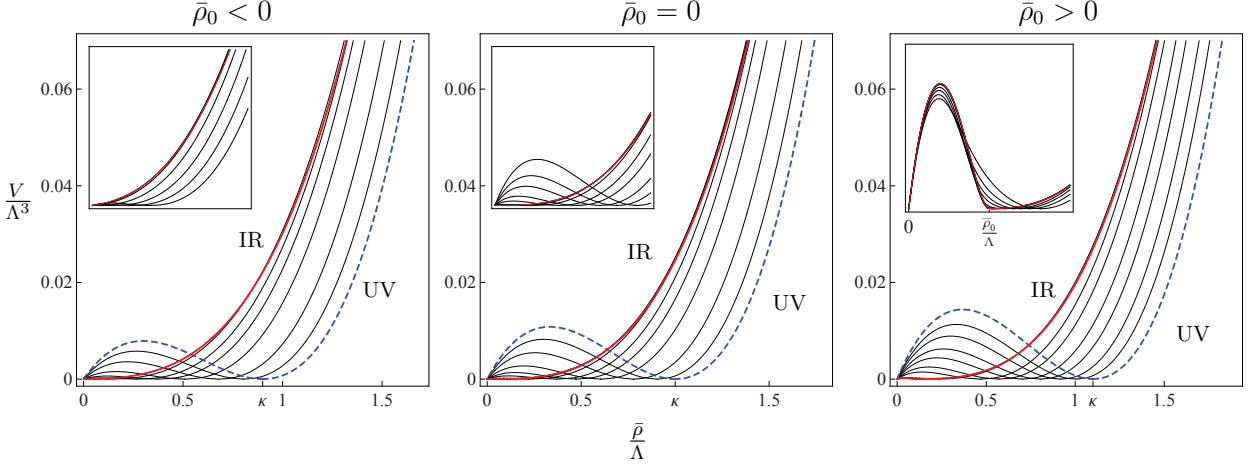


Figure 6.14: RG flow of the effective average potential V_k/Λ^3 as a function of $\bar{\rho}/\Lambda$ according to (6.85) for different values of $\bar{\rho}_0/\Lambda = \{-0.1, 0, 0.1\}$ at weak coupling $c = 3.7$. If $\bar{\rho}_0 < 0$, the system evolves into an $O(N)$ symmetric phase (left panel). Vanishing $\bar{\rho}_0$ corresponds to the phase transition between the $O(N)$ symmetric and the SSB phase and the scale invariant solution is approached in the IR limit (middle panel). If $\bar{\rho}_0 > 0$, the macroscopic theory is characterized by a non-vanishing VEV $\bar{\rho}_0(k \rightarrow 0) = \bar{\rho}_0 > 0$ (right panel). The insets show the potential at small fields approaching the IR limit. Also, the non-analyticity of W' at $\bar{\rho}_0$ in the IR is clearly visible in the right panel.

Three aspects of the potential need to be discussed further: Firstly, there exists a strong coupling domain, where the effective potential shows ambiguities within the physical domain, both in the infinite cutoff limit and the effective theory limit. At strong coupling, the effective potential admits no physical solution for small fields. This result indicates that a description of the theory in terms of an effective superpotential is no longer viable, possibly hinting at the formation of bound states with or without the breaking of supersymmetry.

Secondly, the effective potential is non-analytic at its VEV $\bar{\rho}_0$ in the IR limit, induced by the cusp (6.91) of W' . However, for all finite scales $k > 0$, the second derivative is unique and given by $W''(\bar{\rho}_0(k)) = 1/c = \tau$. Since the radial mass M_ρ is specified by

$$M_\rho^2 = V''(\phi)|_{\phi=\phi_0} = (2\bar{\rho}W''(\bar{\rho}))^2 \Big|_{\rho_0(k)}, \quad (6.93)$$

a uniquely defined radial mass only exists for finite scales $k > 0$, reading

$$M_\rho(k) = 2\tau\bar{\rho}_0(k) = 2\tau(k + \bar{\rho}_0), \quad \bar{\rho}_0 > 0. \quad (6.94)$$

However, the studies at finite N (c.f. section 6.4) indicate that this non-analyticity of W' in the IR is solely due to the large- N limit.

Thirdly, the effective potential in the SSB phase is not convex in the IR limit. As it has already been mentioned in [47], the supersymmetric analogue of the potential in the classical action is the superpotential W . Consequently, the flow drives the approach to convexity of W , but not necessarily of the potential $V = \bar{\rho}W'^2$. The superpotential W is a convex function if and only if the first derivative W' represents a monotonically increasing function

of $\bar{\rho}$. According to (6.85) at $k = 0$, this condition is satisfied as long as $c > c_P$, i.e. in the weakly coupled domain. This fact supports the conjecture that supersymmetry may be broken spontaneously in the strongly coupled domain exhibiting Landau poles.

Thermodynamic Critical Exponents

The three-dimensional supersymmetric $O(N)$ model represents an effective field theory behaving like statistical models near a second-order phase transition. As pointed out in section 6.3.3, the IR fixed point shows Gaussian scaling for all finite couplings c , except for $|c| = c_P, c_I$. Following [31], the *thermodynamic* critical exponents can be extracted as well. The expectation value of the field $\langle\phi\rangle$ serves as order parameter. In the SSB regime it is related to the VEV $\bar{\rho}_0$ via (choose $\phi_i = \delta_{i1}\phi$)

$$\langle\phi\rangle = \lim_{k \rightarrow 0} \sqrt{2\bar{\rho}_0(k)} \equiv \sqrt{2\bar{\rho}_0} = \sqrt{2\delta\kappa\Lambda}. \quad (6.95)$$

The deviation of κ from its critical value $\kappa_{cr} = 1$ may be associated with the deviation of the temperature T from its critical value T_c according to $\delta\kappa\Lambda \sim (T_c - T)$. Thus, the critical exponent β may be quantified:

$$\langle\phi\rangle \sim (\bar{\rho}_0)^\beta \quad \text{with} \quad \beta = \frac{1}{2}. \quad (6.96)$$

Next, consider the critical exponent ν describing the manner in which the correlation length ξ diverges (the mass vanishes) by approaching the phase transition. It has to be distinguished between

$$\begin{aligned} \xi^{-1} = m &\sim (-\bar{\rho}_0)^\nu && \text{(SYM regime, } \bar{\rho}_0 < 0) && \text{and} \\ \xi^{-1} = m &\sim (\bar{\rho}_0)^{\nu'} && \text{(SSB regime, } \bar{\rho}_0 > 0). \end{aligned} \quad (6.97)$$

First, the squared masses (6.76) corresponding to $O(N)$ symmetric ground states are examined. The gap equations (6.78) directly lead to the critical exponent

$$\nu = 1. \quad (6.98)$$

Note that for $|c| = c_P$, ν becomes double-valued. This issue is interpreted in section 6.3.7 in detail. In the SSB regime, there exists a unique $O(N)$ symmetric ground state with mass M given by (6.78) for all $|c| \neq c_P$, implying

$$\nu' = 1. \quad (6.99)$$

Also, a spontaneously $O(N)$ broken ground state characterized by a radial mass according to (6.94) is observed. Since $M_\rho \sim \bar{\rho}_0$, this leads to (6.99) too.

The critical exponent δ is defined by $J|_{\bar{\rho}_0=0} \sim \phi^\delta$, where $J = \partial V/\partial\phi$. Close to the phase transition, the cutoff may be assumed to be much larger than the mass scale, i.e. $W'/\Lambda \ll 1$. The effective potential then reads

$$V(\bar{\rho}) = \frac{1}{A^2} \bar{\rho} (\bar{\rho} - \bar{\rho}_0)^2 \quad (6.100)$$

with $A = c + \pi \operatorname{sgn}(\bar{\rho} - \bar{\rho}_0)$ and $\operatorname{sgn}(0) = 0$. This leads to

$$J|_{\bar{\rho}_0=0} = \frac{3}{4A^2} \phi^\delta \quad \text{with} \quad \delta = 5. \quad (6.101)$$

Finally, the critical exponent γ associated with the susceptibility $\chi = \partial\phi/\partial J = (\partial^2 V/\partial\phi^2)^{-1}$ near the phase transition is discussed. It is given by

$$\begin{aligned} \chi(J)|_{J=0} &\sim (-\bar{\rho}_0)^\gamma \quad (\text{SYM phase, } \bar{\rho}_0 < 0) \\ \chi(J)|_{J=0} &\sim (\bar{\rho}_0)^{\gamma'} \quad (\text{SSB phase, } \bar{\rho}_0 > 0). \end{aligned} \quad (6.102)$$

Using (6.100) and (6.102) yields

$$\gamma = \gamma' = 2. \quad (6.103)$$

Note that the thermodynamic exponents derived above are invariant under changing $c \leftrightarrow -c$, see (6.79). Besides, the thermodynamic scaling exponents can equally be obtained from the leading RG exponent together with scaling relations by using $\nu = 1/\theta$, where $\theta = 1$ is the IR relevant eigenvalue due to the VEV. The scaling exponents of the BMB fixed point with $c = \pm c_P$ are discussed later on in section 6.3.7 in more detail.

6.3.6 Comparison and Discussion

In this section, the phase diagrams obtained by (a) considering the renormalized theory with $\Lambda \rightarrow \infty$ and (b) looking at the effective theory with Λ finite are compared.

Firstly, the phase diagrams derived from the gap equations (6.77) and (6.86) (figure 6.7 and 6.12, left panel) are compared. Apparently, the gap equation (6.86) of the effective theory contains an additional, cutoff and regulator-dependent contribution $H(\mu)$ compared to (6.77). This term implies some modifications of the ‘effective’ phase diagram compared to the ‘renormalized’ one: In the symmetric phase, the parameter range featuring several $O(N)$ symmetric masses is diminished. Besides, up to five different $O(N)$ symmetric phases are observed in the very strong-coupling regime $|c| \ll 1$ and for certain VEV $\bar{\rho}_0(c)$. In the spontaneously broken regime, the function $H(\mu)$ enlarges the parameter range showing a second mass M in addition to M_ρ to infinitely large couplings $\tau = 1/c$. However, the masses in the very strong coupling regime are quite large, i.e. of the order of the cutoff Λ , and regulator-dependent. This strongly indicates that they are of no physical relevance.

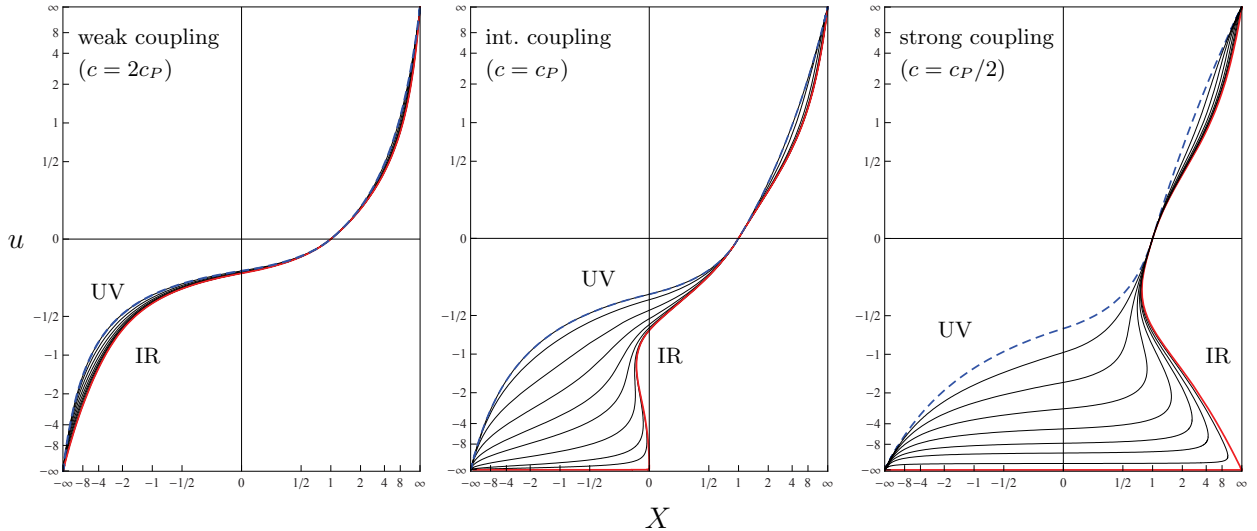


Figure 6.15: Effective field theory with Λ finite: Graphical representation of the dimensionless derivative of the superpotential $u(X)$ as a function of $X = \rho - \bar{\rho}_0/k$ for weak, intermediate and strong superfield coupling $\tau = 1/c$ (from left to right). Each panel shows the RG flow, starting with $u_\Lambda(\rho) = \tau(\rho - \rho_0(\Lambda))$ according to (6.26) in the UV down to the IR limit.

Furthermore, the phase diagrams shown in figure 6.11 and 6.12 (right panel) as deduced from the renormalization group flow at arbitrary k are compared. Here, solutions $W'(\bar{\rho})$ have been claimed to be of physical relevance, if there exists no Landau pole characterized by an infinitely large fermion-boson coupling W'' within the physical domain.

In the *symmetric regime*, the narrow window between the couplings c_L and c_P characterized by two masses m, M vanishes for finite Λ and the effective theory shows only a single mass m . Furthermore, the strong coupling domain is reduced and becomes $\bar{\rho}_0$ -dependent for Λ finite. A comparison of figures 6.8 and 6.15 emphasizes the structural differences of the $O(N)$ symmetric phases of the renormalized and the effective theory. Firstly, the UV properties differ. The renormalized theory (figure 6.8) is plagued by UV Landau poles in the physical domain for superfield couplings stronger than $\tau = c_L^{-1}$. Besides, the potential is not even defined for all fields $\rho > 0$ then. The effective theory, in contrast, always features a well-defined UV limit given by the superpotential $W'_\Lambda = \tau(\bar{\rho} - \bar{\rho}_0(\Lambda))$ at the UV cutoff. Also, the potential is defined for all fields. However, it may show IR ambiguities for sufficiently strong couplings: if $|c| < c_P$ fixed and $-\bar{\rho}_0 \ll 1$, an IR Landau pole occurs at $k_L > 0$ in the physical domain and additional masses appear at the origin by approaching the IR. However, if $|\bar{\rho}_0|$ is chosen large enough, the IR Landau pole drifts out of the physical domain and the effective potential is unique and well-defined for all $\bar{\rho} \geq 0$, leaving a single mass m . This upper limit of $|\bar{\rho}_0|(c)$ simply corresponds to the borderline connecting $(c_P, 0)$ and $(0, -1.077)$ illustrated in figure 6.12, right panel.

Within the *SSB phase*, the weak, Landau and strong coupling domains of the renormalized and the effective model match. As pictured in figures 6.8 and 6.15, both theories exhibit an IR Landau pole for all $|c| < c_P$. Independent of the superfield coupling and the VEV, there

always exists only a single mass M representing an $O(N)$ symmetric ground state. Again, the effective potential is defined for all fields, but may show ambiguities. In contrast, the potential of the renormalized theory is not defined for all fields $\bar{\rho} > 0$ for strong couplings $|c| < c_P$.

The comparison of the renormalized and the effective perspectives of the supersymmetric $O(N)$ model is closed by a graphical illustration of the different mass scales as pictured in figure 6.16. First, notice that these masses represent $O(N)$ symmetric states as they emerge from the curvature of the potential at vanishing field. Besides, the parametrically large masses m observed in the spike-like region (see Fig. 6.12, left panel) are not included in figure 6.16 as they emerge as an artefact of the chosen regularization.

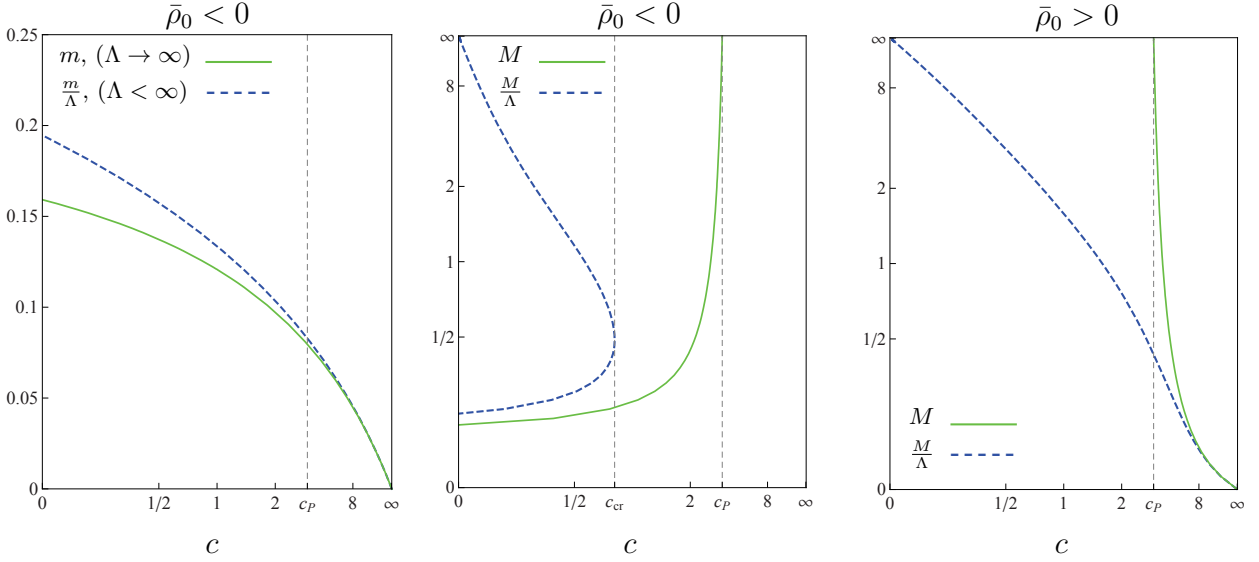


Figure 6.16: *Green, solid lines:* mass scales m , M of the renormalized theory ($\Lambda \rightarrow \infty$) as functions of the coupling c according to the gap equations (6.78) for fixed $\bar{\rho}_0 = \{-0.5, -0.5, 0.5\}$ (left, middle, right panel). *Blue, dashed lines:* Masses m/Λ , M/Λ of the effective theory ($\Lambda < \infty$) as functions of the coupling c according to the gap equations (6.86) for fixed $\bar{\rho}_0/\Lambda = \{-0.5, -0.5, 0.5\}$.

In summary, the SSB phase and the symmetric phase at weak coupling show only minute differences for Λ finite or infinite, resulting in equivalent phase diagrams. More pronounced differences occur within the symmetric phase at strong couplings $c < c_P$: For a finite UV cutoff, the fluctuations of the Goldstone modes have less “RG time” available to built-up non-analyticities in the effective potential. This leads to a shift in the effective boundary between weak and strong coupling, allowing for a substantially larger domain of a regular $O(N)$ symmetric phase. At strong coupling, we also conclude that the absence of an $O(N)$ symmetric phase for $\Lambda \rightarrow \infty$ arises from the theory with Λ finite through an $O(N)$ symmetric phase with anomalously large mass of the order of the UV scale itself.

6.3.7 Spontaneous Breaking of Scale Invariance

In this section it is commented on the supersymmetric analogue of the Bardeen-Moshe-Bander (BMB) phenomenon, the spontaneous breaking of scale invariance and the associated non-classical scaling.

Supersymmetric BMB phenomenon

An introduction to the BMB phenomenon occurring in scalar $(\phi^2)_{d=3}^3$ theories [65, 138–140] has already been given in the preamble of chapter 6. Here, the BMB fixed-point marks the end point of the tricritical line t , characterized by vanishing couplings μ^2 and λ as illustrated in figure 6.1. Contrary, the supersymmetric $O(N)$ model featuring a classical $(\Phi^2)_{d=3}^2$ superpotential corresponding to the microscopic scalar potential (6.92), is determined by only two microscopic couplings τ and κ . The $(\Phi^2)_{d=3}^2$ theory with a quartic superfield potential apparently corresponds, in the scalar sector, to a $(\phi^2)_{d=3}^3$ with a sextic potential. The main new addition due to supersymmetry is that the scalar quartic and sextic couplings are no longer independent of each other. Hence, supersymmetry implies the critical and tricritical theories characterized by $\kappa = \kappa_{\text{cr}}$ to coincide [155, 160].

Now, what picture for the supersymmetric BMB phenomenon emerges by employing the FRG? To begin with, the BMB fixed point has to be identified. If the relevant microscopic coupling $\kappa = \kappa_{\text{cr}}$ is fine-tuned to its critical value $\kappa_{\text{cr}} = 1$, the scaling solution is reached in the IR limit. The analytical solution (6.29) at the origin $\rho = 0$ then takes the form

$$-1 = c u_0 + H(u_0) , \quad (6.104)$$

where $u_0 \equiv u(\rho = 0)$. Thus, (6.104) simply represents the fixed-point solution at vanishing field. The $O(N)$ symmetric ground state is characterized by the mass

$$M^2 = (W'(0))^2 = \bar{\mu}^2 = (u_0 k)^2 \quad (6.105)$$

with $M = -\bar{\mu} > 0$. Evidently, u_0 has to diverge as $1/k$ in order to allow for spontaneous breaking of scale invariance with a finite mass scale M . The transcendental equation (6.104) always has a single zero mass solution $M = 0$, except for $c = c_P$, where it shows an additional, infinitely large solution $u_0 \rightarrow -\infty$. Note that this limit emerges from $u(\rho)$ through negative field squared values $\rho \rightarrow 0^-$, which is a consequence of the chosen regularization. Hence, the specific microscopic parameters

$$(\kappa, \tau) = (1, 1/\pi) \quad (6.106)$$

lead to a macroscopic theory, where the mass of the $O(N)$ bosonic and fermionic quanta is left undetermined. Thus, scale invariance is spontaneously broken in accordance with [155, 156, 160]. A mass is generated by dimensional transmutation. The coupling parameter τ

takes the value (6.106) in our conventions, and the associated degree of freedom is ‘transmuted’ to an arbitrary mass scale M . As supersymmetry is left unbroken, spontaneously broken scale invariance leads to the appearance of a Goldstone boson (dilaton), accompanied by a Goldstone fermion (dilantino). These particles are exactly massless, since τ is not renormalized.

Scaling Exponents

Next, the scaling exponents of the supersymmetric BMB fixed point are studied. Here, the critical exponents (6.97) and (6.102) become double-valued due to a different scaling behaviour of the mass scales m and M in the vicinity of the fixed point. The two masses originate from the finite and the infinite u_0 solution detected at $|c| = c_P$ as shown in figure 6.8. The latter leads to the special non-analytic behaviour at the BMB fixed point. To begin with, the parameter c is fixed to $c = c_P$. Approaching the phase transition from the symmetric regime implies the mass to be $m = -\bar{\rho}_0/2\pi$. Thus, (6.97) yields

$$\nu = 1. \quad (6.107)$$

In turn, approaching the fixed point from the SSB regime, the expression for M in (6.78) is not applicable. This can be appreciated as follows: The RG solution (6.85) at $k = 0$ together with (6.32) yields

$$\bar{\rho} - \bar{\rho}_0 = cW' + \pi|W'| - \frac{3}{\Lambda}W'^2 + \mathcal{O}\left(\frac{W'^4}{\Lambda^3}\right). \quad (6.108)$$

For small masses $W'/\Lambda \ll 1$, the gap equations (6.78) directly follow. However, for $c = c_P$, the expression for M in (6.78) is no more valid as the contribution linear in W' in (6.108) vanishes. The sub-leading quadratic terms take over leading to $M^2 = \frac{\Lambda}{3}\bar{\rho}_0$. Therefore, the supersymmetric BMB exponent ν' is given by

$$\nu'_{\text{BMB}} = \frac{1}{2}. \quad (6.109)$$

Now consider $c = -c_P$. By virtue of the symmetry (6.79), the mass scales $m \leftrightarrow M$ interchange their roles under $c_P \leftrightarrow -c_P$. Consequently, the scaling exponents (6.107) and (6.109) also interchange their values. Therefore, the theory at $|c| = c_P$ displays conventional scaling with (6.107) as well as un-conventional scaling with (6.109). The former is a consequence of the smooth ‘non-BMB-type’ scaling related to finite u_0 , whereas the latter is the BMB scaling associated to infinite u_0 . In either case, and under the above identification, the scaling indices from the symmetric and symmetry broken regimes agree. It should be stressed that the BMB scaling exponent (6.109) is non-classical. Furthermore, it cannot be derived from the RG scaling alone as it is due to non-analyticities in the field dependencies. As a final comment, note that an infinite u_0 , the fingerprint for spontaneous breaking of scale invariance, is stable

under alterations of the RG scheme.

6.4 Physics at Finite N - Radial Mode Fluctuations

This section gives a first account of the phase transition in a theory with finitely rather than infinitely many supermultiplets N , focussing on the existence of a fixed point, the phase transition, and the fate of the supersymmetric BMB phenomenon to leading order in a gradient expansion.

6.4.1 Exact Fixed Point

The fluctuations of the radial mode form the main new addition to the supersymmetric RG flow at infinite N . They imply the quartic coupling τ no longer to be exactly marginal. Instead, the flow of this coupling is governed by terms of order $1/N$. The absence of an exactly marginal coupling causes the line of fixed points found at infinite N to collapse into a finite, possibly empty set of fixed points. Furthermore, the running of the VEV no longer factorizes from the other couplings of the theory resulting in a more complex structure of the RG flow.

In order to study the supersymmetric $O(N)$ model at finite N , it is returned to the evolution equation (6.21), i.e.

$$\partial_t u = -u + \rho u' - \left(1 - \frac{1}{N}\right) u' \frac{1 - u^2}{(1 + u^2)^2} - \frac{1}{N} (3u' + 2u''\rho) \frac{1 - (u + 2\rho u')^2}{(1 + (u + 2\rho u')^2)^2}. \quad (6.110)$$

A global, analytical solution of this PDE is presently not at hand. Thus, it is resorted to approximate solutions instead [177]. Again, the ‘potential’ u is approximated by the polynomial (6.49) of order n expressing it in terms of $(n + 1)$ scale-dependent couplings $(\rho_0, a_1, \dots, a_n)$. Inserting the ansatz into the PDE (6.110) results in a tower of ordinary, coupled differential equations

$$\begin{aligned} \partial_t \rho_0(t) &= -\rho_0(t) + \left(1 - \frac{1}{N}\right) \\ &\quad + \frac{1}{N} \left(3 + 4\rho_0(t) \frac{a_2(t)}{a_1(t)}\right) \frac{(1 - (2\rho_0(t)a_1(t))^2)}{(1 + (2\rho_0(t)a_1(t))^2)^2} \\ &\quad \vdots \\ \partial_t a_n(t) &= f_n(\rho_0(t), a_1(t), a_2(t), \dots, a_{n+2}(t)). \end{aligned} \quad (6.111)$$

Since the right hand side of (6.110) involves up to second derivatives of u , the functions f_n depend on the couplings a_{n+1} and a_{n+2} . The fixed-point solution requires the β functions of all couplings to vanish, c.f. (2.17). By setting the left hand side of (6.111) equal to zero, an

algebraic system of $(n + 1)$ equations for $(n + 3)$ unknowns remains. This system may be solved, tentatively, by setting the last two couplings a_{n+1} and a_{n+2} equal to zero. That way, the fixed-point values

$$\begin{aligned}\rho_{0*}(N) &= 1 - \frac{1}{N} \\ a_{1*}(N) &= \frac{1}{2} \frac{N}{N-1} \\ a_{2*}(N) &= -\frac{3}{8} \frac{N^2}{(N-1)^2}\end{aligned}\tag{6.112}$$

of the first three couplings are obtained. The solution bifurcates into two independent fixed points starting with a_3 . Intriguingly, the recursive relation leads to an *exact analytical solution* of the full system for all N to arbitrarily high expansion order n . The reason for this unlikely outcome is that the fixed point (6.112) is independent of the boundary condition which had been imposed initially on the higher order couplings. This follows from noticing that all fixed point equations (6.111) with $n \geq 2$ are of the form

$$\begin{aligned}0 &= f_n(\rho_0, a_1, \dots, a_{n+2}) \\ &= \tilde{f}_n(\rho_0, a_1, \dots, a_n) + (n+1) \left(\rho_0 - 1 + \frac{1}{N} + \partial_t \rho_0 \right) a_{n+1} - \frac{n+1}{N} \frac{1 - \xi^2}{(1 + \xi^2)^2} [(3 + 2n)a_{n+1} \\ &\quad + 2(n+2)\rho_0 a_{n+2}] - \frac{4\rho_0 \xi (n+1)^2 (3a_1 + 4a_2 \rho_0)(\xi^2 - 3)}{N (1 + \xi^2)^3} a_{n+1}.\end{aligned}\tag{6.113}$$

Here $\xi = 2a_1 \rho_0$, and $\partial_t \rho_0$ is given according to (6.111). At the fixed point (6.112), $\xi_* = 1$ and all terms proportional to a_{n+1} and a_{n+2} vanish. Thus, the fixed point equation for every a_n with $n > 2$ is independent of a_{n+1} and a_{n+2} , provided the first three couplings take the values (6.112). Hence, a closed system of $(n + 1)$ equations for $(n + 1)$ couplings has been found, allowing for an exact solution order by order.

6.4.2 Exact Critical Exponents

The new fixed point (6.112) has two branches, one of which is IR attractive in all couplings except for the running VEV which remains an IR relevant operator. The second fixed point is IR relevant in all couplings and is thus not pursued any further. The universal scaling exponents of the Wilson-Fisher type fixed point can be determined analytically. From the eigenvalues of the stability matrix B_i^j it follows that the lowest coupling ρ_0 represents an IR unstable direction with a critical index

$$\theta_0 = 1.\tag{6.114}$$

Note that the leading critical exponent $\nu = 1/\theta_0$ in (6.114) is identical to the leading exponent (6.57) obtained at infinite N . Apparently, it does not receive corrections due to the fluctuations of the radial mode in LPA. Therefore it cannot be used to distinguish universality classes of different N . All other couplings a_i , $i = 1, 2, 3, \dots$ define IR attractive directions with sub-leading critical exponents

$$\theta_i = 1 - i - \frac{i(i+1)}{6} \left(\sqrt{\frac{N+17}{N-1}} - 1 \right), \quad i \in \mathbb{N}. \quad (6.115)$$

The universal eigenvalues θ_i are strictly negative for all $N > 1$. In particular, the formerly exactly marginal ϕ^6 coupling has now become irrelevant.

The Gaussian critical exponents (6.57) of the theory in the large- N limit are recovered from (6.114), (6.115) in the limit $1/N \rightarrow 0$. Similarly, the fixed-point values of the couplings (6.112) converge to the large- N fixed-point values for $N \rightarrow \infty$. In the presence of the radial fluctuations, the N -dependent quartic superfield couplings $\tau_*(N)$ is given by the coefficient $a_{1*}(N)$, see (6.112). Taking the limit of infinite N singles out the unique value

$$\lim_{N \rightarrow \infty} \tau_*(N) = \frac{1}{2} \quad (6.116)$$

for the quartic superfield coupling, meaning that the line of non-trivial fixed points parametrized by the exactly marginal superfield coupling τ has shrunk to a single point. Notice also that the fixed point value (6.116) is different from the supersymmetric BMB value $\tau = 1/c_P$ for $N \rightarrow \infty$ within the same regularization scheme. This serves as a strong indication for the non-existence of a supersymmetric BMB fixed point in the presence of the radial fluctuations and $N > 1$.

6.4.3 Global Scaling Solution

The infinite N limit (6.116) of the quartic superfield coupling belongs to the strong coupling domain. Here, the fixed-point solution for the derivative of the superpotential u_* displays two branches, neither of which extends towards arbitrarily small fields. The latter, signalled through the divergence of $du_*/d\rho$ at some finite field value $\rho \geq 0$, is responsible for the occurrence of a Landau scale. It remains to be seen whether the fixed point at finite N continues to belong to the strongly coupled regime or not.

To answer this question and to compare the fixed points at finite and infinite N , a numerical study of the finite- N potential at small fields is necessary. The Taylor series (6.49) of the scaling solution has a finite radius of convergence. Alternatively, one may expand the inverse fixed point solution $\rho(u)$ in powers of u . At infinite N , the analytical scaling solution $\rho = 1 + cu_* + H(u_*) = \sum_{i=0}^{\infty} b_i u_*^i$ has a finite radius of convergence r set by the gap of the inverse propagator (here: $r = 1$) [165]. Either expansion is limited to a finite range in field

space. In order to cover the full field space, and to make potential non-analyticities of the form $u'_*(\rho) \rightarrow \infty$ visible, the differential equation of the inverse function $\rho(u_*)$ instead of $u_*(\rho)$ is integrated numerically. It reads

$$0 = \rho - u_*\rho' - \left(1 - \frac{1}{N}\right) \frac{(1 - u_*^2)}{(1 + u_*^2)^2} - \frac{1}{N}(3\rho'^2 - 2\rho\rho'') \frac{\rho'^2 - (u_*\rho' + 2\rho)^2}{(\rho'^2 + (u_*\rho' + 2\rho)^2)^2} \quad (6.117)$$

subject to suitable boundary conditions. The boundary conditions $\rho(0) = \rho_{0*}$ and $\rho'(0) = 2\rho_{0*}$ correspond to a singular point of (6.117) and cannot be used. Instead, the boundary conditions for $\rho(u_*)$, $\rho'(u_*)$ for $|u_*| = 0.01 \ll 1$ are extracted from the polynomial approximation⁹ to $u_*(\rho)$ of the order $n = 9$.

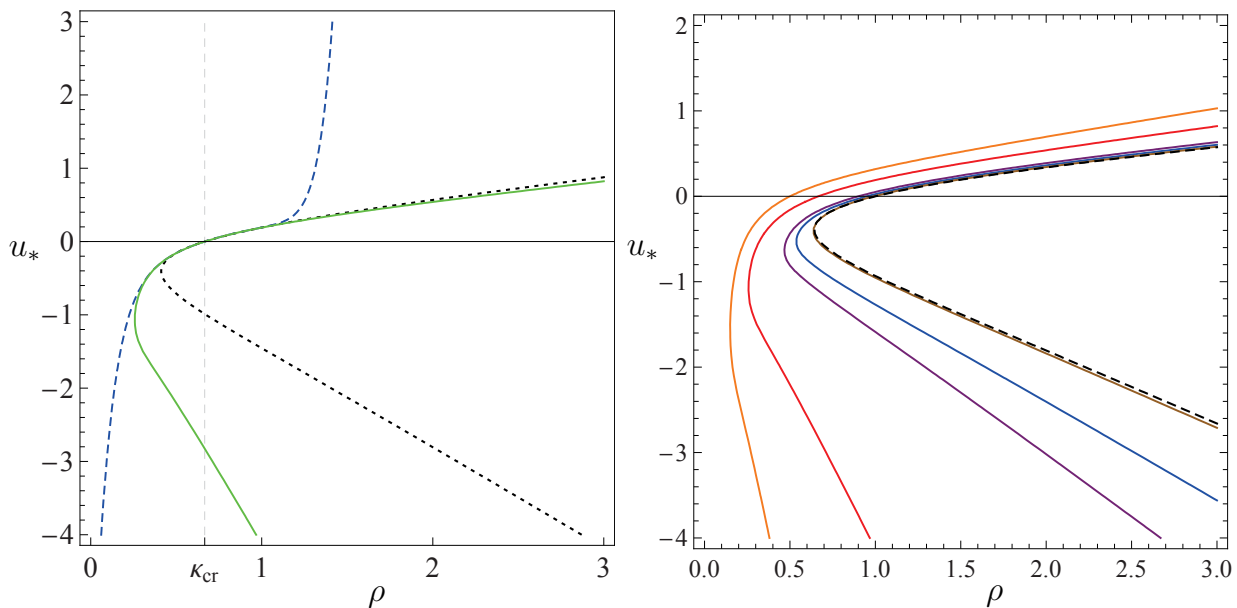


Figure 6.17: *Left panel:* Fixed-point solution $u_*(\rho)$ for $N = 3$. The figure compares the polynomial approximation (blue, dashed line) with the non-perturbative integration (green, solid line) and a large- N like solution (black, dotted line). *Right panel:* Scaling solution $u_*(\rho)$ for various $N > 1$, showing $N = 2, 3, 10, 20$ and 100 from left to right (full lines) in comparison with the infinite N result (dashed line). With increasing N , the solutions converges to the exact infinite- N result with $\tau(N)$ approaching (6.116).

Figure 6.17 (left panel) compares the polynomial approximation of the scaling solution with the numerical one for $N = 3$. The graph also contains the analytical solution of the theory at infinite N . The latter is given by the fixed-point solution of (6.110), where the contribution of the radial mode is neglected and the free parameter of the solution to $a_{1*}(N = 3)$ fixed according to (6.112).

As figure 6.17 (left panel) illustrates, the large- N solution is found to approximate the finite- N solution very well in the vicinity of the node ρ_{0*} and above, largely independently of the chosen value for $N > 1$. This is entirely due to the structure of the fixed point (6.112),

⁹The combined use of polynomial expansions and subsequent numerical integration is a well-tested technique in critical scalar theories. See e.g. [177] for further reading.

where $2a_{1*}\rho_{0*} \equiv 1$. The numerical solutions illustrate further that the fixed-point solution at finite N shows a similar non-analytic behaviour characterized by a diverging mass term $u'_* \rightarrow \infty$, as it appears in the large- N limit for strong quartic superfield coupling (cf. section 6.3).

Now, it is turned to the N -dependence of the scaling solution (6.112). Figure 6.17 (right panel) displays the scaling solution for various $N > 1$. It shows that the fixed-point solution always generates a diverging $du/d\rho$ for some positive field value $\rho = \rho_c(N)$, with $0 < \rho_c(N) < \rho_{0*}(N)$. The solution $u_*(\rho)$ does not exist for small $0 \leq \rho < \rho_c$, for all N considered. Also, $u_*(\rho_c)$ becomes increasingly large in magnitude with decreasing N . Hence, the main effect of the competition between the radial mode and the Goldstone mode fluctuations, with decreasing N , is a shift of the end point $\rho_c(N)$ and the VEV $\rho_{0*}(N)$ towards smaller field values. Continuity in N suggests that this pattern persists for all $N > 1$ where $\rho_{0*} > 0$.

In case of the supersymmetric Ising model where $N = 1$, the Goldstone modes are absent and the RG dynamics is solely controlled by the fluctuations of the radial mode. In the limit $N \rightarrow 1$, (6.112) predicts a vanishing VEV, $\rho_{0*} = 0$ and implies the existence of a supersymmetric Ising fixed point valid for all fields, though at the expense of a non-analytic behaviour of $u_*(\rho)$ at vanishing field. Note that a direct study of the $N = 1$ case using the same RG equations [48] has also detected a regular Ising fixed point analytic in the fields, whose critical eigenvalue $\theta_0 = 3/2$ is different from (6.114). Furthermore, the divergence of all higher order couplings in the limit $N \rightarrow 1$, together with the continuity of the fixed point in N suggests that $\rho_c \rightarrow 0$ and $|u_*(\rho_c)| \rightarrow \infty$ in this limit. This behaviour is intriguing inasmuch as the diverging of $u_*(\rho \rightarrow 0)$ is the fingerprint for the spontaneous breaking of scale invariance. It may thus qualify for a novel supersymmetric BMB phenomenon which originates from the radial mode rather than the Goldstone fluctuations. It would seem worth to test this picture directly in the supersymmetric Ising model without relying on the limit $N \rightarrow 1$ adopted here.

To conclude, the fixed point (6.112) is of the strongly-coupled type for all $N > 1$ as signalled by the same qualitative behaviour seen previously at infinite N in section 6.3. Furthermore, the fluctuations of the Goldstone modes are central for the existence of the endpoint in field space $\rho_c > 0$ of strongly coupled fixed-point solutions. At infinite N , and as a consequence of $\rho_c > 0$, the phase diagram at strong coupling is governed by non-analyticities at finite RG scales. Due to $\rho_c(N) > 0$ for $N > 1$, the same type of non-analyticities with an associated Landau scale k_L control the phase transition associated with the fixed point (6.112) at finite N . The above behaviour at strong coupling is thus generic for supersymmetric $(\Phi^2)^2$ theories with $N > 1$.

Chapter 7

Conclusions

This work aimed at gaining new insight into the non-perturbative regimes of supersymmetric field theories within the functional renormalization group framework.

We thus formulated a supersymmetric renormalization group flow that connects physics on microscopic and macroscopic scales by successively taking into account quantum fluctuations. Most importantly, its applicability is not restricted to the perturbative regimes characterized by a small parameter. It rather allows for exploring deeply non-perturbative physics.

We considered theories both with unbroken and spontaneously broken supersymmetry via a manifestly supersymmetric formulation of the evolution equations. Only then, a precise investigation of the nature of the supersymmetry breaking mechanism becomes feasible. Therefore, the flow equations were formulated in superspace. This implies the ansatz of the effective average action and the regulator to be solely a functional of superfields and supercovariant derivatives. The flow of the truncated action was regularized by a suitable regulator functional that links bosonic and fermionic degrees of freedom to conform to supersymmetry. As specific truncation scheme we applied the supercovariant derivative expansion - an approach of intrinsically non-perturbative nature. Here, the action is expanded in operators containing a successively increasing number of supercovariant derivatives. Contrary to the derivative expansion in non-supersymmetric theories, this scheme is not an expansion in momenta rather than in the auxiliary field.

Supersymmetric quantum mechanics served as the first testing ground of the renormalization group approach described above. Since quantum mechanical observables as excited state energies are well-known to numerical precision, the convergence properties of the expansion scheme could directly be valued. Indeed, we showed the supercovariant derivative expansion to be systematic in the sense that physically measurable quantities converged by increasing the order of truncation.

First, we studied quantum mechanical systems with unbroken supersymmetry. The supercovariant derivative expansion enabled us to apply a simple projection scheme: by extracting the coefficients of an expansion in the auxiliary field, the evolution equations

were derived. We obtained high-accuracy results for the first excited state energy within a truncation containing all operators up to and including fourth-order derivative terms. We achieved a relative error of the energy gap below one percent for a wide range of couplings, including the non-perturbative regime where tunnelling effects become important. However, for quite large couplings, i.e. pronounced non-convex microscopic potentials, the derivative expansion broke down. This is expected since this regime is dominated by non-local instanton contributions which have not been comprised in our truncation.

Furthermore, we investigated supersymmetric quantum mechanics with spontaneously broken supersymmetry. We revealed the expansion in the auxiliary field around vanishing expansion point to fail, as an infrared regularization is not viable any more. Intuitively, this is already clear since spontaneous supersymmetry breaking implies the auxiliary field to take a non-vanishing expectation value which has to be accounted for. Consequently, we proposed a new projection scheme exhibiting an expansion in the auxiliary field around its vacuum expectation value. By studying the flow of the superpotential with constant wave-function renormalization, we determined the ground state energies in agreement to the exact results within a few percent.

The three-dimensional $\mathcal{N} = 1$ Wess-Zumino theories provided the second testing ground of our renormalization group approach to supersymmetry. We focussed on physics at criticality as described by the fixed-point solution of the flow equations. The latter separates the phase of unbroken supersymmetry from the phase allowing for spontaneous supersymmetry breaking. In particular, we identified the supersymmetric analogue of the Wilson-Fisher scaling solution of spherical scalar theories. Via spectral methods, we determined the global scaling solution and leading critical exponents in next-to-next-to-leading order in the derivative expansion. Again, the physical quantities at the phase transition - the universal critical exponents - converged quite nicely by increasing the order of truncation. Quite special to the model and unknown in standard spin systems is a connection between the critical exponent of the infrared-unstable direction and the anomalous dimension, called superscaling relation. We proved this relation to hold to all orders in the supercovariant derivative expansion. Additionally, we generalized and verified it for all dimensions $d \geq 2$.

Finally, we elaborately provided a renormalization group study of interacting supersymmetric $O(N)$ theories in three dimensions. In particular, we analysed supersymmetric $O(N)$ theories with microscopic $(\Phi^2)^2$ superpotential which we pointed out to have many common characteristics to spherical scalar $(\phi^2)^3$ theories. We derived the evolution equation for the superpotential within the superspace formalism in leading order in the supercovariant derivative expansion. The implementation of $O(N)$ symmetry in the supersymmetric action thereby leads to a scalar potential with vanishing ground state and thus unbroken supersymmetry. Due to the highly non-linear structure of this partial differential equation, we focussed on the large- N limit first. It offers two advantages: firstly, the local potential

approximation becomes exact as higher order operators are suppressed by N . Secondly, the evolution equation may be solved analytically then. Consequently, we determined the exact analytical solution of the flow equation for the superpotential.

Special interest was devoted to the fixed-point solution describing the phase transition between the $O(N)$ symmetric and the spontaneously $O(N)$ broken phase. We showed the phase diagram in the large- N limit to be controlled by two free physical parameters: the exactly marginal quartic superfield coupling and the infrared relevant vacuum expectation value. We demonstrated the theory to locally exhibit an infinitely extended line of fixed points, parametrized by the quartic superfield coupling. However, globally we found this line to terminate at a critical value: starting at the trivial Gaussian fixed point with vanishing coupling, the line bifurcates at some coupling in two solutions, both of which terminate at a critical coupling. If the quartic superfield coupling is increased further, we showed Landau-type poles to appear in physical field space, implying the scaling solution to be no more globally defined. We specified the universal critical exponents by showing the fixed points to obey Gaussian scaling, quite similar to the scalar $(\phi^2)^3$ models. However, we further showed the scaling solution with asymptotically large superfield coupling to deviate from this Gaussian scaling. We resolved this interesting behaviour by directly linking this fixed point to the Wilson-Fisher scaling solution of the 3d spherical model. In particular, we showed remnants of the non-Gaussian critical exponents of the scalar model to become visible then. Two important differences induced by supersymmetrizing the scalar $O(N)$ model could be devised: Firstly, supersymmetry is responsible for the absence of the redundant relevant exponent of $\theta = 3$ corresponding to overall shifts of the potential. Secondly, supersymmetry links the quartic and sextic couplings, implying criticality to be achieved by fine-tuning merely a single microscopic parameter - the vacuum expectation value.

We presented a detailed analysis of the phase diagram from an effective as well as a renormalized field theory perspective. At weak coupling, we found the theory to display a second-order phase transition between the $O(N)$ symmetric and a symmetry broken phase with Gaussian scaling and conserved global supersymmetry. At strong coupling, the global effective potential becomes multi-valued in certain regions of field space, signalled by divergences in the fermion-boson interactions at a finite Landau scale. We thus resolved the long-standing puzzle about peculiar degenerate $O(N)$ symmetric ground states by showing those states to arise from the integrating-out of strongly-coupled long wave-length fluctuations. We suspect supersymmetry to be spontaneously broken in this strong-coupling regime. Besides, we demonstrated the phase structure described above to be largely insensitive to whether the ultraviolet cutoff is finite or infinite.

At infinite N , we identified a supersymmetric analogue of the Bardeen-Moshe-Bander (BMB) fixed point characterized by spontaneously broken scale-invariance. We showed supersymmetry to remain intact. The broken scale invariance occurs at a single value of the

quartic superfield coupling, whose degree of freedom is transmuted to an arbitrary mass scale. Besides, an exactly massless dilaton and dilatino appear. We verified the scaling exponents of the BMB fixed-point to be double-valued. They obey Gaussian as well as non-Gaussian scaling due to non-analyticities in the superpotential.

We completed our studies on supersymmetric $O(N)$ theories by exploring the influence of the radial fluctuations arising at finite N . We illustrated the latter to lift the degeneracy of the quartic superfield coupling implying the line of fixed points to collapse to a single non-trivial scaling solution. Locally, we identified a new supersymmetric Wilson-Fisher fixed point characterized by non-Gaussian exponents and super-universal scaling of the relevant coupling. Globally, however, the fixed point belongs to the strongly coupled regime, plagued by Landau poles in physical field space. Interestingly, we observed the domain in field space showing Landau poles to shrink with decreasing N . As soon as the Goldstone fluctuations are absent, the scaling solution extends over all physical field space, though at the expense of a non-analyticity at vanishing field. Lastly, we showed the BMB phenomenon to disappear at finite $N > 1$.

From a structural point of view, we revealed the build-up of multi-valued effective potentials accompanied by Landau poles to be the most distinctive new feature due to supersymmetry. We gave evidence that this behaviour arises primarily through the fluctuations of the Goldstone modes. The occurrence of similar non-analyticities in the random-field Ising model with Parisi-Sourlas supersymmetry hints at a possible spontaneous breakdown of supersymmetry at strong couplings. Conversely, we propose that the existence of a Landau scale is the signature of a multi-valued effective potential in disordered Ising models. Finally, we stress that the utilization of the functional renormalization group was decisive to achieve the stated results. Only by virtue of the fully integrated renormalization group flow at all scales, the structure of the effective potential has become transparent.

Nevertheless, some findings in the deeply non-perturbative regimes require a critical glance: In unbroken supersymmetric quantum mechanics, the breakdown of our truncation was accompanied by the effective potential becoming purely imaginary and the appearance of additional, parametrically large masses. Similarly, we observed a multi-valued effective potential not globally defined and masses of the order of the UV cutoff in the strongly coupled supersymmetric $O(N)$ model. These similarities might indicate a possible breakdown of the expansion scheme at large couplings in supersymmetric $O(N)$ theories as well. Therefore, we suggest further investigations by applying different truncations or methods. One might utilize e.g. the vertex expansion (or similarly Dyson-Schwinger equations) since this truncation may be regarded as complementary to the derivative expansion in the sense that the expansion coefficients are arbitrary functions of the momenta.

Appendix A

Technical Details for SUSY-QM

This appendix describes the derivation of the flow equations for SUSY-QM in NNLO in the supercovariant derivative expansion. A rough sketch of the derivation is already given in section 4.2.3. According to (4.23), i.e.

$$\begin{aligned}
 \partial_k \Gamma_k |_{\dot{\phi}=\dot{F}=\dot{\psi}=\dot{\bar{\psi}}=0} &= \int d\tau \left(i \partial_k W' F + \frac{1}{2} \partial_k Z'^2 F^2 + \frac{i}{4} \partial_k Y'_2 F^3 \right) \\
 &= \frac{1}{2} \int \frac{dq}{2\pi} \frac{dq'}{2\pi} d\theta d\bar{\theta} d\theta' d\bar{\theta}' (\partial_k R_k)(q', q, \theta', \theta) G_k(q, q', \theta, \theta') \\
 &= \frac{1}{2} \int d\tau \frac{dq}{2\pi} \left[i (\partial_k r_1) (b + c + d + e) + \partial_k (r_2 Z'^2(\bar{\phi})) (f + a q^2 - e q + d q) \right], \quad (\text{A.1})
 \end{aligned}$$

the flow equations for W' , Z' and Y'_2 are extracted by the projection of the right hand side onto the contributions in F , F squared and F cubed respectively. Thereby, the functions (a, b, c, d, e, f) denote the coefficients of the Taylor expansion of the Greens function G_k in Grassmann variables according to the ansatz (4.22). The coefficients are determined by solving the relation

$$1 = G_k \left(\Gamma_k^{(2)} + R_k \right) \quad (\text{A.2})$$

via the method of equating the coefficients. This yields

$$\begin{aligned}
a &= \frac{(B + \frac{3}{2}iFY'_2)}{\frac{1}{16}(4A + F(3FY''_2 - 8iZ'Z''))^2 + (B + \frac{3}{2}iFY'_2)C} \\
b = c &= \frac{-\left(iA + \frac{3}{4}iF^2Y''_2 + 2FZ'Z''\right)}{\left(\frac{1}{16}(4A + F(3FY''_2 - 8iZ'Z''))^2 + (B + \frac{3}{2}iFY'_2)C\right)} \\
d &= \frac{4i}{4A - 4iBq + F(FY''_2 + 4qY'_2 - 4iZ'Z'')} \\
e &= \frac{4i}{4A + 4iBq + F(FY''_2 - 4qY'_2 - 4iZ'Z'')} \tag{A.3} \\
f &= \frac{1}{\left(B + \frac{3}{2}iFY'_2\right)} + \frac{\left(iA + \frac{3}{4}iF^2Y''_2 + 2FZ'Z''\right)^2}{\left(B + \frac{3}{2}iFY'_2\right)\left(\frac{1}{16}(4A + 3F^2Y''_2 - 8iFZ'Z'')^2 + \left(B + \frac{3}{2}iFY'_2\right)C\right)},
\end{aligned}$$

where the abbreviations

$$\begin{aligned}
A &= W'' + r_1 + \frac{1}{2}(Y'_1 + Y_2)q^2 \\
B &= Z'^2 + r_2Z_k'^2(\bar{\phi}) \\
C &= Bq^2 + \frac{i}{4}F^3Y_2''' + F^2(Z''^2 + Z'''Z') + \frac{i}{2}F(q^2(2Y'_2 + Y_1'') + 2W''') \tag{A.4}
\end{aligned}$$

have been used. By inserting the solutions (A.3) into (A.1), the different flows can be projected out. They read

$$\begin{aligned}
\partial_k W'_k(\phi) &= \frac{1}{2} \int_{-\infty}^{\infty} \frac{dq}{2\pi} \left[\partial_k r_1 \frac{2(Z'Z''(A^2 - B^2q^2) - BAA')}{(B^2q^2 + A^2)^2} \right. \\
&\quad \left. + \partial_k(r_2Z'^2(\bar{\phi})) \frac{(A'(A^2 - B^2q^2) + 4Bq^2AZ'Z'')}{(B^2q^2 + A^2)^2} \right] \\
\partial_k Z'_k(\phi) &= \frac{1}{2} \int_{-\infty}^{\infty} \frac{dq}{2\pi} \left[\frac{\partial_k r_1}{2Z'(A^2 + B^2q^2)^3} \left\{ -2A^4Y_2'' + 2B^3q^2(Bq^2Y_2'' - 4Z'Z''(A' + q^2Y_2')) \right. \right. \\
&\quad - AB^2(q^2(10A'Y_2' + 4BZ^{(3)}Z' + 4Z''^2(B - 9Z'^2) + q^2Y_2'^2) + 4A'^2) \\
&\quad \left. \left. + A^3(6A'Y_2' - 4BZ^{(3)}Z' - 4Z''^2(B + 3Z'^2) - q^2Y_2'^2) + 24A^2BZ'Z''(A' + q^2Y_2') \right\} \right. \\
&\quad + \frac{\partial_k(r_2Z'^2(\bar{\phi}))}{4Z'(A^2 + B^2q^2)^3} \left\{ 4A^4(Z''^2 + Z^{(3)}Z') - B^3q^2(4A'^2 + 2q^2(2A'Y_2' + 2B(Z^{(3)}Z' + Z''^2) \right. \\
&\quad \left. \left. - 12Z'^2Z''^2 + q^2Y_2'^2)) + 8AB^2q^2(6Z'Z''(A' + q^2Y_2') - Bq^2Y_2'') - 8A^3(2Z'Z''(A' + q^2Y_2') \right. \right. \\
&\quad \left. \left. + Bq^2Y_2'') + A^2B(4A'^2 - 2q^2(-14A'Y_2' + q^2Y_2'^2 + 36Z'^2Z''^2)) \right\} \right] \tag{A.5}
\end{aligned}$$

$$\begin{aligned}
\partial_k Y_2'(\phi) = & \frac{1}{2} \int_{-\infty}^{\infty} \frac{dq}{2\pi} \left[\frac{2\partial_k r_1}{(A^2 + B^2 q^2)^4} \left\{ -10A^5 Y_2'' Z' Z'' - 24A^4 B Z' Z''^3 - 28A^4 Z'^3 Z''^3 \right. \right. \\
& - A^5 B Y_2^{(3)} - 2A^3 B^3 q^2 Y_2^{(3)} + 20A^3 B^2 q^2 Y_2'' Z' Z'' - 16A^2 B^3 q^2 Z' Z''^3 + 168A^2 B^2 q^2 Z'^3 Z''^3 \\
& + 4ABq^4 Y_2'^3 (A^2 + B^2 q^2) + 4AB^3 A^3 + 2q^2 Y_2'^2 Z' Z'' (3A^4 - 38A^2 B^2 q^2 + 7B^4 q^4) \\
& + 8BZ^{(3)} Z'^2 Z'' (-3A^4 - 2A^2 B^2 q^2 + B^4 q^4) + 2Y_2' (Y_2'' (6A^4 B q^2 + 4A^2 B^3 q^4 - 2B^5 q^6) \\
& + AZ^{(3)} Z' (-3A^4 + 2A^2 B^2 q^2 + 5B^4 q^4) + AZ''^2 (-3A^4 + 2A^2 B^2 q^2 + 72Bq^2 Z'^2 (A^2 - B^2 q^2) \\
& + 5B^4 q^4)) + 4BA'^2 (2BZ' Z'' (B^2 q^2 - 5A^2) - 3AY_2' (A^2 - B^2 q^2)) + A' (6ABq^2 Y_2'^2 (3B^2 q^2 \\
& - 5A^2) + B (8A (BZ^{(3)} Z' (A^2 + B^2 q^2) + Z''^2 (B (A^2 + B^2 q^2) + 12Z'^2 (A^2 - B^2 q^2))) \\
& + Y_2'' (9A^4 + 6A^2 B^2 q^2 - 3B^4 q^4)) + 4Y_2' Z' Z'' (9A^4 - 34A^2 B^2 q^2 + 5B^4 q^4)) - AB^5 q^4 Y_2^{(3)} \\
& \left. + 30AB^4 q^4 Y_2'' Z' Z'' + 8B^5 q^4 Z' Z''^3 - 28B^4 q^4 Z'^3 Z''^3 \right\} \\
& + \frac{\partial_k (r_2 Z'^2(\bar{\phi}))}{(A^2 + B^2 q^2)^4} \left\{ A^6 Y_2^{(3)} + 16A^5 Z' Z''^3 + A^4 B^2 q^2 Y_2^{(3)} - 60A^4 B q^2 Y_2'' Z' Z'' - A^2 B^4 q^4 Y_2^{(3)} \right. \\
& - 32A^3 B^2 q^2 Z' Z''^3 - 224A^3 B q^2 Z'^3 Z''^3 + 16AZ^{(3)} Z'^2 Z'' (A^2 - 3B^2 q^2) (A^2 + B^2 q^2) \\
& - 40A^2 B^3 q^4 Y_2'' Z' Z'' + 16ABq^4 Y_2'^2 Z' Z'' (5A^2 - 7B^2 q^2) - 4B^2 A^3 (A^2 - B^2 q^2) \\
& + Y_2'^3 (-2A^4 q^4 + 4A^2 B^2 q^2 + 6B^4 q^8) + 2A'^2 (16ABZ' Z'' (A^2 - 2B^2 q^2) \\
& + 3Y_2' (A^4 - 6A^2 B^2 q^2 + B^4 q^4)) + 4q^2 Y_2' (Y_2'' (-2A^5 + 4A^3 B^2 q^2 + 6AB^4 q^4) \\
& + BZ^{(3)} Z' (-7A^4 - 6A^2 B^2 q^2 + B^4 q^4) + Z''^2 (-18Z'^2 (A^4 - 6A^2 B^2 q^2 + B^4 q^4) + B^5 q^4 \\
& - 7A^4 B - 6A^2 B^3 q^2)) + A' (32ABq^2 Y_2' Z' Z'' (7A^2 - 5B^2 q^2) + 3Y_2'^2 (5A^4 q^2 + B^4 q^6 \\
& - 26A^2 B^2 q^4) + 2 (4BZ^{(3)} Z' (B^4 q^4 - A^4) + Y_2'' (-3A^5 + 6A^3 B^2 q^2 + 9AB^4 q^4) \\
& - 4Z''^2 (A^4 B + 6Z'^2 (A^4 - 6A^2 B^2 q^2 + B^4 q^4) - B^5 q^4)) - 48AB^4 q^4 Z' Z''^3 \\
& \left. + 224AB^3 q^4 Z'^3 Z''^3 - B^6 q^6 Y_2^{(3)} + 20B^5 q^6 Y_2'' Z' Z'' \right\} . \tag{A.6}
\end{aligned}$$

In order to close the system of coupled differential equations, the flow of $Y_1' + Y_2$ is finally determined. Therefore, an expansion of the inverse propagator around field configurations of F and ϕ exhibiting a small momentum dependence according to (4.24) is required, quite analogously the procedure applied in scalar models [125, 126]. Again, the fermionic fields ψ and $\bar{\psi}$ are set to zero and only the bosonic part of the superfield in the inverse propagator is considered. Now, the inverse Green's function $\Gamma_k^{(2)} + R_k$ is expanded up to the order $\mathcal{O}(\delta\phi(Q)\delta F(-Q))$. Hence, the inverse propagator may be written in the form

$$(\Gamma_k^{(2)} + R_k)(z, z') = [\Gamma_0(q, q') + \Gamma_\phi(q, q') + \Gamma_F(q, q') + \Gamma_{\phi F}(q, q')] \delta(\theta, \theta'), \tag{A.7}$$

corresponding to an expansion in powers of $\delta\phi$ and δF . The terms read in detail

$$\begin{aligned}
\Gamma_0(q, q') &= \hat{\Gamma}_0(q)\delta(q - q') \quad \text{with} \\
\hat{\Gamma}_0(q) &= \left(i(W'' + r_1) - BK(q) + \frac{i}{2}(Y'_1 + Y_2)q^2 \right) \\
\hat{\Gamma}_0^{-1}(q) &= \frac{-i(W'' + r_1 + \frac{1}{2}(Y'_1 + Y_2)q^2) - BK(q)}{B^2q^2 + (W'' + r_1 + \frac{1}{2}(Y'_1 + Y_2)q^2)^2} \\
\Gamma_\phi(q, q') &= \hat{\Gamma}_\phi(q, Q)\delta(q - q' - Q) + \hat{\Gamma}_\phi(q, -Q)\delta(q - q' + Q) \quad \text{with} \\
\hat{\Gamma}_\phi(q, Q) &= \left(iW'''' + Z'Z''Q^2\bar{\theta}\theta - Z'Z''(K(q) + K(q - Q)) - \frac{i}{2}Y'_2Q^2\bar{\theta}\theta K(q - Q) \right. \\
&\quad \left. - \frac{i}{2}Y'_2Q^2K(q)\bar{\theta}\theta + \frac{i}{2}Y'_2K(q)K(q - Q) + \frac{i}{4}Y''_1(q^2 + Q^2 + (q - Q)^2) \right) \delta\phi(Q) \\
\Gamma_F(q, q') &= \hat{\Gamma}_F(q, Q)\delta(q - q' - Q) + \hat{\Gamma}_F(q, -Q)\delta(q - q' + Q) \quad \text{with} \\
\hat{\Gamma}_F(q, Q) &= \left(iW''''\bar{\theta}\theta + Z'Z'' - Z'Z''K(q)\bar{\theta}\theta - Z'Z''\bar{\theta}\theta K(q - Q) - \frac{i}{2}Y'_2K(q) \right. \\
&\quad \left. - \frac{i}{2}Y'_2K(q - Q) + \frac{i}{2}Y'_2K(q)\bar{\theta}\theta K(q - Q) + \frac{i}{4}Y''_1(q^2 + Q^2 + (q - Q)^2)\bar{\theta}\theta \right) \delta F(Q) \\
\Gamma_{\phi F}(q, q') &= \hat{\Gamma}_{\phi F}(q)\delta(q - q') \quad \text{with} \\
\hat{\Gamma}_{\phi F}(q) \Big|_{\mathcal{O}(Q^2)} &= \frac{i}{2}(Y''_2 + Y''_1)Q^2\bar{\theta}\theta(\delta\phi(Q)\delta F(-Q) + \delta F(Q)\delta\phi(-Q)). \quad (\text{A.8})
\end{aligned}$$

Thereby, only terms quadratic in Q in $\Gamma_{\phi F}(q, q')$ are listed as other terms do not contribute to the flow. Note that the operator K occurring in eq. (A.8) is a function of the momentum as well as the Grassmann variables $\bar{\theta}, \theta$. Next, the Green's function as the inverse operator of (A.7) has to be determined. An inversion of (A.7) yields with $\Gamma_0(q, q') = \hat{\Gamma}_0(q)\delta(q - q')$ the propagator

$$\begin{aligned}
(G_k)(z, z')_{(\delta\phi\delta F)} &= \left\{ -\hat{\Gamma}_0^{-1}(q)\Gamma_{\phi F}(q, q')\hat{\Gamma}_0^{-1}(q) \right. \\
&\quad \left. + \int_{\tilde{q}} \hat{\Gamma}_0^{-1}(q)\Gamma_\phi(q, \tilde{q})\hat{\Gamma}_0^{-1}(\tilde{q})\Gamma_F(\tilde{q}, q')\hat{\Gamma}_0^{-1}(q) \right. \\
&\quad \left. + \int_{\tilde{q}} \hat{\Gamma}_0^{-1}(q)\Gamma_F(q, \tilde{q})\hat{\Gamma}_0^{-1}(\tilde{q})\Gamma_\phi(\tilde{q}, q')\hat{\Gamma}_0^{-1}(q) \right\} \delta(\theta, \theta'), \quad (\text{A.9})
\end{aligned}$$

where only contributions quadratic in the fluctuations $\sim (\delta F)(\delta\phi)$ have been kept. Now, all ingredients are gathered and the final flow equation reads

$$\begin{aligned}
\frac{i}{2}\partial_k(Y'_1 + Y_2) &= \lim_{Q^2 \rightarrow 0} \frac{\partial}{\partial Q^2} \frac{\delta}{\delta\phi(Q)} \frac{\delta}{\delta F(-Q)} \frac{1}{2} \int \frac{dq}{2\pi} \partial_k \left[ir_1 - Z_k'^2(\bar{\phi})r_2K(q, \theta') \right] \delta(\theta', \theta) \times \\
&\quad \left[-\hat{\Gamma}_0^{-1}(q)\hat{\Gamma}_{\phi F}(q)\hat{\Gamma}_0^{-1}(q) + \hat{\Gamma}_0^{-1}(q)\hat{\Gamma}_\phi(q, Q)\hat{\Gamma}_0^{-1}(q - Q)\hat{\Gamma}_F(q - Q, -Q)\hat{\Gamma}_0^{-1}(q) \right. \\
&\quad \left. + \hat{\Gamma}_0^{-1}(q)\hat{\Gamma}_F(q, -Q)\hat{\Gamma}_0^{-1}(q + Q)\hat{\Gamma}_\phi(q + Q, Q)\hat{\Gamma}_0^{-1}(q) \right] \delta(\theta, \theta') \Big|_{\bar{\theta}\theta\bar{\theta}'\theta'}. \quad (\text{A.10})
\end{aligned}$$

The flow of $(Y'_1 + Y_2)$ is then obtained by inserting the expressions (A.8) into (A.10) and integrating over all Grassmann variables. Note that (A.10) contains contributions of the form $r_1(q \pm Q)$ and $r_2(q \pm Q)$, carrying a dependence on the external momentum Q (c.f. (A.8)). Thus, the specific form of the flow of $(Y'_1 + Y_2)$ depends on the regulator functions chosen.

Appendix B

Pseudo-Spectral Methods

We obtained the numerical results in this work in part with so-called (pseudo-)spectral methods. Spectral methods were studied from a mathematical point of view already some decades ago, however, they were only applied in certain fields of physics up to now, e.g. in numerical relativity, meteorology or fluid mechanics. The basic idea behind spectral methods is to expand the solution into orthogonal polynomials which should be chosen to fit the problem. A well-known example is the Fourier series of a periodic function. In our case, we chose a combination of Chebyshev and rational Chebyshev polynomials in order to resolve the operators globally. On the other hand, in RG-time-direction, we chose to map the (infinite) time axis onto a finite interval, then slicing it into smaller pieces and apply a Chebyshev spectralization in this direction. With a stabilized Newton-Raphson iteration scheme, we demanded that the flow equations are satisfied on collocation points up to a certain tolerance. This twofold application of spectral methods was considered too expensive in former times, but thanks to the progress in computing power, it is feasible now. This point is also undermined by the recent application of this method to gain exact solutions to the Einstein field equations for axisymmetric and stationary space times [128, 178].

The reason to use spectral methods is their extraordinary speed of convergence. For well-behaved functions, a spectral method may convergence exponentially, i.e. faster than any power law. Another advantage is that the expansion coefficients give a rough estimate of the maximal error in the interpolation of the solution. A general rule of thumb is that the error is bounded by roughly the absolute value of the last coefficient retained. For an extensive review of spectral methods, see e.g. [127].

Appendix C

Technical Details for the $\mathcal{N} = 1$ Wess-Zumino Model

Similarly to the analysis in SUSY quantum mechanics, the Greens function

$$G_k(q, q', \theta, \theta') = \left(a + b \bar{\theta}\theta + c \bar{\theta}'\theta' + d \bar{\theta}\theta' + e \bar{\theta}\theta\bar{\theta}'\theta' + f \bar{\theta}'\theta\theta' \right) \delta(q, q') \quad (\text{C.1})$$

is determined by solving the equation

$$\int \frac{d^3 q'}{(2\pi)^3} d\theta' d\bar{\theta}' G_k^{-1}(q, q', \theta, \theta') G_k(q', q'', \theta', \theta'') = \delta(q, q'') \delta(\theta, \theta'') \quad (\text{C.2})$$

for the coefficients (a, b, c, d, e, f) . This yields

$$\begin{aligned} a &= \frac{8(2B - 3FY_2')}{8C(2B - 3FY_2') - (4A - 3F^2Y_2'' + 8FZ'Z'')^2} \\ b = c &= \frac{8A - 6F^2Y_2'' + 16FZ'Z''}{(4A - 3F^2Y_2'' + 8FZ'Z'')^2 + 8C(3FY_2' - 2B)} \\ d &= -\frac{4\left(A - \frac{1}{4}F^2Y_2'' + FZ'Z''\right)}{4\left(A - \frac{1}{4}F^2Y_2'' + FZ'Z''\right)^2 - 4q^2(B - FY_2')^2} \\ e &= \frac{4C}{8C(2B - 3FY_2') - (4A - 3F^2Y_2'' + 8FZ'Z'')^2} \\ f &= -\frac{16(B - FY_2')}{(4A - 4Bq + F(-FY_2'' + 4qY_2' + 4Z'Z''))(4A + 4Bq - F(FY_2'' + 4qY_2' - 4Z'Z''))}, \end{aligned} \quad (\text{C.3})$$

where the abbreviations

$$\begin{aligned}
A &= W''' + r_1 - \frac{1}{2}(Y_1' + Y_2)q^2 \\
B &= Z'^2 + r_2 Z_k'^2(\bar{\phi}) \\
C &= Bq^2 - \frac{1}{4}F^3 Y_2''' + F^2 (Z''^2 + Z''' Z') + \frac{1}{2}F (2W''' - q^2 (2Y_2' + Y_1'')) \quad (C.4)
\end{aligned}$$

have been used. A projection of the right hand side of the Wetterich equation onto terms in F, F^2 and F^3 for constant component fields and vanishing Majorana spinors then provides the scale dependence of W', Z', Y_2' according to

$$\begin{aligned}
\partial_k \Gamma_k |_{\partial_\mu \phi = \partial_\mu F = \psi = \bar{\psi} = 0} &= \int d^3 x \left(\partial_k W' F + \frac{1}{2} \partial_k Z'^2 F^2 - \frac{1}{4} \partial_k Y_2' F^3 \right) \\
&= \frac{i}{2} \int \frac{d^3 q}{(2\pi)^3} \frac{d^3 q'}{(2\pi)^3} d\theta d\bar{\theta} d\theta' d\bar{\theta}' (\partial_k R_k)(q', q, \theta', \theta) G_k(q, q', \theta, \theta') \\
&= \frac{i}{2} \int d^3 x \frac{d^3 q}{(2\pi)^3} \left[(2\partial_k r_1)(b + c + d) + \partial_k (r_2 Z_k'^2(\bar{\phi}))(-2fq^2 + aq^2 + 4e) \right], \quad (C.5)
\end{aligned}$$

where (a, b, c, d, e, f) are given by (C.3).

Appendix D

Technical Details for Supersymmetric $O(N)$ Theories

This appendix contains the derivation of the evolution equation for the superpotential $W_k(\rho)$ of the three-dimensional $\mathcal{N} = 1$ SUSY $O(N)$ model. The scale dependence of Γ_k is thereby encoded solely in the superpotential, i.e. it is restricted to the local potential approximation. To begin with, the second functional derivative with respect to the superfields of the truncated action (6.8) with $Z_k(R) = 1$ and $Y_k(R) = 0$ has to be calculated¹. This leads to

$$\begin{aligned} (\Gamma_k^{(2)})_{mn}(z, z') &= -K(q, \theta)\delta_{mn}\delta(z - z') + 2 \int_x W'_k(R)\delta_{mn}\delta(\bar{\theta} - \bar{\theta}')\delta(\theta - \theta')e^{i(q-q')x} \\ &+ 2 \int_x W''_k(R) \left(\int_{\tilde{q}} \Phi_m(\tilde{q}, \theta)e^{-i(\tilde{q}-q)x} \right) \left(\int_{\hat{q}} \Phi_n(\hat{q}, \theta)e^{-i(\hat{q}+q')x} \right) \delta(\bar{\theta} - \bar{\theta}')\delta(\theta - \theta'). \end{aligned} \quad (\text{D.1})$$

Here, $K = 1/2(\bar{\mathcal{D}}\mathcal{D} - \mathcal{D}\bar{\mathcal{D}})$ represents the kinetic operator and $z = (q, \theta)$ summarizes momentum and Grassmann coordinates. The evolution equation of W_k can now be obtained by setting ψ_i, F_i equal to zero, i.e. by considering purely scalar fields. Furthermore, the scalars are assumed to be constant in position space and it is projected onto one single component according to

$$\Phi_i(q, \theta) = \phi \delta_{i1}\delta(q). \quad (\text{D.2})$$

Hence, (D.1) turns into

$$(\Gamma_k^{(2)})_{mn}(z, z') = [-\delta_{mn}K(q, \theta) + 2W'_k(\bar{\rho})\delta_{mn} + 4W''_k(\bar{\rho})\bar{\rho}\delta_{m1}\delta_{n1}] \delta(z - z'). \quad (\text{D.3})$$

Next, an adequate regulator term ΔS_k has to be chosen with $\Delta S_k^{(2)} = R_k$ preserving supersymmetry as well as $O(N)$ symmetry. In order to guarantee the one-loop structure of the flow equation, it should be quadratic in the superfields. According to (6.11) it may be

¹Subsequently, it is worked in momentum space.

chosen as

$$\Delta S_k = -\frac{1}{2} \int \frac{d^3 q}{(2\pi)^3} d\theta d\bar{\theta} \Phi_i \left[r_2(q^2, k) K \delta_{ij} \right] \Phi_j \quad (\text{D.4})$$

where the regulator function r_1 has been set to zero. The remaining dimensionless function $r_2(q^2, k)$ then determines the shape of the momentum cutoff. Consequently, the inverse propagator is given by

$$(\Gamma_k^{(2)} + R_k)_{mn}(z, z') = [-h\delta_{mn}K(q, \theta) + 2W'_k(\bar{\rho})\delta_{mn} + 4W''_k(\bar{\rho})\bar{\rho}\delta_{m1}\delta_{n1}] \delta(z - z'), \quad (\text{D.5})$$

where $h := 1 + r_2$. Since it is worked in Minkowski spacetime, the Wetterich equation in superspace reads

$$\partial_t \Gamma_k = \frac{i}{2} \int dz dz' (\partial_t R_k)_{mn}(z, z') (\Gamma_k^{(2)} + R_k)_{nm}^{-1}(z', z). \quad (\text{D.6})$$

Inserting the regulator (D.4) as well as the inverse Green's function (D.3) into the Wetterich equation then yields

$$\begin{aligned} \partial_t \Gamma_k &= 2\delta(0) \int d\theta d\bar{\theta} \partial_t W_k(\bar{\rho}) \\ &= \frac{i}{2} \int dz dz' [-\partial_t r_2 K(z') \delta_{mn} \delta(z' - z)] [(-h\delta_{nm}K(z) + 2W'_k \delta_{nm} + 4W''_k \bar{\rho} \delta_{n1} \delta_{m1}) \delta(z - z')]^{-1} \\ &= -\frac{i}{2} \delta(0) \int \frac{d^3 q}{(2\pi)^3} d\theta d\bar{\theta} d\theta' d\bar{\theta}' [\partial_t r_2 e^{-\bar{\theta}' \not{q} \theta}] \left[\left((N-1) \frac{hK(z) + 2W'}{h^2 q^2 - W'^2} \right. \right. \\ &\quad \left. \left. + \frac{hK(z) + 2(W' + 2W''\bar{\rho})}{h^2 q^2 - (W' + 2W''\bar{\rho})^2} \right) \delta(\bar{\theta} - \bar{\theta}') \delta(\theta - \theta') \right] \\ &= -i\delta(0) \int \frac{d^3 q}{(2\pi)^3} d\theta d\bar{\theta} \partial_t r_2 \left[(N-1) \frac{W'}{h^2 q^2 - W'^2} + \frac{W' + 2W''\bar{\rho}}{h^2 q^2 - (W' + 2W''\bar{\rho})^2} \right]. \end{aligned} \quad (\text{D.7})$$

Hence, the flow of the superpotential in Minkowski spacetime follows as

$$\partial_t W_k = -\frac{i}{2} \int \frac{d^3 q}{(2\pi)^3} (\partial_t r_2) \left[(N-1) \frac{W'}{h^2 q^2 - W'^2} + \frac{W' + 2W''\bar{\rho}}{h^2 q^2 - (W' + 2W''\bar{\rho})^2} \right]. \quad (\text{D.8})$$

By performing a Wick rotation of the zeroth component of the momentum, i.e. $q^0 \rightarrow iq^0, q^2 \rightarrow -q^2$, the final Euclidean version

$$\partial_t W_k = -\frac{1}{2} \int \frac{d^3 q}{(2\pi)^3} (\partial_t r_2) \left[(N-1) \frac{W'}{h^2 q^2 + W'^2} + \frac{W' + 2W''\bar{\rho}}{h^2 q^2 + (W' + 2W''\bar{\rho})^2} \right] \quad (\text{D.9})$$

of the flow (D.8) is extracted.

References

- [1] Georges Aad et al. Observation of a new particle in the search for the Standard Model Higgs boson with the ATLAS detector at the LHC. *Phys.Lett.*, B716:1–29, 2012.
- [2] Serguei Chatrchyan et al. Observation of a new boson at a mass of 125 GeV with the CMS experiment at the LHC. *Phys.Lett.*, B716:30–61, 2012.
- [3] M.R. Buckley and Berkeley University of California. *Colliders, Cosmology, and Problems in the Standard Model*. University of California, Berkeley, 2008.
- [4] Stephen P. Martin. A Supersymmetry primer. *Adv.Ser.Direct.High Energy Phys.*, 21:1–153, 2010.
- [5] Nir Polonsky. Supersymmetry: Structure and phenomena. Extensions of the standard model. *Lect.Notes Phys.*, M68:1–169, 2001.
- [6] J. Polchinski. String theory. Vol. 1: An introduction to the bosonic string. 1998.
- [7] J. Polchinski. String theory. Vol. 2: Superstring theory and beyond. 1998.
- [8] Edward Witten. Five-branes and M theory on an orbifold. *Nucl.Phys.*, B463:383–397, 1996.
- [9] Petr Horava and Edward Witten. Eleven-dimensional supergravity on a manifold with boundary. *Nucl.Phys.*, B475:94–114, 1996.
- [10] D. Kazakov, S. Lavignac, and J. Dalibard. *Particle Physics beyond the Standard Model: Lecture Notes of the Les Houches Summer School 2005*. Les Houches. Elsevier Science, 2006.
- [11] Rudolf Haag, Jan T. Lopuszanski, and Martin Sohnius. All Possible Generators of Supersymmetries of the s Matrix. *Nucl.Phys.*, B88:257, 1975.
- [12] Gudrun Hiller and Martin Schmaltz. Solving the strong CP problem with supersymmetry. *Phys.Lett.*, B514:263–268, 2001.
- [13] Gianfranco Bertone, Dan Hooper, and Joseph Silk. Particle dark matter: Evidence, candidates and constraints. *Phys.Rept.*, 405:279–390, 2005.
- [14] John Ellis and Keith A. Olive. *Supersymmetric Dark Matter Candidates*. 2010.
- [15] S. Dimopoulos, S. Raby, and Frank Wilczek. Supersymmetry and the Scale of Unification. *Phys.Rev.*, D24:1681–1683, 1981.
- [16] Georges Aad et al. Search for supersymmetry in events with large missing transverse momentum, jets, and at least one tau lepton in 20 fb⁻¹ of $\sqrt{s} = 8$ TeV proton-proton collision data with the ATLAS detector. *JHEP*, 1409:103, 2014.

- [17] John R. Ellis, Giovanni Ridolfi, and Fabio Zwirner. Radiative corrections to the masses of supersymmetric Higgs bosons. *Phys.Lett.*, B257:83–91, 1991.
- [18] John Ellis. Supersymmetric Fits after the Higgs Discovery and Implications for Model Building. *Eur.Phys.J.*, C74:2732, 2014.
- [19] Alok Jha. *One year on from the Higgs boson find, has physics hit the buffers?* The Guardian, 06.08.2013.
- [20] J. Wess and B. Zumino. Supergauge Transformations in Four-Dimensions. *Nucl.Phys.*, B70:39–50, 1974.
- [21] Edward Witten. Dynamical Breaking of Supersymmetry. *Nucl.Phys.*, B188:513, 1981.
- [22] Edward Witten. Constraints on Supersymmetry Breaking. *Nucl.Phys.*, B202:253, 1982.
- [23] A. Wipf. *Statistical approach to quantum field theory : an introduction*. Lecture Notes in Physics. Springer, 2013.
- [24] Georg Bergner. *Ausgewählte Approximationsmethoden für supersymmetrische Modelle*. Diplomarbeit, 2005.
- [25] Joshua W. Elliott, Joel Giedt, and Guy D. Moore. Lattice four-dimensional N=4 SYM is practical. *Phys.Rev.*, D78:081701, 2008.
- [26] Joel Giedt. Progress in four-dimensional lattice supersymmetry. *Int.J.Mod.Phys.*, A24:4045–4095, 2009.
- [27] Michael G. Endres. Dynamical simulation of N=1 supersymmetric Yang-Mills theory with domain wall fermions. *Phys.Rev.*, D79:094503, 2009.
- [28] Maarten F.L. Golterman and Donald N. Petcher. A Local Interactive Lattice Model With Supersymmetry. *Nucl.Phys.*, B319:307–341, 1989.
- [29] I. Montvay. Tuning to N=2 supersymmetry in the SU(2) adjoint Higgs-Yukawa model. *Nucl.Phys.*, B445:399–428, 1995.
- [30] Simon Catterall, David B. Kaplan, and Mithat Unsal. Exact lattice supersymmetry. *Phys.Rept.*, 484:71–130, 2009.
- [31] Juergen Berges, Nikolaos Tetradis, and Christof Wetterich. Nonperturbative renormalization flow in quantum field theory and statistical physics. *Phys.Rept.*, 363:223–386, 2002.
- [32] Holger Gies. Introduction to the functional RG and applications to gauge theories. *Lect.Notes Phys.*, 852:287–348, 2012.
- [33] Jens Braun and Holger Gies. Chiral phase boundary of QCD at finite temperature. *JHEP*, 0606:024, 2006.
- [34] Jens Braun, Lisa M. Haas, Florian Marhauser, and Jan M. Pawłowski. Phase Structure of Two-Flavor QCD at Finite Chemical Potential. *Phys.Rev.Lett.*, 106:022002, 2011.
- [35] Holger Gies and Michael M. Scherer. Asymptotic safety of simple Yukawa systems. *Eur.Phys.J.*, C66:387–402, 2010.
- [36] Holger Gies and René Sondenheimer. Higgs Mass Bounds from Renormalization Flow for a Higgs-top-bottom model. 2014.

- [37] Astrid Eichhorn, Holger Gies, Joerg Jaeckel, Tilman Plehn, Michael M. Scherer, et al. The Higgs Mass and the Scale of New Physics. 2015.
- [38] R.J. Furnstahl. The Renormalization Group in Nuclear Physics. *Nucl.Phys.Proc.Suppl.*, 228:139–175, 2012.
- [39] Matthias Drews, Thomas Hell, Bertram Klein, and Wolfram Weise. Thermodynamic phases and mesonic fluctuations in a chiral nucleon-meson model. *Phys.Rev.*, D88(9):096011, 2013.
- [40] Matthias Drews and Wolfram Weise. Functional renormalization group approach to neutron matter. *Phys.Lett.*, B738:187–190, 2014.
- [41] J. Berges and David Mesterhazy. Introduction to the nonequilibrium functional renormalization group. *Nucl.Phys.Proc.Suppl.*, 228:37–60, 2012.
- [42] Jürgen Berges, Björn Schenke, Sören Schlichting, and Raju Venugopalan. Turbulent thermalization process in high-energy heavy-ion collisions. 2014.
- [43] M. Reuter. Nonperturbative evolution equation for quantum gravity. *Phys.Rev.*, D57:971–985, 1998.
- [44] Alessandro Codello and Roberto Percacci. Fixed points of higher derivative gravity. *Phys.Rev.Lett.*, 97:221301, 2006.
- [45] Alessandro Codello, Roberto Percacci, and Christoph Rahmede. Investigating the Ultraviolet Properties of Gravity with a Wilsonian Renormalization Group Equation. *Annals Phys.*, 324:414–469, 2009.
- [46] Dario Benedetti, Pedro F. Machado, and Frank Saueressig. Asymptotic safety in higher-derivative gravity. *Mod.Phys.Lett.*, A24:2233–2241, 2009.
- [47] Franziska Synatschke, Georg Bergner, Holger Gies, and Andreas Wipf. Flow Equation for Supersymmetric Quantum Mechanics. *JHEP*, 0903:028, 2009.
- [48] Franziska Synatschke, Jens Braun, and Andreas Wipf. N=1 Wess Zumino Model in d=3 at zero and finite temperature. *Phys. Rev.*, D81:125001, 2010.
- [49] Franziska Synatschke, Holger Gies, and Andreas Wipf. The Phase Diagram for Wess-Zumino Models. *AIP Conf. Proc.*, 1200:1097–1100, 2010.
- [50] Franziska Synatschke, Holger Gies, and Andreas Wipf. Phase Diagram and Fixed-Point Structure of two dimensional N=1 Wess-Zumino Models. *Phys. Rev.*, D80:085007, 2009.
- [51] Franziska Synatschke-Czerwonka, Thomas Fischbacher, and Georg Bergner. The two dimensional N=(2,2) Wess-Zumino Model in the Functional Renormalization Group Approach. *Phys. Rev.*, D82:085003, 2010.
- [52] Holger Gies, Franziska Synatschke, and Andreas Wipf. Supersymmetry breaking as a quantum phase transition. *Phys.Rev.*, D80:101701, 2009.
- [53] Hidenori Sonoda and Kayhan Ulker. Construction of a Wilson action for the Wess-Zumino model. *Prog.Theor.Phys.*, 120:197–230, 2008.
- [54] Hidenori Sonoda and Kayhan Ulker. An Elementary proof of the non-renormalization theorem for the Wess-Zumino model. *Prog.Theor.Phys.*, 123:989–1002, 2010.

- [55] Oliver J. Rosten. On the Renormalization of Theories of a Scalar Chiral Superfield. *JHEP*, 1003:004, 2010.
- [56] Marianne Heilmann, Tobias Hellwig, Benjamin Knorr, Marcus Ansorg, and Andreas Wipf. Convergence of Derivative Expansion in Supersymmetric Functional RG Flows. 2014.
- [57] Daniel F. Litim, Marianne C. Mastaler, Franziska Synatschke-Czerwonka, and Andreas Wipf. Critical behavior of supersymmetric $O(N)$ models in the large- N limit. *Phys.Rev.*, D84:125009, 2011.
- [58] M. Mastaler, F. Synatschke-Czerwonka, and A. Wipf. Supersymmetric renormalization group flows. *Phys.Part.Nucl.*, 43:593–599, 2012.
- [59] Marianne Heilmann, Daniel F. Litim, Franziska Synatschke-Czerwonka, and Andreas Wipf. Phases of supersymmetric $O(N)$ theories. *Phys.Rev.*, D86:105006, 2012.
- [60] Michael Dine and John D. Mason. Supersymmetry and Its Dynamical Breaking. *Rept.Prog.Phys.*, 74:056201, 2011.
- [61] M. Reuter and C. Wetterich. Average action for the Higgs model with Abelian gauge symmetry. *Nucl.Phys.*, B391:147–175, 1993.
- [62] M. Bonini, M. D’Attanasio, and G. Marchesini. Renormalization group flow for $SU(2)$ Yang-Mills theory and gauge invariance. *Nucl.Phys.*, B421:429–455, 1994.
- [63] Jan M. Pawłowski. Aspects of the functional renormalisation group. *Annals Phys.*, 322:2831–2915, 2007.
- [64] Leonie Canet, Bertrand Delamotte, Dominique Mouhanna, and Julien Vidal. Nonperturbative renormalization group approach to the Ising model: A Derivative expansion at order partial**4. *Phys.Rev.*, B68:064421, 2003.
- [65] N. Tetradis and D.F. Litim. Analytical solutions of exact renormalization group equations. *Nucl.Phys.*, B464:492–511, 1996.
- [66] Uwe C. Tauber. Renormalization Group: Applications in Statistical Physics. *Nucl.Phys.Proc.Suppl.*, 228:7–34, 2012.
- [67] Michael E. Peskin and Daniel V. Schroeder. An Introduction to quantum field theory. 1995.
- [68] J. Zinn-Justin. *Quantum Field Theory and Critical Phenomena*. International series of monographs on physics. Clarendon Press, 2002.
- [69] Steven Weinberg. *The Quantum Theory of Fields, Volume 1: Foundations*. Cambridge University Press, 2005.
- [70] Murray Gell-Mann and F.E. Low. Quantum electrodynamics at small distances. *Phys.Rev.*, 95:1300–1312, 1954.
- [71] Kenneth G. Wilson. Renormalization group and critical phenomena. 1. Renormalization group and the Kadanoff scaling picture. *Phys.Rev.*, B4:3174–3183, 1971.
- [72] Kenneth G. Wilson. Renormalization group and critical phenomena. 2. Phase space cell analysis of critical behavior. *Phys.Rev.*, B4:3184–3205, 1971.

- [73] Kenneth G. Wilson. The Renormalization Group: Critical Phenomena and the Kondo Problem. *Rev.Mod.Phys.*, 47:773, 1975.
- [74] K.G. Wilson and John B. Kogut. The Renormalization group and the epsilon expansion. *Phys.Rept.*, 12:75–200, 1974.
- [75] L.P. Kadanoff. Scaling laws for Ising models near $T(c)$. *Physics*, 2:263–272, 1966.
- [76] C. Wetterich. Average Action and the Renormalization Group Equations. *Nucl.Phys.*, B352:529–584, 1991.
- [77] Christof Wetterich. Exact evolution equation for the effective potential. *Phys. Lett.*, B301:90–94, 1993.
- [78] C. Bagnuls and C. Bervillier. Exact renormalization group equations and the field theoretical approach to critical phenomena. *Int.J.Mod.Phys.*, A16:1825, 2001.
- [79] Janos Polonyi. Lectures on the functional renormalization group method. *Central Eur.J.Phys.*, 1:1–71, 2003.
- [80] Bertrand Delamotte. An Introduction to the nonperturbative renormalization group. *Lect.Notes Phys.*, 852:49–132, 2012.
- [81] Oliver J. Rosten. Fundamentals of the Exact Renormalization Group. *Phys.Rept.*, 511:177–272, 2012.
- [82] Daniel F. Litim and Jan M. Pawłowski. Completeness and consistency of renormalisation group flows. *Phys.Rev.*, D66:025030, 2002.
- [83] Daniel F. Litim and Jan M. Pawłowski. Perturbation theory and renormalization group equations. *Phys.Rev.*, D65:081701, 2002.
- [84] C. Wetterich. Quadratic Renormalization of the Average Potential and the Naturalness of Quadratic Mass Relations for the Top Quark. *Z.Phys.*, C48:693–705, 1990.
- [85] Stefan Bornholdt and Christof Wetterich. Average action for models with fermions. *Z.Phys.*, C58:585–594, 1993.
- [86] Jordi Comellas, Yuri Kubyshin, and Enrique Moreno. Exact renormalization group study of fermionic theories. *Nucl.Phys.*, B490:653–686, 1997.
- [87] Holger Gies and Christof Wetterich. Renormalization flow of bound states. *Phys.Rev.*, D65:065001, 2002.
- [88] Daniel F. Litim. Optimized renormalization group flows. *Phys.Rev.*, D64:105007, 2001.
- [89] S. Weinberg. *Ultraviolet divergences in quantum theories of gravitation*, in: *General Relativity: An Einstein centenary survey*, Eds. S.W. Hawking and W. Israel. Cambridge University Press, first edition edition, 1979. 790-831.
- [90] Daniel F. Litim. Renormalisation group and the Planck scale. *Phil. Trans. R. Soc.*, A 369:2759–2778, 2011. arXiv:1102.4624 [hep-th].
- [91] Peter Brockway Arnold. Quark-Gluon Plasmas and Thermalization. *Int.J.Mod.Phys.*, E16:2555–2594, 2007.

- [92] Holger Gies and Lukas Janssen. UV fixed-point structure of the three-dimensional Thirring model. *Phys.Rev.*, D82:085018, 2010.
- [93] Peter Kopietz, Lorenz Bartosch, and Florian Schutz. Introduction to the functional renormalization group. *Lect.Notes Phys.*, 798:1–380, 2010.
- [94] Stanislaw D. Glazek and Kenneth G. Wilson. Limit cycles in quantum theories. *Phys.Rev.Lett.*, 89:230401, 2002.
- [95] Andre LeClair, Jose Maria Roman, and German Sierra. Log periodic behavior of finite size effects in field theories with RG limit cycles. *Nucl.Phys.*, B700:407–435, 2004.
- [96] Daniel Litim and Alejandro Satz. Limit cycles and quantum gravity. 2012.
- [97] Yu.A. Golfand and E.P. Likhtman. Extension of the Algebra of Poincare Group Generators and Violation of p Invariance. *JETP Lett.*, 13:323–326, 1971.
- [98] D.V. Volkov and V.P. Akulov. Possible universal neutrino interaction. *JETP Lett.*, 16:438–440, 1972.
- [99] D.V. Volkov and V.P. Akulov. Is the Neutrino a Goldstone Particle? *Phys.Lett.*, B46:109–110, 1973.
- [100] Pierre Ramond. Dual Theory for Free Fermions. *Phys.Rev.*, D3:2415–2418, 1971.
- [101] A. Neveu and J.H. Schwarz. Factorizable dual model of pions. *Nucl.Phys.*, B31:86–112, 1971.
- [102] Sidney R. Coleman and J. Mandula. All Possible Symmetries of the S Matrix. *Phys.Rev.*, 159:1251–1256, 1967.
- [103] S. Weinberg. *The Quantum Theory of Fields: Supersymmetry*. The Quantum Theory of Fields. Cambridge University Press, 2000.
- [104] Peter C. West. Introduction to supersymmetry and supergravity. 1990.
- [105] H. Kalka and G. Soff. Supersymmetry. (In German). 1997.
- [106] Andreas Wipf. Non-perturbative methods in supersymmetric theories. 2005.
- [107] Adel Bilal. Introduction to supersymmetry. 2001.
- [108] Abdus Salam and J.A. Strathdee. Supergauge Transformations. *Nucl.Phys.*, B76:477–482, 1974.
- [109] Savas Dimopoulos and Howard Georgi. Softly Broken Supersymmetry and SU(5). *Nucl.Phys.*, B193:150, 1981.
- [110] Abdus Salam and J.A. Strathdee. On Goldstone Fermions. *Phys.Lett.*, B49:465–467, 1974.
- [111] Kenneth A. Intriligator and Nathan Seiberg. Lectures on Supersymmetry Breaking. *Class.Quant.Grav.*, 24:S741–S772, 2007.
- [112] Yael Shadmi and Yuri Shirman. Dynamical supersymmetry breaking. *Rev.Mod.Phys.*, 72:25–64, 2000.
- [113] H. Nicolai. Supersymmetry and Spin Systems. *J.Phys.*, A9:1497–1506, 1976.

- [114] E. Schrödinger and Dublin Institute for Advanced Studies. *Further Studies on Solving Eigenvalue Problems by Factorization*. Proceedings of the Royal Irish Academy, Section A, mathematical, astronomical and physical science. Hodges, Figgis, 1941.
- [115] Fred Cooper, Avinash Khare, and Uday Sukhatme. Supersymmetry and quantum mechanics. *Phys.Rept.*, 251:267–385, 1995.
- [116] R. Adhikari, R. Dutt, A. Khare, and U.P. Sukhatme. Higher Order WKB Approximations in Supersymmetric Quantum Mechanics. *Phys.Rev.*, A38:1679–1686, 1988.
- [117] Georg Junker. Quantum and classical stochastic dynamics: Exactly solvable models by supersymmetric methods. 1998.
- [118] Edward Witten. Supersymmetry and Morse theory. *J.Diff.Geom.*, 17:661–692, 1982.
- [119] Georg Bergner, Tobias Kaestner, Sebastian Uhlmann, and Andreas Wipf. Low-dimensional Supersymmetric Lattice Models. *Annals Phys.*, 323:946–988, 2008.
- [120] Christian Wozar and Andreas Wipf. Supersymmetry Breaking in Low Dimensional Models. *Annals Phys.*, 327:774–807, 2012.
- [121] David Baumgartner and Urs Wenger. Exact results for supersymmetric quantum mechanics on the lattice. *PoS, LATTICE2011*:239, 2011.
- [122] Atsushi Horikoshi, Ken-Ichi Aoki, Masa-aki Taniguchi, and Haruhiko Terao. Nonperturbative renormalization group and quantum tunneling. pages 194–203, 1998.
- [123] M. Weyrauch. Functional renormalization group and quantum tunnelling. *J.Phys.*, A39:649–666, 2006.
- [124] G. Junker. Supersymmetric methods in quantum and statistical physics. 1996.
- [125] N. Tetradis and C. Wetterich. Critical exponents from effective average action. *Nucl.Phys.*, B422:541–592, 1994.
- [126] Christof Wetterich. The Average action for scalar fields near phase transitions. *Z.Phys.*, C57:451–470, 1993.
- [127] John P. Boyd. *Chebyshev and Fourier Spectral Methods*. Dover Publications, 2nd edition, 2000.
- [128] Marcus Ansorg, A. Kleinwachter, and R. Meinel. Highly accurate calculation of rotating neutron stars: detailed description of the numerical methods. *Astron.Astrophys.*, 405:711, 2003.
- [129] D. Zappala. Improving the renormalization group approach to the quantum mechanical double well potential. *Phys.Lett.*, A290:35–40, 2001.
- [130] D. Bailin and A. Love. *Supersymmetric Gauge Field Theory and String Theory*. Graduate Student Series in Physics. Taylor & Francis, 1994.
- [131] M. Reuter and C. Wetterich. Effective average action for gauge theories and exact evolution equations. *Nucl.Phys.*, B417:181–214, 1994.
- [132] M. Reuter and C. Wetterich. Gluon condensation in nonperturbative flow equations. *Phys.Rev.*, D56:7893–7916, 1997.

- [133] Rui Neves, Yuri Kubyshev, and Robertus Potting. Polchinski ERG equation and 2-D scalar field theory. pages 159–167, 1998.
- [134] Robert D. Pisarski and Frank Wilczek. Remarks on the Chiral Phase Transition in Chromodynamics. *Phys.Rev.*, D29:338–341, 1984.
- [135] Frank Wilczek. Application of the renormalization group to a second order QCD phase transition. *Int.J.Mod.Phys.*, A7:3911–3925, 1992.
- [136] Krishna Rajagopal and Frank Wilczek. Static and dynamic critical phenomena at a second order QCD phase transition. *Nucl.Phys.*, B399:395–425, 1993.
- [137] Krishna Rajagopal. The Chiral phase transition in QCD: Critical phenomena and long wavelength pion oscillations. 1995.
- [138] Francois David, David A. Kessler, and Herbert Neuberger. The Bardeen-Moshe-Bander Fixed Point and the Ultraviolet Triviality of ϕ^6 IN three-dimensions. *Phys. Rev. Lett.*, 53:2071, 1984.
- [139] Francois David, David A. Kessler, and Herbert Neuberger. A Study of $(\Phi^2)_3^3$ at $N = \infty$. *Nucl.Phys.*, B257:695–728, 1985.
- [140] William A. Bardeen, Moshe Moshe, and Myron Bander. Spontaneous Breaking of Scale Invariance and the Ultraviolet Fixed Point in $O(n)$ Symmetric $(\phi^6$ in Three-Dimensions) Theory. *Phys. Rev. Lett.*, 52:1188, 1984.
- [141] Frithjof Karsch and Hildegard Meyer-Ortmanns. Phase structure of $O(N)$ symmetric ϕ_3^6 models at small and intermediate N . *Phys.Lett.*, B193:489, 1987.
- [142] L. Dolan and R. Jackiw. Symmetry Behavior at Finite Temperature. *Phys.Rev.*, D9:3320–3341, 1974.
- [143] K. Takahashi. PERTURBATIVE CALCULATIONS AT FINITE TEMPERATURES. *Z.Phys.*, C26:601–613, 1985.
- [144] M.E. Carrington. The Effective potential at finite temperature in the Standard Model. *Phys.Rev.*, D45:2933–2944, 1992.
- [145] J.R. Espinosa, M. Quiros, and F. Zwirner. On the phase transition in the scalar theory. *Phys.Lett.*, B291:115–124, 1992.
- [146] William A. Bardeen and Moshe Moshe. Phase Structure of the $O(N)$ Vector Model. *Phys.Rev.*, D28:1372, 1983.
- [147] M. Reuter, N. Tetradis, and C. Wetterich. The Large N limit and the high temperature phase transition for the ϕ^4 theory. *Nucl.Phys.*, B401:567–590, 1993.
- [148] A. Codello, N. Defenu, and G. D’Odorico. Critical exponents of $O(N)$ models in fractional dimensions. 2014.
- [149] Nicolo Defenu, Andrea Trombettoni, and Alessandro Codello. Fixed Points Structure & Effective Fractional Dimension for $O(N)$ Models with Long-Range Interactions. 2014.
- [150] Roberto Percacci and Gian Paolo Vacca. Are there scaling solutions in the $O(N)$ -models for large N in $d > 4$? *Phys.Rev.*, D90(10):107702, 2014.

- [151] Leonie Canet, Bertrand Delamotte, Dominique Mouhanna, and Julien Vidal. Optimization of the derivative expansion in the nonperturbative renormalization group. *Phys.Rev.*, D67:065004, 2003.
- [152] J.-P. Blaizot, Ramon Mendez Galain, and Nicolas Wschebor. A New method to solve the non perturbative renormalization group equations. *Phys.Lett.*, B632:571–578, 2006.
- [153] Jean-Paul Blaizot, Ramon Mendez-Galain, and Nicolas Wschebor. Non perturbative renormalisation group and momentum dependence of n-point functions (I). *Phys.Rev.*, E74:051116, 2006.
- [154] F. Benitez, J.-P. Blaizot, H. Chate, B. Delamotte, R. Mendez-Galain, et al. Non-perturbative renormalization group preserving full-momentum dependence: implementation and quantitative evaluation. *Phys.Rev.*, E85:026707, 2012.
- [155] William A. Bardeen, Kiyoshi Higashijima, and Moshe Moshe. Spontaneous Breaking of Scale Invariance in a Supersymmetric Model. *Nucl. Phys.*, B250:437, 1985.
- [156] Moshe Moshe and Jean Zinn-Justin. Quantum field theory in the large N limit: A review. *Phys. Rept.*, 385:69–228, 2003.
- [157] John F. Dawson, Bogdan Mihaila, Per Berglund, and Fred Cooper. Supersymmetric approximations to the 3D supersymmetric $O(N)$ model. *Phys. Rev.*, D73:016007, 2006.
- [158] Tsuneo Suzuki. Three-dimensional $O(N)$ model with Fermi and scalar fields. *Phys. Rev.*, D32:1017, 1985.
- [159] Tsuneo Suzuki and Hisashi Yamamoto. A nontrivial Ultraviolet fixed point and stability of three-dimensional $O(N)$ model with fermions and bosons. *Prog. Theor. Phys.*, 75:126, 1986.
- [160] Ragnheidur Gudmundsdottir and Gunnar Rydneil. On a supersymmetric version of $(\phi^2)_3^3$ theory. *Nucl. Phys.*, B254:593, 1985.
- [161] J. Feinberg, M. Moshe, Michael Smolkin, and J. Zinn-Justin. Spontaneous breaking of scale invariance and supersymmetric models at finite temperature. *Int. J. Mod. Phys.*, A20:4475–4483, 2005.
- [162] Yoshimi Matsubara, Tsuneo Suzuki, Hisashi Yamamoto, and Ichiro Yotsuyanagi. On a phase with spontaneously broken scale invariance in three-dimensional $O(N)$ models. *Prog. Theor. Phys.*, 78:760, 1987.
- [163] Moshe Moshe and Jean Zinn-Justin. Phase structure of supersymmetric models at finite temperature. *Nucl. Phys.*, B648:131–160, 2003.
- [164] Daniel F. Litim. Critical exponents from optimized renormalization group flows. *Nucl.Phys.*, B631:128–158, 2002.
- [165] Daniel F. Litim. Optimisation of the exact renormalisation group. *Phys. Lett.*, B486:92–99, 2000. hep-th/0005245.
- [166] Daniel F. Litim. Mind the gap. *Int.J.Mod.Phys.*, A16:2081–2088, 2001. hep-th/0104221.
- [167] Gerard 't Hooft. A Planar Diagram Theory for Strong Interactions. *Nucl.Phys.*, B72:461, 1974.
- [168] D.J. Amit. Field Theory, the Renormalization Group, and Critical Phenomena. 1978.

- [169] Jens Braun, Holger Gies, and Daniel D. Scherer. Asymptotic safety: a simple example. *Phys.Rev.*, D83:085012, 2011.
- [170] Matthieu Tissier and Gilles Tarjus. Supersymmetry and Its Spontaneous Breaking in the Random Field Ising Model. *Phys.Rev.Lett.*, 107:041601, 2011.
- [171] Matthieu Tissier and Gilles Tarjus. Nonperturbative Functional Renormalization Group for Random Field Models. III: Superfield formalism and ground-state dominance. *Phys.Rev.*, B85:104202, 2012.
- [172] Matthieu Tissier and Gilles Tarjus. Nonperturbative Functional Renormalization Group for Random Field Models. IV: Supersymmetry and its spontaneous breaking. *Phys.Rev.*, B85:104203, 2012.
- [173] Jordi Comellas and Alex Travesset. O (N) models within the local potential approximation. *Nucl.Phys.*, B498:539–564, 1997.
- [174] D. Litim and N. Tetradis. Approximate solutions of exact renormalization group equations. 1995. hep-th/9501042.
- [175] Daniel F. Litim. Derivative expansion and renormalization group flows. *JHEP*, 0111:059, 2001. hep-th/0111159.
- [176] Daniel F. Litim. Wilsonian flow equation and thermal field theory. 1998. hep-ph/9811272.
- [177] Claude Bervillier, Andreas Juttner, and Daniel F. Litim. High-accuracy scaling exponents in the local potential approximation. *Nucl.Phys.*, B783:213–226, 2007.
- [178] Rodrigo P. Macedo and Marcus Ansorg. Axisymmetric fully spectral code for hyperbolic equations. 2014.

Zusammenfassung

Das die elektromagnetische, schwache und starke Wechselwirkung beschreibende Standardmodell der Elementarteilchen gilt seit seiner Entwicklung in den 1970er Jahren als großer wissenschaftlicher Erfolg. Mit der Entdeckung des 125 GeV schweren Higgs Bosons durch die ATLAS- und CMS-Experimente am Large Hadron Collider 2012 ist nun erstmals das vollständige Teilchenspektrum des Standardmodells verifiziert. Dennoch werden einige physikalische Phänomene und Beobachtungen nicht (hinreichend) durch das Standardmodell beschrieben. Hierzu zählen die vollständige Implementation der Gravitation, die Beschreibung dunkler Materie und Energie, der Ursprung des Hierarchieproblems und die Erklärung der Neutrinomassen. Das Standardmodell wird deshalb nicht als eine fundamentale, auf allen Skalen gültige Theorie, sondern vielmehr als die niederenergetische effektive Beschreibung der Natur angesehen. Verschiedenartige Ansätze für theoretische Konzepte jenseits des Standardmodells wurden und werden seither entworfen. Beispiele sind das minimal supersymmetrische Standardmodell (MSSM), Stringtheorie, M-Theorie sowie Extradimensionen. Das populäre und vielversprechende Konzept der Supersymmetrie verknüpft jedes Boson mit einem entsprechenden Fermion bzw. „Superpartner“ gleicher Masse und erweitert somit das Teilchenspektrum des Standardmodells immens. Da bisher keine Superpartner experimentell bei Energien unter 1 TeV nachgewiesen werden konnten, muss Supersymmetrie im Niederenergiebereich spontan brechen. Der Brechungsmechanismus - wahrscheinlich induziert durch nicht-perturbative Quanteneffekte - ist bisher nicht vollständig verstanden.

In der vorliegenden Arbeit werden skalare supersymmetrische Feldtheorien - vereinfachte Modellierungen des MSSM - mittels der funktionalen Renormierungsgruppe (FRG) untersucht.

Die Methode der FRG verbindet durch die Konstruktion einer skalenabhängigen effektiven Wirkung klassische Physik auf mikroskopischen mit effektiver Physik auf makroskopischen Skalen. Die Skalenabhängigkeit der Wirkung ist dabei durch eine funktionale Differentialgleichung bestimmt, die aus einer Reformulierung des Pfadintegrals hervorgeht.

Diese Arbeit wurde durch folgende Fragestellungen motiviert: *Welche physikalische Erkenntnisse supersymmetrischer Theorien, insbesondere in der Nähe von Phasenübergängen und im nicht-perturbativen Regime, können mittels der FRG gewonnen werden? Wie ist die Qualität der gewonnenen Resultate zu bewerten?*

Die Methodik der FRG wurde in dieser Dissertation auf drei supersymmetrische Modelle angewandt: supersymmetrische Quantenmechanik, dreidimensionale $\mathcal{N} = 1$ Wess-Zumino Theorien sowie $\mathcal{N} = 1$ supersymmetrische $O(N)$ Modelle in drei Dimensionen. Zunächst wurde der Renormierungsgruppenfluss der Wirkung manifest supersymmetrisch formuliert. Dies garantiert eine unverfälschte Untersuchung der spontanen Supersymmetriebrechung. Des Weiteren wurde mit einer Entwicklung in Ableitungsoperatoren ein adäquater, intrinsisch nicht-perturbativer Ansatz für die skalenabhängige Wirkung gewählt.

Zunächst lag der Fokus auf der supersymmetrischen Quantenmechanik, da hier das Energiespektrum numerisch exakt bestimmt werden kann, was eine quantitative Bewertung der verwendeten Methodik ermöglicht. Die supersymmetrische Quantenmechanik betreffend konnten folgende Erkenntnisse gewonnen und Ergebnisse erzielt werden: es wurde gezeigt, dass die superkovariante Ableitungsentwicklung systematisch in dem Sinne ist, dass physikalische Observablen bei Erhöhung der Trunkierungsordnung konvergieren. Für die Quantenmechanik mit erhaltener Supersymmetrie konnte die erste angeregte Energie in vierter Ordnung in der Ableitungsentwicklung für Kopplungsstärken hinein in den nicht-perturbativen Bereich mit einem relativen Fehler kleiner 1% bestimmt werden. Für sehr starke Kopplungen zeigte sich jedoch eine limitierte Anwendbarkeit und die hier dominierenden nicht-lokalen Instantoneffekte konnten nicht hinreichend beschrieben werden. Anschließend wurde die spontane Supersymmetriebrechung in der Quantenmechanik studiert. Ein neues Projektionsschema zur Bestimmung der Flussgleichungen wurde entwickelt und die Grundzustandsenergien mit einem relativen Fehler von wenigen Prozent bestimmt.

Als zweites Untersuchungsobjekt fungierten dreidimensionale $\mathcal{N} = 1$ Wess-Zumino Theorien. Dabei lag der Fokus auf der Untersuchung des kritischen Verhaltens nahe dem Phasenübergang zwischen der supersymmetrischen und der spontan gebrochenen Phase. Mittels spektraler Methoden konnte eine globale Fixpunktlösung in vierter Ordnung in der Ableitungsentwicklung bestimmt werden. Es wurden die universellen führenden kritischen Exponenten mit hoher Präzision bestimmt. Auch hier konnte die Systematik der Trunkierung anhand der guten Konvergenz der kritischen Exponenten bestätigt werden. Es wurde außerdem eine in gewöhnlichen Spinsystemen nicht existente Superskalenrelation zwischen dem führenden kritische Exponenten und der anomalen Dimension hergeleitet und auf beliebige Dimensionen $d \geq 2$ verallgemeinert.

Zuletzt wurden dreidimensionale supersymmetrische $O(N)$ Theorien eingehend in führender Ordnung in der Ableitungsentwicklung untersucht. Besonderes Augenmerk wurde auf Modelle mit mikroskopischem $(\Phi^2)^2$ -Potential gelegt. Aufgrund der hochgradig nichtlinearen Struktur der Differentialgleichung wurde zunächst der Limes $N \rightarrow \infty$ betrachtet. Folgende Erkenntnisse konnten hier gewonnen werden: Die Flussgleichung wurde in diesem Grenzfall mittels der Methode der Charakteristiken exakt gelöst und die Phasenstruktur aufgezeigt. Die Theorie wurde durch zwei frei wählbare, physikalische Parameter charakterisiert. Die Analyse des

Phasendiagramms zeigte eine Linie von Fixpunkten mit Gaußschem Skalierungsverhalten, parametrisiert durch die quartische Superfeldkopplung. Ab einer kritischen Kopplung treten jedoch Landau-Pole mit divergenter Fermion-Boson Kopplung auf, die möglicherweise spontane Supersymmetriebrechung indizieren. Gemeinsamkeiten und Unterschiede zu skalaren sphärischen $(\phi^2)^3$ Theorien wurden herausgearbeitet. Des Weiteren wurde die Phasenstruktur aus der Perspektive einer effektiven Theorie mit endlichem cutoff als auch einer renormierten Theorie mit unendlichem cutoff analysiert. Dies ermöglichte durch die Betrachtung des skalenabhängigen Potentials die Erklärung einiger bisher ungeklärter Sachverhalte wie z.B. dem Auftreten mehrerer $O(N)$ symmetrischer Grundzustände. Es wurde gezeigt, dass die Phasenstrukturen der effektiven und renormierten Theorie im weitesten Sinne übereinstimmen. An einem ausgezeichneten Fixpunkt wurde das Phänomen der spontanen Brechung der Skaleninvarianz beobachtet.

Der Studie für $N \rightarrow \infty$ schloss sich dann eine Analyse des Modells für endliche N in Anwesenheit radialer Fluktuationen mit folgenden Feststellungen an: Für endliche N kollabiert die einparametrische Schar von Fixpunktlösungen zu genau einer nicht-trivialen Lösung. Dieser supersymmetrische Wilson-Fisher Fixpunkt mit nicht-Gaußschem Skalenverhalten ist jedoch nur lokal wohldefiniert. Global wurden Nichtanalytizitäten im physikalischen Feldraum identifiziert. Eine weitere wichtige Erkenntnis war das Verschwinden des Fixpunktes mit gebrochener Skaleninvarianz in Anwesenheit radialer Fluktuationen.

Strukturell konnte diese Arbeit zeigen, dass Supersymmetrie im sphärischen Modell das Vorhandensein eines nicht-eindeutigen effektiven Potentials zusammen mit Landau-Polen induziert. Dieses Verhalten wird durch die Goldstone Moden hervorgerufen. Ähnlich wie in Ising Modellen mit Parisi-Sourlas Supersymmetrie könnten die Nichtanalytizitäten auf eine spontane Brechung der Supersymmetrie im stark nicht-perturbativen Regime hindeuten. Die Verwendung der funktionalen Renormierungsgruppengleichungen war insbesondere zur detaillierten Untersuchung der Supersymmetriebrechung und der Phasenstruktur des $O(N)$ Modells maßgebend. Nur durch die Bestimmung des skalenabhängigen Potentials wurden viele Ergebnisse transparent.

Dennoch ist das in dieser Arbeit entwickelte Bild der supersymmetrischen Modelle im stark nicht-perturbativen Regime noch nicht vollständig verstanden und bedarf weiterer Untersuchungen. Hierfür würde sich z.B. eine Vertexentwicklung als komplementärer Ansatz zur Ableitungsentwicklung anbieten.

Danksagung

An erster Stelle gilt mein Dank Prof. Andreas Wipf für die gute, kontinuierliche Betreuung, angefangen von meiner Studienarbeit über die Diplomarbeit hinweg bis zum Ende meiner Dissertation.

Des Weiteren möchte ich mich für die fruchtbaren Kollaborationen bei Daniel Litim, Franziska Synatschke-Czerwonka, Tobias Hellwig, Benjamin Knorr und Markus Ansorg bedanken. Ohne ihre fachlichen Impulse und Anregungen wäre die Dissertation in dieser Form nicht zustande gekommen.

In zahlreichen fachlichen Diskussionen (meistens korreliert mit Kaffeekonsum) mit Kollegen des Theoretisch-Physikalischen Instituts Jena konnte ich mein Wissen erweitern und Probleme lösen. Hierfür möchte ich Tobias Hellwig, Björn Wellegehausen, Lukas Jansen, Ulrich Theis, Georg Bergner, Benjamin Knorr, Holger Gies, Jens Braun, Albrecht Werner, Daniel Körner und Reinhard Meinel herzlich danken. Benjamin Knorr gilt mein Dank auch für das kritische Korrekturlesen dieser Arbeit.

Zu großem Dank verpflichtet bin ich meiner ganzen Familie, insbesondere meinem Mann Christoph und meinem Sohn Oskar für ihre mentale Unterstützung.

Ehrenwörtliche Erklärung

Ich erkläre hiermit ehrenwörtlich, dass ich die vorliegende Arbeit selbständig, ohne unzulässige Hilfe Dritter und ohne Benutzung anderer als der angegebenen Hilfsmittel und Literatur angefertigt habe. Die aus anderen Quellen direkt oder indirekt übernommenen Daten und Konzepte sind unter Angabe der Quelle gekennzeichnet.

Ergebnisse, die in Zusammenarbeit mit den Mitgliedern des Lehrstuhles für Quantenfeldtheorie in Jena und anderen Kooperationen entstanden sind, sind in der Arbeit entsprechend benannt.

Weitere Personen waren an der inhaltlich-materiellen Erstellung der vorliegenden Arbeit nicht beteiligt. Insbesondere habe ich hierfür nicht die entgeltliche Hilfe von Vermittlungs- bzw. Beratungsdiensten (Promotionsberater oder andere Personen) in Anspruch genommen. Niemand hat von mir unmittelbar oder mittelbar geldwerte Leistungen für Arbeiten erhalten, die im Zusammenhang mit dem Inhalt der vorgelegten Dissertation stehen.

Die Arbeit wurde bisher weder im In- noch im Ausland in gleicher oder ähnlicher Form einer anderen Prüfungsbehörde vorgelegt.

Die geltende Promotionsordnung der Physikalisch-Astronomischen Fakultät ist mir bekannt.

Ich versichere ehrenwörtlich, dass ich nach bestem Wissen die reine Wahrheit gesagt und nichts verschwiegen habe.

Jena, den 01. Februar 2015

Marianne Heilmann

Lebenslauf

Persönliche Daten

Name	Marianne Heilmann, geb. Mastaler
Geburtsdatum	22.01.1986
Geburtsort	Suhl
Familienstand	verheiratet, ein Kind (2 Jahre)

Schule

1992-1996	Grundschule „Gerhart-Hauptmann“, Schleusingen
1996-2004	Hennebergisches Gymnasium „Georg-Ernst“, Schleusingen
26.06.2004	Abitur

Studium

10/2004-07/2005	Humanmedizin, Albert-Ludwigs-Universität Freiburg
10/2005-12/2010	Physik (Diplom), Friedrich-Schiller-Universität Jena
04.01.2008	Vordiplom in Physik
31.01.2011	Diplom in Physik
seit 01/2011	Promotion in Physik, Friedrich-Schiller-Universität Jena

Jena, den 01. Februar 2015

Marianne Heilmann

